TEXTILE RESEARCH JOURNAL

VOLUME XXIII April, 1953 *NUMBER 4*

PUBLICATION OF

TEXTILE RESEARCH INSTITUTE

Editorial Office: 10 East 40th Street, New York 16, N. Y.

All these
AT NEW LOW COST...

Stabilization

Crush Resistance

Glazing and Embossing–

with RHONITE R-2

To give you the greater economy and improved efficiency of RHONITE R-2 we have not sacrificed these other familiar RHONITE advantages—(1) storage stability; (2) easy handling; (3) excellent durability.

P. S. *It's a good finish for nylons, too.*

RHONITE *is a trademark Reg. U.S. Pat. Off. and in principal foreign countries*

CHEMICALS FOR INDUSTRY

ROHM & HAAS COMPANY

WASHINGTON SQUARE, PHILADELPHIA 5, PA.

Representatives in principal foreign countries

TEXTILE RESEARCH JOURNAL

VOL. XXIII, No. 4 April, 1953

In This Issue

Bending Modulus of Fibers Measured with the Resonance Frequency Method
E. Marianne Kärrholm and Bengt Schröder 207

Relationship Between Various Surface Properties of Wool Fibers
Part II: Frictional Properties
Joel Lindberg 225

Summer Courses, Polytechnic Institute of Brooklyn 236

Mechanical Properties of Cotton Fibers
Part I: Relaxation in Air and Water
J. A. Lasater, E. L. Nimer, and H. Eyring 237

The X-Ray Pattern of Sericin and Silk Wax from *Bombyx mori*
E. H. Mercer and F. H. Meyer 243

The Identification of Synthetic Fibers by Their Refractive Indices and Birefringence
A. N. J. Heyn 246

Magnetic Anisotropy of Cellulosic Materials
L. Loeb and L. A. Welo 251

Letters to the Editor
The Birefringence of Dacron Polyester Fiber 258
The Rapid Identification of Fibers by the Christiansen Effect 259

INDUSTRIAL SECTION

The Measurement of Fabric Thickness
R. E. Seaman 262

A Theoretical Investigation of Cap and Ring Spinning Systems
J. Crank 266

Gordon Research Conference on Textiles 276

Editor: Julian S. Jacobs *Production Editor:* Lois E. Emma

Associate Editors

H. J. Ball
Earl E. Berkley
Henry Eyring
Milton Harris
K. L. Hertel
H. Mark
E. R. Schwarz
Kyle Ward, Jr.

TEXTILE RESEARCH JOURNAL, published monthly at Prince and Lemon Streets, Lancaster, Pa., is devoted to the interest of research in textile and allied industries. It is published by Textile Research Institute.

Manuscripts and communications should be sent to the editorial office, 10 East 40th Street, New York 16, N. Y.

Subscription rates:
$15.00 per year; additional for postage, 50 cents to Canada, $1.00 to all other countries. Single copies, $1.50 each.

Entered as second-class matter, April 27, 1945, at the post office at Lancaster, Pa , under the Act of August 24, 1912. Accepted for mailing at special rate of postage provided for in paragraph (d-2), Section 34.40, P. L. & R. of 1948, authorized May 9, 1950.

Contents copyrighted 1953 by Textile Research Institute.

Advertising rates supplied on request.

NOW | . . . an invaluable reference volume for textile chemists, physicists, engineers

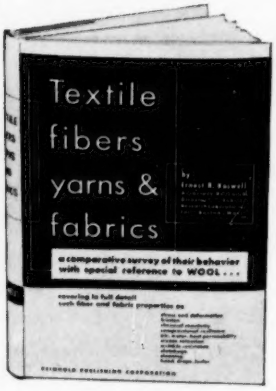

by ERNEST R. KASWELL

Associate Research Director, Fabric Research Laboratories, Inc., Boston, Mass.

Textile

FIBERS, YARNS AND FABRICS

A Comparative Survey of Their Behavior with Special Reference to Wool

Based directly on the research results of over 400 investigators, this eagerly awaited book is the first to evaluate the engineering, physical and chemical behavior of natural and synthetic textile fibers, yarns and fabrics.

The first section of the book deals with the intrinsic properties of fibers. Here, such characteristics as stress and strain, energy absorption, elastic modulus, repeated stress, chemical, thermal, biological and environmental resistance are fully discussed. In the second section, the relationships of these fiber properties to such fundamental fabric requirements as abrasion resistance, crease retention, wrinkle resistance, hand, thermal conductivity and air-water permeability are explained in unusual detail. All fibers including such recent synthetics as Dacron, Vicara, X-51, etc., are fully covered.

Written primarily for textile chemists, physicists and engineers, this book will serve as an ideal reference source for all scientifically trained personnel in textile research, development, service, production or management.

1953, 450 pages, $11.00

Send for an Examination Copy Today!

REINHOLD PUBLISHING CORPORATION

Dept. M-505, 330 West 42nd Street, New York 36, N. Y.

Chemical Specialties

FOR TEXTILE PROCESSING

LUPOMIN*
A series of cationic nitrogen compounds for softening and finishing textiles.

BENSAPOL*
Liquid detergent derived from Monopole Oil for wool scouring.

ORATOL L-48*
A neutralized sulphonated ester of a higher alkanolamide for increased scouring efficiency.

SULPHONATED OILS
A wide range of types available in numerous concentrations, grades and degrees of sulphonation.

MONOPOLE OIL*
Double sulphonated castor oil for bleaching, dyeing, finishing and as a dispersant for dye solutions.

PARNOL NO. 85
An anionic dodecyl-benzene sulphonate with exceptional wetting properties and high detergent characteristics.

LOMAR PW*
A condensation product of alkyl aryl sulphonates used as dispersing agent for insoluble pigments.

SUPERCLEAR*
Product of natural vegetable gums with complete solubility and outstanding penetrating properties for fine printing.

WETSIT CONC.*
A liquid wetting agent of the alkyl aryl type with rapid wetting and penetrating properties.

HYDROSULFITES OF SODA CONC.
($Na_2S_2O_4$). Reducing agent for vat dyeing.

HYDROSULFITE AWC
($NaHSO_2.CH_2O.2H_2O$). For discharge printing, stripping, and application printing of vat colors.

HYDROZIN
($Zn(OH)HSO_2.H.CHO$). A clear-dissolving, soluble Zinc Formaldehyde Sulphoxylate, for discharge printing and stripping.

GUMS
A wide range of gums including Arabic, Tragacanth, Karaya, Irish Moss, etc. In both liquid and powder form.

*Reg. Trademark

Write for our Chemicals & Specialties Catalog.

WOLF BRAND CHEMICAL SPECIALTIES

JACQUES WOLF & CO.

Chemicals PASSAIC, N. J.

Branches: Carlstadt, N. J. • Los Angeles, Calif.

TEXTILE RESEARCH JOURNAL

VOL. XXIII, No. 4 April, 1953

Bending Modulus of Fibers Measured with the Resonance Frequency Method

E. Marianne Kärrholm and Bengt Schröder*

Swedish Institute for Textile Research, Gothenburg, Sweden

NUMEROUS investigations of the elastic properties of textile fibers treat the problem by studying the fibers in the stretched condition. Very few consider the bending properties of fibers. This is due mostly to the experimental difficulties involved, especially when static or quasi-static methods are employed.

When a fiber which is free at one end and rigidly clamped at the other end is submitted to a concentrated load, the deflection of the free end is a function of its bending modulus. Khayatt and Chamberlain [10] used this principle for the measurement of the bending modulus of wool and hair. The same principle was utilized by Sen [18] for jute fibers, with the modification that 150 fibers were tested at a time. Müller [15] constructed an apparatus for the determination of the bending properties of single fibers. He remarked, however, that the results are not very accurate due to the experimental difficulties encountered. The bending modulus of nylon monofils with a diameter of at least 0.3 mm. was investigated by Carlene [3] according to the following procedure. The fiber is treated as a beam which is freely supported at the ends and loaded in the center with a concentrated load. The loading is performed with the Cambridge Fiber Extensometer.

Carlene [4] applied another static method which is suitable for both yarns and single fibers of ordinary dimensions. The fiber or yarn is bent into a ring loop of known diameter. An applied weight produces a distortion in the ring shape, from which the flexural rigidity can be calculated.

Textile fibers show a delayed elastic deformation even for loads below the yield point. This means that the rate of loading will influence the stress and strain of the fiber. When the experimental conditions are such that the stress and strain are independent of time, the method is referred to as "static." A "dynamic" method gives the stress-strain relationships under conditions where the stress and strain are usually sinusoidal functions of time. According to these definitions, the testing methods described above may be classified as "quasi-static."

With ideal elastic bodies—*e.g.*, steel—the same value for Young's modulus should be obtained when static and dynamic methods are applied. However, the values obtained for fibers will differ appreciably, the dynamic values being higher than the static ones. Hermanne [7] dealt with this in a perspicuous way in a paper on the elastic properties of rayon.

* Parts I and III of this paper report work done by Mrs. Kärrholm, and Part II reports work done by Mrs. Kärrholm and Mr. Schröder.

Some dynamic methods for the determination of the stretching properties of fibers have been published. Meyer and Lothmar [14] used an acoustic method, which was improved by Ballou and Silverman [2]. Asmussen and Andersen [1] constructed an apparatus with which both static and dynamic measurements can be made. The dynamic elastic properties of rubber-like materials were extensively investigated by Nolle [16].

Lochner [11] studied the dynamic bending properties of textile fibers in the only publication existing on this subject. However, his original intention was to study the damping capacity of fibers. For this purpose he measured the resonance frequency of the fibers using methods which, in some cases, are similar to those used herein.

PART I: THEORETICAL

Fundamental Equations

The differential equation for an elastic beam subjected to forced vibrations can be written

$$m\ddot{y} + r\dot{y} + ky = Ce^{iwt}, \tag{1}$$

where w = exciting frequency, m = mass of the body, r = frictional constant, k = constant ("spring constant"), t = time, y = displacement of the body from its equilibrium position, $\dot{y} = dy/dt$, $\ddot{y} = d^2y/dt^2$, and $i = \sqrt{-1}$.

The resonance frequency of this system, ν_n, is obtained from

$$2\pi\nu_n = w_n = \sqrt{\frac{k}{m} - \frac{r^2}{2m^2}}; \tag{2}$$

for the undamped system ($r = 0$),

$$2\pi\nu_n = w_n = \sqrt{\frac{k}{m}}. \tag{3}$$

For details the reader is referred to the literature on the subject—*e.g.*, Courant [5].

The following equation can be deduced for the free transversal vibrations of a prismatic bar with cross section A, weight per volume γ, and flexural rigidity EI assumed constant along the bar (Timoshenko [20]):

$$-\frac{\gamma A}{g}\frac{\partial^2 z}{\partial t^2} = EI\frac{\partial^4 z}{\partial x^4}, \tag{4a}$$

where E = Young's modulus of elasticity, g = acceleration of gravity, I = moment of inertia, and z is the product of a function of the time, t, and a function of x:

$$z(x,t) = u(x)\cdot y(t). \tag{4b}$$

The vibration axis of the bar lies in the direction of the x-axis.

According to Timoshenko,

$$\frac{\partial^4 z}{\partial x^4} = \frac{s^4 z}{l^4}, \tag{4c}$$

where l is the length of the bar and s is a constant depending on the mode of vibration and the boundary conditions.

Combining equations (4*a*), (4*b*), and (4*c*) gives

$$\frac{\gamma A}{g}\ddot{y} + EI\frac{s^4}{l^4}y = 0. \tag{4d}$$

Equation (4*d*) is of the same type as equation (1) if $r = C = 0$. The resonance frequency can then be obtained from equation (3) by inserting in it the values of k and m, where $k = EI(s^4/l^4)$ and $m = \gamma A/g$, which gives

$$4\pi^2\nu_n^2 = \frac{EIs^4 g}{l^4 A\gamma},$$

or

$$EI = \frac{4\pi^2 A\gamma l^4}{gs^4}\nu_n^2. \tag{5}$$

If one end of the bar is built in and the other end is free: $s_o = 1.875$ for the fundamental mode of vibration, $s_1 = 4.694$ for the first harmonic, and $s_2 = 7.855$ for the second harmonic.

This assumes that Hooke's law is valid and that the length of the bar is large compared to its cross section. Further, the damping has been neglected.

Equation (5) is valid irrespective of the shape of the cross section. For a circular cross section, the moment of inertia, $I = \pi d^4/64$.

According to equation (5) we get

$$E = \frac{64\pi^2\gamma l^4}{gs^4 d^2}\nu_n^2. \tag{6}$$

Equation (6) is valid for an elliptical cross section also; d then means the axis perpendicular to the bending axis.

In deriving the bending stiffness, all damping forces have been neglected. If the amplitude is plotted against the frequency of the forced vibrations, the width of the curve obtained will increase with the damping forces. (The relationship is much more complicated than is indicated here. For details the reader is referred to Courant [5], p. 514.) The damping forces will also influence

the value of the resonance frequency, but to a smaller degree. A lower value of the resonance frequency is obtained with damped oscillations, producing, according to equation (5), too low a value of the bending modulus. The damping effect depends partly on the friction losses in the vibrating body (internal damping) and partly on the damping of the surrounding medium (in this case air damping). By performing the measurements in vacuum, the influence of the air damping can be eliminated. Measurements under vacuum will involve more complicated apparatus, and, what is more important, there is the possibility that fibers will have different elastic properties in a vacuum than in air. It is, of course, also necessary to work at a constant known water vapor pressure in the absence of air.

For these reasons it is desirable that the method be used under atmospheric pressure. This calls for a quantitative determination of the influence of air damping on the value of the resonance frequency.

If a damping force proportional to the time derivative dy/dt acts on the system, equation (4*a*) can be written

$$\frac{\gamma A}{g}\frac{\partial^2 z}{\partial t^2} + r\frac{\partial z}{\partial t} + EI\frac{\partial^4 z}{\partial x^4} = 0.$$

Further, if an external force with the angular velocity w is acting on the system,

$$\frac{\gamma A}{g}\frac{\partial^2 z}{\partial t^2} + r\frac{\partial z}{\partial t} + EI\frac{\partial^4 z}{\partial x^4} = Ce^{iwt},$$

where C is usually a function of x.

If the frequency of the oscillating system approaches the resonance frequency corresponding to s_n, we can write with good approximation

$$\frac{\gamma A}{g}\ddot{y} + r\dot{y} + EI\frac{(s_n)^4}{l^4}y = C_n e^{iwt}, \qquad (7)$$

where C_n = constant and $y(t) = z/u$ according to equation (4*b*). Equation (7) is of the same type as equation (1). Equation (2) can therefore be used to calculate the resonance frequency.

Theoretical Calculation of the Influence of the Air Damping

The magnitude of the air damping of fine quartz fibers ($d = 15\mu$) used in electrometers was calculated by Ising [9]. He pointed out that it is impossible to calculate the friction produced by a long cylinder moving with constant velocity perpendicular to its axis in a viscous medium unless the medium has definite limitation. This was also proved by Lord Rayleigh [12].

Oberbeck [17] calculated the frictional resistance against an ellipsoid moving with constant low velocity in a viscous medium. If the semiaxes of the ellipsoid are denoted by a, c, and d, where $c = d$ and $a \gg d$ and the direction of the motion is perpendicular to the a-axis, the frictional resistance per unit length of the cylinder, α, is given by the following expression:

$$\alpha = \frac{8\pi\eta v}{2\ln\left(\frac{2a}{d} + 1\right)}, \qquad (8)$$

where η = viscosity of the medium and v = velocity of the ellipsoid.

Combining equation (7) and equation (2) and having $r = \alpha/g$, the flexural rigidity, EI, is obtained as

$$EI = \left(4\pi^2 A\gamma\nu_n^2 + \frac{\alpha^2}{2A\gamma}\right)\frac{l^4}{gs^4}. \qquad (9)$$

The assumptions made in deriving α do not correspond to the actual case, as the velocity is not constant.

Stokes [19] calculated the frictional resistance against a cylinder oscillating in an unlimited mass of fluid. The cylinder moves in a direction perpendicular to its axis along a straight line, y, according to

$$\frac{dy}{dt} = ce^{iwt},$$

where c is a constant and w = the angular velocity $= 2\pi\nu$.

According to Stokes, the force per unit length of the cylinder, f, exerted by the medium is

$$f = -kM'\frac{d^2y}{dt^2} - k'M'w\frac{dy}{dt}, \qquad (10a)$$

where

$$M' = \frac{\pi d^2\rho}{4}, \qquad (10b)$$

d = diameter of the cylinder, ρ = density of the medium, k and k' are functions of the quantity m, where

$$m = \frac{d}{4}\sqrt{\frac{w\rho}{\eta}}, \qquad (10c)$$

and η = viscosity of the medium.

If $m < 0.1$, the following expressions for k and k' are valid:

$$k - 1 = \frac{1}{m^2} \cdot \frac{\pi/4}{L^2 + (\pi/4)^2}, \qquad (10d)$$

$$k' = \frac{1}{m^2} \cdot \frac{-L}{L^2 + (\pi/4)^2}, \qquad (10e)$$

where

$$L = 0.577 + \ln m. \qquad (10f)$$

k and k' have been calculated and tabulated by Stokes ([19], p. 52) for larger values of m.

The term containing d^2y/dt^2 in equation (10*a*) is an expression for the amount of the medium (in this case air) which follows the cylinder. With very small values of the diameter, this amount of air will be considerably less than is evident from equation (10*a*). According to Stokes ([19], p. 67), the resistance is best described merely by a function of the velocity, when fine fibers are being considered:

$$f = -k'M'w\frac{dy}{dt}. \qquad (11)$$

Equation (7) then becomes

$$\frac{\gamma A}{g}\ddot{y} + \frac{k'M'w}{g}\dot{y} + EI\frac{(s_n)^4}{l^4}y = C_n e^{iwt}. \qquad (12a)$$

The resonance frequency, ν_n, is obtained from equation (2) by having

$$m = \frac{\gamma A}{g}, \qquad (12b)$$

$$r = \frac{k'M'w}{g}, \qquad (12c)$$

$$k = EI\frac{s^4}{l^4}, \qquad (12d)$$

$$w = 2\pi\nu.$$

From equation (12*a*) the flexural rigidity, EI, can be calculated:

$$EI = \frac{4\pi^2 A\gamma l^4}{gs^4}\nu_n^2(1 + \varphi^2), \qquad (13a)$$

where

$$\varphi = \frac{1}{\sqrt{2}}\frac{k'M'}{A\gamma}. \qquad (13b)$$

For a circular cross section, $A = \pi d^2/4$ and M' is obtained from equation (10*b*) where $M' = A\rho$.

Combining equations (10*b*) and (13*b*) gives

$$\varphi = \frac{1}{\sqrt{2}}\frac{k'\rho}{\gamma}. \qquad (13c)$$

TABLE I. CALCULATED RELATIONSHIP BETWEEN FIBER DIAMETER, RESONANCE FREQUENCY, AND INFLUENCE OF AIR DAMPING

Fiber	Max. influence of air damping according to eq. (13*c*)	Smallest fiber diameter at a resonance frequency of: 50 c.p.s.	100 c.p.s.
Viscose rayon	1%	32μ (11 denier)	23μ (5.7 denier)
	5%	20μ (4.3 denier)	13μ (1.8 denier)
Nylon	1%	38μ (11.7 denier)	27μ (5.9 denier)
	5%	24μ (4.6 denier)	16μ (2.1 denier)

The value of φ increases with decreasing values of diameter and resonance frequency. The percentage influence of the air damping on the bending modulus is obtained from equation (13*a*), and is equal to $100\varphi^2$. Conversely, if φ^2 is allowed to influence the modulus, E, by at most 1% to 5%, it is possible by successive approximations to calculate the minimum fiber diameter that fulfills this condition at a given resonance frequency. The density of the fiber will influence the results; hence, the calculations have been made for nylon fibers (density 1.14) and for viscose rayon (density 1.52). Circular cross section is assumed as well. The results are given in Table I. From this table it is evident that accurate results can be obtained at atmospheric pressure when the fiber diameter

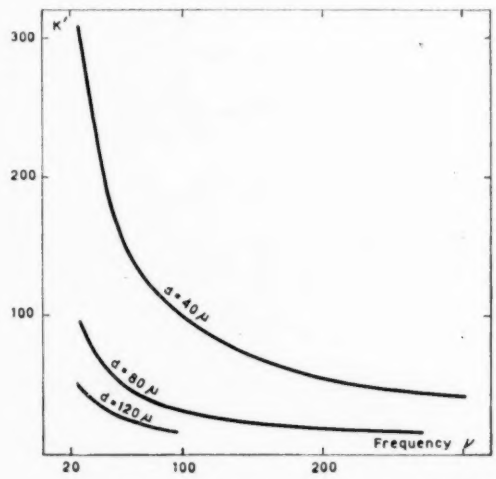

FIG. 1. k' *as a function of the frequency, ν, for different fiber diameters.*

is large enough and the resonance frequency sufficiently high. The latter condition can be realized by varying the fiber length, since the resonance frequency is inversely proportional to the fiber length.

Experimental Determination of the Magnitude of the Air Damping

At two frequencies straddling the resonance frequency the amplitude of the vibrations is $1/\sqrt{2}$ times the maximum amplitude. The difference between these two frequencies is called the "band width" of the frequency curve; it can be determined experimentally and can be used as a measure of the damping effect.

It can be shown (Appendix 1) that the band width, $\Delta\nu$, is equal to

$$\Delta\nu = \frac{r}{2m\pi}, \tag{14}$$

where r and m are the constants of equation (1). By combining equation (14) with equations (12*b*) and (12*c*), the following equation is obtained:

$$\frac{\Delta\nu}{\nu} = \frac{k'M'}{\gamma A}. \tag{15a}$$

For a circular cross section, $M'/A = \rho$, and we have $\frac{\Delta\nu}{\nu} = \frac{k'\rho}{\gamma}$. But, according to equation (13*c*),

$$\varphi = \frac{1}{\sqrt{2}}\frac{k'\rho}{\gamma},$$

which gives

$$\varphi = \frac{\Delta\nu}{\sqrt{2}\nu}, \text{ or } \varphi^2 = \frac{\Delta\nu^2}{2\nu^2} \tag{15b}$$

Inserting the value of φ^2 in equation (13*a*) gives

$$EI = \frac{4\pi^2 A\gamma l^4}{s_n{}^4 g}\,\nu_n{}^2\left(1 + \frac{(\Delta\nu)^2}{2\nu_n{}^2}\right). \tag{16}$$

The same expression was derived by Nolle [16] with the help of an electric analogy. In that case, $\Delta\nu$ refers to the experimentally determined band width, regardless of the cause of the damping effect. With the assumptions made in this paper in deriving equation (16), $\Delta\nu$ refers only to that part of the damping caused by the air, but equation (16) is valid if the internal damping is considered and is assumed to be proportional to the time derivative, dy/dt. In the latter case, $\Delta\nu$ is the over-all band width, as in Nolle's equation.

The value of the band width obtained in vibration experiments is a measure of the over-all damping. In order to obtain only that part caused by air damping, it is necessary to determine the magnitude of the internal damping. The function φ decreases with increasing values of fiber diameter and resonance frequency. Figure 1 shows k', which is directly proportional to φ, as a function of the resonance frequency, ν_n, for different values of the fiber diameter. The corresponding theoretical value of the band width can be calculated from equation (15*b*), which, as shown above refers only to the effect of the air damping. Figure 2 shows the band width thus calculated as a function of the resonance frequency for different values of the fiber diameter. The calculation is made for viscose fibers ($\gamma = 1.52$). For large values of the diameter, the band width is small. For viscose fibers with a diameter of about 200μ the experimentally de-

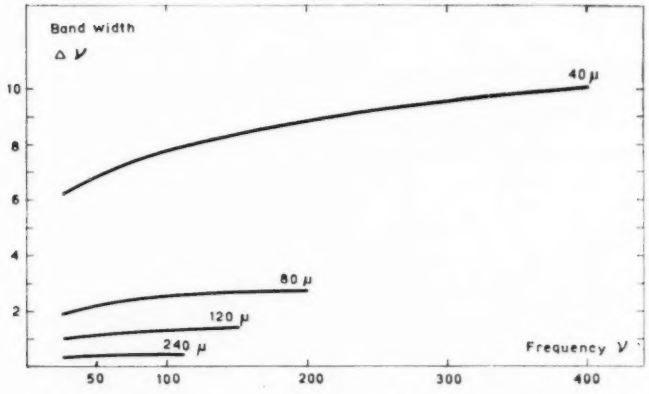

Fig. 2. *Calculated band width referring only to air damping as a function of the resonance frequency for different fiber diameters.*

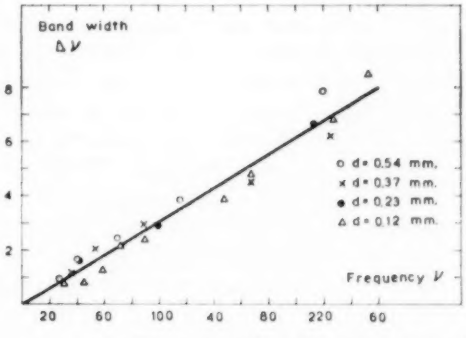

Fig. 3. *The band width referring to internal damping as a function of the frequency for thick model filaments.*

TABLE II. DETERMINATION OF THE BAND WIDTH CAUSED BY INTERNAL DAMPING*

Fiber diameter† (μ)	Resonance frequency ν_0	Total band width $\Delta\nu$	Calculated band width (depending only on air damping)	Band width (depending only on internal damping)
540	41.2	1.68	<0.1	1.68
(×0)	69.5	2.48		2.48
	116.0	3.90		3.90
	221.0	7.85		7.85
370	35.5	1.17	<0.1	1.17
(×50)	57.0	2.06		2.06
	89.3	2.96		2.96
	168.5	4.50		4.50
	225.0	6.20		6.20
230	28.2	1.20	0.30	0.90
(×0)	42.0	1.93	0.30	1.63
	100.0	3.30	0.40	2.90
	214.0	7.10	0.50	6.60
120	30.9	1.67	1.00	0.67
(×50)	44.8	1.85	1.05	0.80
	59.4	2.40	1.15	1.25
	72.1	3.40	1.20	2.20
	90.2	3.70	1.20	2.50
	148.0	5.20	1.35	3.85
	167.0	6.20	1.40	4.80
	228.0	8.30	1.50	6.80
	254.0	10.0	1.50	8.50

* The values in columns 2 and 3 are mean values of six determinations.

† ×0 means that the fiber was not stretched; ×50 means that the fiber was stretched 50% in the xanthate state.

termined band width will be caused by the internal damping for the most part. These fibers are therefore suitable for the measurement of internal damping. In these experiments circular model filaments having diameters of 120μ and 370μ, respectively, and stretched 50% in the xanthate state were used. Unstretched model filaments of diameters of 230μ and 540μ, respectively, were also used. (The production of the filaments is described in Part III.) The band width was determined for two different amplitudes of two and four times the fiber diameter. Within these limits the band width was independent of the amplitude. The experimental results for different resonance frequencies are given in Table II. The values given are the means of six determinations. In column 4 the theoretically calculated band widths (from equation (15b)), depending only on air damping, are given For the fiber diameters of 120μ and 230μ, the values are measurable quantities

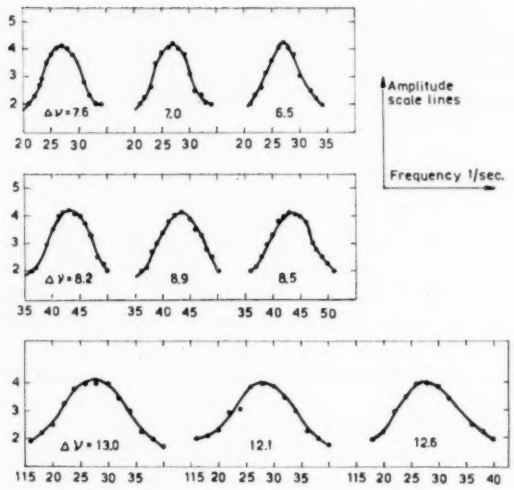

FIG. 4. *Amplitude-frequency curves for the same viscose fiber at three different lengths.*

(see Figure 2). Figure 3 shows the band width, $\Delta\nu$, as a function of ν. These values of $\Delta\nu$ have been corrected for the air damping (column 5, Table II). The band width caused by internal damping increases rectilinearly with the resonance frequency. (The fiber is subjected only to small stresses; see below.)

The equation of the regression line may be written

$$\Delta\nu = 0.0310\nu - 0.06.$$

This equation is valid for the internal damping of viscose fibers independent of fiber diameter and degree of stretching within a frequency range of 25–250 c.p.s.

The experimental errors in the determination of the resonance frequency are small compared with the errors in the determination of the band widths. The standard error, $V(\Delta\nu)$, of a predicted value of $\Delta\nu$ corresponding to a given value ν_1 may be calculated from the following expression (Davies [6], p. 131):

$$V(\Delta\nu) = s^2\left(\frac{1}{n} + \frac{(\nu_1 - \bar{\nu})^2}{\Sigma(\nu - \bar{\nu})^2}\right),$$

where s^2 = variance around the regression line, n = number of observations, and $\bar{\nu}$ = mean value of ν. For the values in Table II, $s^2 = 0.230$ and $n = 22$.

The values of $V(\Delta\nu)$ have been calculated for three values of the resonance frequency, ν, and are

TABLE III. Experimentally Determined Band Widths at Different Resonance Frequencies for Viscose Fibers of Circular Cross Section

Fiber	Resonance frequency ν_0	Band width $\Delta\nu_0$	Resonance frequency ν_0	Band width $\Delta\nu_0$	Resonance frequency ν_0	Band width $\Delta\nu_0$
		7.8		8.3		12.8
1	27.5	8.2	42.1	8.1	126.5	13.1
		7.3		7.5		13.8
		7.0		7.5		11.5
2	27.0	7.0	41.8	7.8	132.1	11.4
		7.6		7.8		12.5
		7.2		7.5		13.7
3	26.3	7.9	41.2	8.0	129.9	13.4
		7.4		7.9		14.6
		7.6		8.2		13.0
4	27.0	7.0	43.2	8.9	127.9	12.1
		6.5		8.5		12.6
		7.6		9.5		13.9
5	26.8	6.7	41.8	9.4	127.1	13.6
		7.2		9.5		12.9
		7.8		10.4		13.5
6	26.4	8.2	44.0	10.6	132.8	14.6
		8.0		10.6		13.9
Mean value	26.83	7.44	42.35	8.67	129.4	13.16

TABLE IV

Source of variance	Sums of squares	Degrees of freedom	Mean squares
Between frequencies	3 2 6 2 4	2	16312***
Between fibers	1 9 3 3	5	366.5
Interaction	1 2 4 5	10	124.5***
Between groups of 3	3 5 8 0 2	17	2106
Within groups of 3 = residual = experimental error	6 4 3	36	17.9
Total	3 6 4 4 5	53	

TABLE V

Resonance frequency	Source of variance	Sums of squares	Degrees of freedom	Mean squares
26.8	Between groups of 3	216.5	5	43.3
	Within groups of 3	200	12	16.7
	Total	416.5	17	
	Within frequencies			
42.4	Between groups of 3	2961	10	296.1***
129.4	Within groups of 3	443	24	18.5
	Total	3404	34	

given in Table VI together with the confidence limits for $\Delta\nu$ calculated with Student's t-test ($P = 0.95$).

In order to determine the influence of air damping, circular viscose fibers of smaller diameter, $d = 40\mu$, were used. (The production of these fibers is described in Part III.) In order to obtain the highest possible accuracy, the whole frequency-amplitude curve was determined. The measurements were performed at three different resonance frequencies—roughly 25, 40, and 130 c.p.s.—on the same fiber. The experiments were begun at the lowest resonance frequency, after which the fiber length was decreased by cutting down the free end until the next desired value of the resonance frequency was obtained. Three amplitude-frequency curves were taken at each resonance frequency. Six fibers were examined, which means that 54 frequency curves in all were determined. It is important that straight fibers be used for measurements of band width. If the fiber is curved, it usually does not vibrate in one plane at resonance, but turns round its length axis, and too high values of the band widths are obtained. The fibers were therefore wetted and straightened by loading with a small weight (0.2 g.) for 10 min. at 65% R.H. They were then conditioned from the dry state at 65% R.H.

During the tests the amplitude was kept constant at about four times the fiber diameter. This was the smallest possible amplitude that could be used in order to keep the reading errors small. At very large amplitudes (10 to 20 times the diameter) the band width increased about 30%. This increase may be dependent upon an increase of internal damping.

The results are given in Table III, and Figure 4 shows typical amplitude-frequency diagrams.

An analysis of variance* of the data in Table III has been performed in order to calculate the confidence limits of the mean values of each frequency. The errors in the determination of the resonance frequency are small compared with the errors in determination of the band width, and they have been neglected to simplify the calculations. The analysis of variance is given in Appendix 2.

* The results of the analysis are given in Tables IV and V.

TABLE VI. EXPERIMENTALLY DETERMINED VALUES OF THE BAND WIDTH

1	2	3	4	5	6	7
Resonance frequency ν_0	Total band width $\Delta\nu_{tot}$	Variance of the mean value of $\Delta\nu_{tot}$	Band width caused by internal damping $\Delta\nu_i$	Variance of $\Delta\nu_i$	$\Delta\nu_{tot} - \Delta\nu_i$ (2 − 4)	Variance of $(\Delta\nu_{tot} - \Delta\nu_i)$ (3 + 5)
26.8	7.44 ± 0.40	0.02405	0.77 ± 0.33	0.0254	6.67 ± 0.57	0.0495
42.4	8.67 ± 0.90	0.1645	1.25 ± 0.30	0.0206	7.42 ± 0.96	0.1851
129.4	13.16 ± 0.90	0.1645	3.95 ± 0.22	0.0112	9.21 ± 0.93	0.1757

TABLE VII. INFLUENCE OF THE AIR DAMPING ACCORDING TO EXPERIMENTS AND ACCORDING TO CALCULATIONS

Resonance frequency ν_0	$\Delta\nu_{max}$	$\Delta\nu_{min}$	$\frac{(\Delta\nu_{max})^2}{2\nu_0^2} \times 100$	$\frac{(\Delta\nu_{min})^2}{2\nu_0^2} \times 100$	Calculated value of $\varphi^2 \times 100$ (according to Stokes) 1	2
26.8	7.44 ± 0.40	6.67 ± 0.57	3.85 ± 0.41	3.10 ± 0.53	2.69	(9.05)
42.4	8.67 ± 0.90	7.42 ± 0.96	2.09 ± 0.44	1.53 ± 0.40	1.24	(6.04)
129.4	13.2 ± 0.90	9.21 ± 0.93	0.52 ± 0.07	0.25 ± 0.05	0.20	(2.69)

The experimentally determined results are summarized in Table VI together with the confidence limits of the mean values.

That part of the band width which is produced by internal damping was calculated from the equation of the regression line,

$$\Delta\nu = 0.0310\nu - 0.06 \text{ (column 4, Table VI).}$$

Further, these band widths were subtracted from the experimentally determined ones, and the differences, representing the influence of air damping only, are given in column 6. The variances of these values were obtained by adding the variances in columns 3 and 5. The calculated quantity $\varphi^2 \times 100$ and the experimentally determined quantity $\frac{\Delta\nu^2}{2\nu^2} \times 100$ are both expressions for the influence of air damping on the bending modulus. The values of these quantities are given in Table VII together with the values of the band widths. The latter are denoted by $\Delta\nu_{max}$ when internal damping is not taken into account, and by $\Delta\nu_{min}$ when correction has been made for internal damping.

Further, the values indicating the influence of air damping were calculated with equation (10*a*) presumed valid instead of equation (11). These values appear in the last column of Table VII within brackets. For reasons presented earlier, equation (11) corresponds more closely to the experimental conditions than equation (10*a*). The continuous curve in Figure 5 represents the theoretical influence of air damping on the bending modulus calculated as described. The dots represent values of $\frac{(\Delta\nu_{min})^2}{2\nu^2} \times 100$ obtained from Table VII. Despite the difficulties encountered in the theoretical calculation of air damping, the experimental agreement obtained must be considered more than satisfactory.

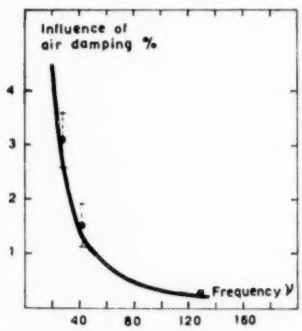

FIG. 5. *The curve represents the theoretical influence of the air damping on the resonance frequency as a function of this frequency. The dots represent experimentally determined points.*

PART II: EXPERIMENTAL PROCEDURE

In deriving the equations in Part I, the bending stiffness was assumed to be constant along the fiber. If this assumption is valid, the bending stiffness of any reasonably straight fiber can be determined by the resonance frequency method. A numerical value of the bending modulus, how-

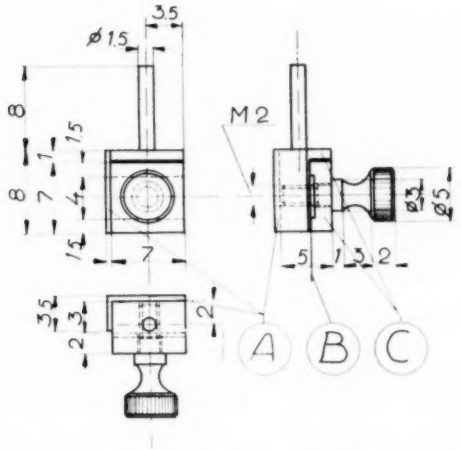

FIG. 6. *The fiber clamp used for the investigation. A—Soft iron plate. B—Fiber. C—Clamp, made of Perspex. The screw is made of brass.*

ever, can be obtained only if the moment of inertia is known. This means that the cross section of the fiber must have a simple geometric shape. This limitation is, however, common to all methods of measuring bending moduli. Model filaments of viscose rayon are especially suitable, as they can be manufactured with an almost perfectly circular cross section. Cuprammonium rayon, nylon filaments, human hair, and coarse wool having little crimp can also be used.

For calculation of the bending modulus the following quantities must be determined: the resonance frequency, the length and radius (or semiaxis for elliptical cross section), and the density of the fiber.

Mounting the Fiber

The stress in a bent fiber rigidly clamped at one end with the other end free is a maximum at the point where the fiber emerges from the clamp. The cross section, therefore, must not be distorted at this point. Different types of clamps and adhesives have been tried Figure 6 shows the type of clamp found most suitable for the experiments. If it is made of Perspex, no distortion of the fiber occurs. A distortion is obtained, however, if stainless steel is used. This can be checked by measuring the diameter of the fiber under a microscope in two perpendicular directions at the point where it emerges from the clamp.

Further, it is necessary to have a well-defined fiber length. The fiber length plotted against $1/\sqrt{\nu}$ (where ν = resonance frequency) should produce a straight line which passes through the origin if perfect mounting is achieved. With the Perspex clamp, according to Figure 6, straight lines passing through the origin were obtained for all cases tested (see Figures 9, 12, and 13). Picien wax was also tried, with good results. But since the Perspex clamps are more convenient, they were preferred in this investigation.

Excitation of the Fiber

The A.C. voltage from a frequency generator is transformed into mechanical vibrations which are then used to excite the fiber to resonance.

The following methods of excitation have been tried: (*a*) A small rod of aluminum was fastened to the membrane of a headphone, so that it was perpendicular to it. The clamp with the fiber was screwed to this rod, while the headphone was coupled to the frequency generator. Measurements within the range of the resonance frequencies of the mechanical system could not be obtained, however. (*b*) The frequency generator was connected to a loud-speaker. The vibrations of the membrane were then transmitted to the fiber through the air. (Methods (*a*) and (*b*) have both been used on the same fiber; in each case the same value of the resonance frequency was obtained.) (*c*) By connecting an electromagnetic pickup to a frequency generator, an alternating magnetic field is obtained which can be employed as a means of making the clamp vibrate. This can be done by fastening a thin plate of soft iron to the clamp. The fiber may be made to vibrate in two perpendicular directions if two iron plates are used, one being fastened to the back and the other to the side of the clamp (see Figure 6). Thus, with this technique the clamp and the pickup are never brought into contact. It should be noticed that the pickup in this case is used to generate vibrations.

The vibrations of the clamp have been analyzed with a cathode-ray oscillograph. With method (*c*), pure sinusoidal vibrations without harmonics were obtained. This was not the case when methods (*a*) and (*b*) were used. For this reason, plus the fact that it is very convenient, method (*c*) was considered to be the best.

The frequency range of interest is 20–1,000 c.p.s. The following information will serve to give the

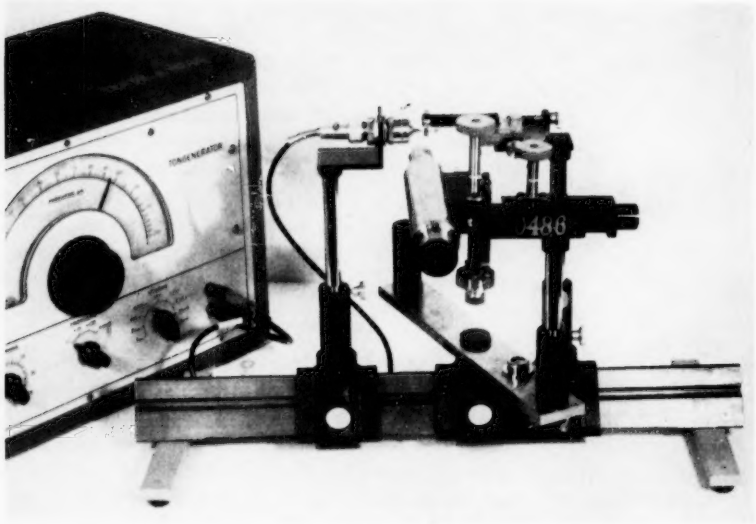

FIG. 7a. *The apparatus for measuring the bending modulus of single fibers.*

reader an idea of the order of magnitude of the various factors in question: a circular viscose fiber, diameter 40μ, has a resonance frequency of about 65 c.p.s. at a length of 1.5 cm.

The Philips magnetic pickup type GM 5527 and the frequency generator type GM 2305 were used for this investigation. The frequency generator was calibrated before each series of experiments against General Radio frequency standard (Type 1105-A) at the Research Laboratory of Electronics of Chalmers University of Technology, which in effect increased the accuracy of the results.

The reading error was approximately 0.5%. A larger scale having a longer dial indicator was made for the measurement of band widths. In this way the reading error was reduced to 0.2%–0.3%.

The free end of the fiber was observed through a microscope of low magnification (2.5 × 10). The microscope was equipped with an ocular scale which facilitated the measurement of resonance frequencies and made the measurement of band widths possible. Figure 7a shows a photograph of the apparatus, and Figure 7b illustrates its essential parts. The microscope is mounted so that it can be moved in three directions by means of adjustment screws.

Determination of Fiber Length and Fiber Diameter

The fiber is held vertically during the determination of the resonance frequency (see Figures 7a and 7b). The length of the fiber is measured by moving the microscope vertically, starting from the point where the fiber emerges from the clamp, until the free end of the fiber coincides with an index on the ocular scale. The fiber is kept vertical during this measurement by means of a small tong-shaped clamp (weight 0.2 g.). The lower end of the fiber protrudes from this small clamp (see Figure 8).

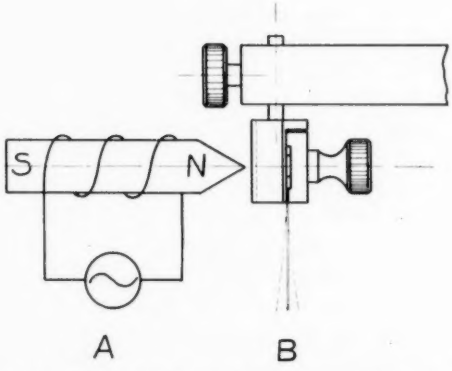

FIG. 7b. *Principal parts of the apparatus shown in Figure 7a:* A, *electromagnetic vibration pickup;* B, *Perspex clamp with fiber.*

The vertical movement of the microscope can be measured with an accuracy of 0.005 mm. By plotting the fiber length against $1/\sqrt{\nu}$, the deviations from straight lines obtained can be used in controlling the accuracy of the measurements of

FIG. 8. *Arrangement for measurement of fiber length.*

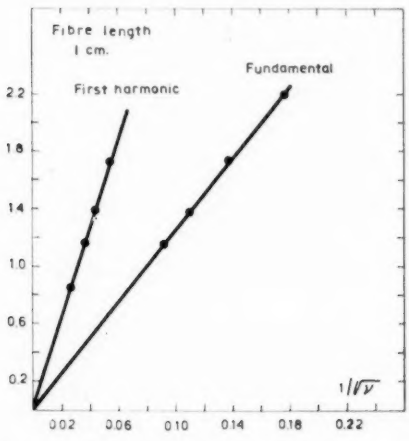

FIG. 9. *The fiber length as a function of $l/\sqrt{\nu}$ for a circular viscose fiber.*

fiber length. Figure 9 illustrates this, and shows that the measuring accuracy is satisfactory.

A special device was constructed for determination of the cross section of the fiber (see Figure 10). The clamp, holding the fiber, was fastened to a rotatory axis, and the free end of the fiber was threaded through a hole. The fiber could thus be rotated while being viewed under a microscope and the diameter measured with an ocular scale. Fibers with circular and elliptical cross sections were measured at ten points along their longitudinal axis, after which the fibers were rotated 90° and the measurements repeated. (Magnification 35 × 5 was used.)

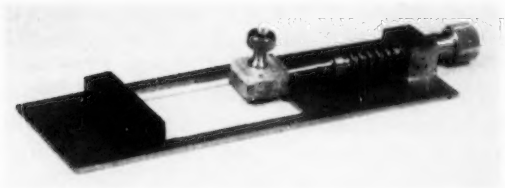

FIG. 10. *The device for the measurement of fiber cross section.*

Determination of the Bending Modulus of Steel and Some Textile Fibers

In the vibration experiments the stress is proportional to the amplitude and varies along the fiber length. The largest stress is obtained at the point where the fiber emerges from the clamp.

At not too large amplitudes, the stresses are small. In viscose fibers ($d = 40\mu$) the maximum stress is about 5 kg./cm.^{2} for an amplitude of 4 times the fiber diameter. This corresponds to a total load of about 0.06 g.

The resonance frequency of the fundamental mode of vibration, or sometimes the first harmonic, was used in the calculation of the bending modulus. The first harmonic and the fundamental gave the same value of the bending modulus for viscose fibers (see Table VIII). This means that the modulus is independent of the frequency above 30 c.p.s. When human hair was used, the agreement was not as good, probably due to the irregularity of its shape.

Comparison of the Results Obtained by Bending and Stretching Experiments on the Same Steel Filaments

In order to verify equation (16) (Part I) experimentally, thin filaments of steel were used. The elastic properties of steel should be independent of time factors, since steel behaves as an ideal elastic body below the yield point. Dynamic and static methods, therefore, should produce the same results. Further, bending and stretching experiments should also give the same value of the Young's modulus. The latter can be determined very accurately by static stretching methods, and this value can be used as a standard of comparison for the dynamic bending experiments.

A conventional extensometer was used in the stretching experiments, and the bending experiments were performed with the method described

above. Values of Young's modulus obtained by bending were 15% higher than those obtained by stretching.

This is probably due to the outer part of the steel filaments having a larger modulus of elasticity than the inner parts, which condition is brought about in the manufacturing of the filaments. In order to minimize this condition, a piece of the steel filament was heated at 600°C for several hours, and then allowed to cool slowly over a period of 24 hrs. Later the filament was mechanically conditioned—*i.e.*, loaded and unloaded with small loads until a constant value of the modulus of elasticity was obtained by stretching. In this manner a value of $E = 1.94 \times 10^{12}$ dynes/cm.^{2} was obtained (see Figure 11).

The bending modulus was determined with the same piece of filament that was used for the stretching experiments. The resonance frequencies of the fundamental in two mutually perpendicular directions were 109.7 and 110.2, respectively, for a fiber length of 2.577 cm. and diameter of 101μ (the band width was less than 1 c.p.s.). The density as determined was 7.62. These values when inserted in equation (6) result in an E value of 2.04×10^{12} dynes/cm.^{2} Thus, values about 5% higher are obtained with the bending experiments. This is still higher than the experimental error. The agreement, however, must be considered as satisfactory.

The steel filaments used contained 18% chromium, 8% nickel, and 0.06%–0.07% carbon.

The Accuracy of the Method

The accuracy of the method is determined for the most part by the properties of the fibers investigated. Important are the approximations which must be made regarding the shape of the cross section, together with the fact that the cross section very often varies along the fiber. If the behavior of the material conforms exactly with the assumptions made, the method is extremely accurate.

The circular viscose fibers show the best agreement with the assumptions made, as seen from the very low dispersion of the points in Figure 9.

Some examples of the applicability of the method are given below. All measurements were made at 65% R.H. (conditioned from the dry state) and 20°C.

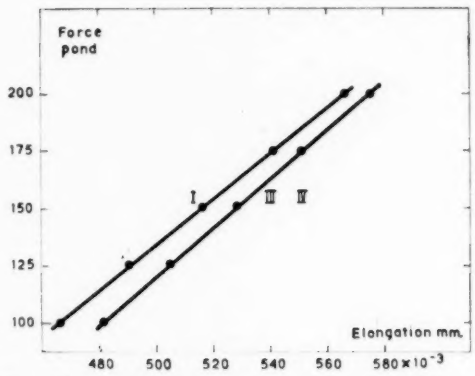

FIG. 11. *Load-elongation curves for steel filaments. Curve I represents the first loading. Curves III and IV represent the third and fourth loadings.*

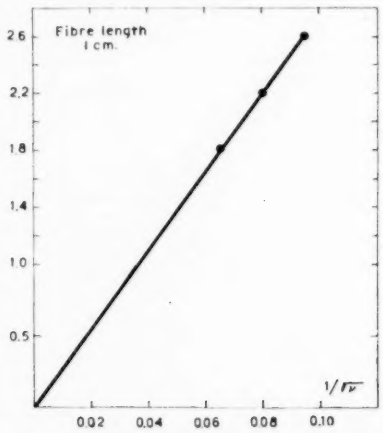

FIG. 12. *The fiber length as a function of $1/\sqrt{\nu}$ for a nylon fiber.*

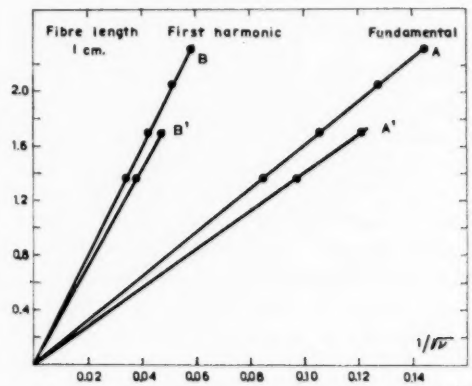

FIG. 13. *The fiber length as a function of $1/\sqrt{\nu}$ for human hair. A and A' and B and B' represent two perpendicular directions of vibration.*

Nylon Fibers

Cold-drawn nylon filaments with a diameter of 45μ were used. Figure 12 shows the fiber length plotted against $1/\sqrt{\nu}$ for one fiber. With the help of equation (16) the bending modulus was calculated from the mean value of the resonance frequencies of the first harmonic measured in two perpendicular directions. The mean value of the bending modulus of three fibers was 4.04×10^{10} dynes/cm.^{2}, with a range of 0.2×10^{10} dynes/cm.^{2} (The range is the difference between the highest and lowest values obtained.) The low dispersion of the values was due to the regularity and uniformity of the cross section of the fibers along their length.

Human Hair

Nonmedullated, blond hairs of a 4-year-old child were used. The axes of the elliptical cross section were measured with the arrangement described previously. The ratio between the major and minor axes varied between 1.3–1.6 for different hairs. In Figure 13 the fiber length is plotted against $1/\sqrt{\nu}$ for the fundamental and first harmonic. The fiber was caused to vibrate in two perpendicular directions, producing two different values of the resonance frequency. The ratio between these values is equal to the ratio between the axes of the ellipse.

The clamp with the fiber was rotated about the longitudinal axis of the fiber, and the resonance frequency was measured for each rotation of 30°. Only two values of the resonance frequency were obtained, representing vibrations around the principal axis of inertia.

Due to the irregular shape of the hair, the dispersion of the bending moduli values is rather high. The mean value of the bending modulus obtained from the fundamental mode of vibration is 4.9×10^{10} dynes/cm.^{2}, with a range of 1.8×10^{10} dynes/cm.^{2}

Wool Fibers

Wool fibers are generally unsuitable for vibration experiments because of their crimp and the spiraling of the plane containing the major axis along the fiber, which often exists.

Some experiments, however, have been made on coarse, straight Lincoln wool not having a medulla (diameter about 55μ). By plotting the fiber length against $1/\sqrt{\nu}$, straight lines through the origin were obtained with these fibers, also. The mean value of the bending modulus obtained for three fibers was 6.16×10^{10} dynes/cm.^{2}, with a range of 0.70×10^{10} dynes/cm.^{2} Again the fundamental mode of vibration was used.

PART III: COMPARISON OF VALUES OF YOUNG'S MODULUS OF VISCOSE RAYON OBTAINED BY BENDING AND BY STRETCHING

Circular viscose fibers were manufactured according to the method recommended by Hermans [8]. The viscose was first spun in a bath containing only ammonium sulfate (sp. gr. 1.08). If desired, the fibers may be stretched in the xanthate state, and then the cellulose regenerated in dilute sulfuric acid. The free sulfur formed is solved in the usual manner, and the fibers are washed and dried.

The thick fibers (d = 120–540μ) that were used to determine internal damping were spun through glass capillaries, using the method described by Hermans. The finer fibers (d = 40μ) were made by a viscose plant. A spinning machine for laboratory purpose was used, the fibers being spun through a spinneret having 18 holes.* In Figure 14 are shown photomicrographs of cross sections of these fibers. The fibers are almost perfectly cir-

* The authors are indebted to AB Svenskt Konstsilke, Borås, Sweden, and the head of their laboratory, Mr. P. O. Törnkvist, for the manufacturing of these fibers.

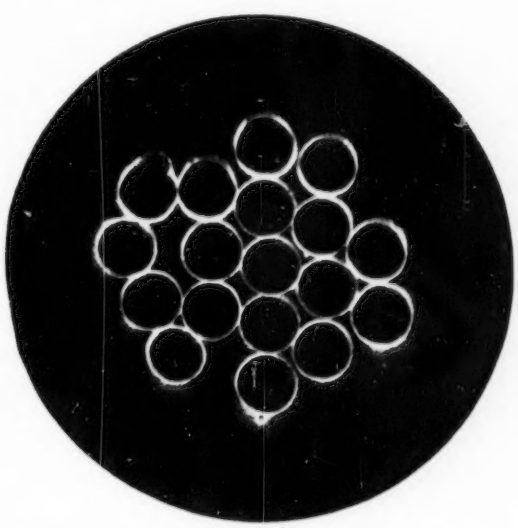

FIG. 14. *Photomicrographs of the cross sections of viscose fibers (diameter about 40μ).*

TABLE VIII. DETERMINATION OF THE MODULUS OF ELASTICITY BY BENDING FOR VISCOSE FIBERS

Fiber	Resonance frequency ν_o (fundamental)	Resonance frequency ν_o (fundamental in perpendicular direction)	Band width $\Delta\nu$	Resonance frequency ν_1 (first harmonic)	Fiber length (cm.)	Fiber diameter (μ)	Modulus of elasticity E_o (dynes/cm.^{2}) (from fundamental)	Modulus of elasticity E_1 (dynes/cm.^{2}) (from first harmonic)
1	65.5	60.3	13	390	1.545	40.6	1.08×10^{11}	1.05×10^{11}
2	48.6	48.1	10	307	1.732	40.2	1.03	1.02
3	39.7	39.7	10	258	1.912	40.9	1.01	1.05
4	58.5	57.1	10	360	1.638	41.5	1.10	1.07
5	49.5	53.3	10	324	1.701	40.6	1.06	1.05
				Mean value		40.8	1.06×10^{11}	1.05×10^{11}

cular. This conforms with the results obtained from measurements of diameter and resonance frequencies in two perpendicular directions.

Young's moduli of five fibers were determined by bending with the method described above. The moduli determined by stretching were then measured on the same fibers using a dynamic method. The fibers were thereby subjected to longitudinal vibrations. The latter experiments were performed in cooperation with Dr. Andersen at the Danish Institute for Textile Research in Copenhagen, Denmark, using the apparatus constructed and described by Asmussen and Andersen [1]. All measurements were performed at 65% R.H. (conditioned from the wet state) and 20°C.

Measurement of Young's Modulus by Bending

The fibers were extracted with alcohol and ether, steeped in water to relax any stresses that may have developed in the manufacture of the fibers, and then conditioned at 65% relative humidity and 20°C. The resonance frequency was measured in two perpendicular directions, the fundamental mode of vibration being determined ten times in each direction. The first harmonic was also measured, but fewer measurements were made. The diameter was measured in air by the method described in Part II. It was sometimes difficult to focus on the two edges of the fibers simultaneously. Therefore, the measurements were made at two magnifications at ten points along the fiber. As the fibers were almost circular, the difference between the resonance frequencies in two perpendicular directions was less than the error obtained in measuring the diameter. The mean value of the resonance frequencies in the two directions and the mean value of the diameters in the same directions were therefore used. (Determination of resonance frequency in two perpendicular directions is a much more sensitive measure of deviation from circularity than a direct measurement of diameter.) The results are given in Table VIII. The modulus of elasticity was calculated from equation (16), Part I. (The value of the density $\gamma = 1.53$ was used.)

The mean variance value, Vm, of the frequencies, ν_o, of all determinations of the fundamental (but within ν_o) = 0.297. Vm is thus a measure of the error in ν_o. The confidence limits of ν_o are $\pm \dfrac{1.98 \times 0.297}{10} = \pm 0.34$. ($\nu_o$ is the mean value of ten determinations.)

Measurement of Young's Modulus by Stretching

The apparatus described by Asmussen and Andersen for measurement of the elastic properties of fibers can be used in both static and dynamic experiments. In this case the dynamic method is of interest. The fiber is subjected to free, damped, longitudinal vibrations that are recorded on a photographic film with the aid of an electronic apparatus. The dynamic stiffness of the fiber, S, can be calculated from the following equation (Asmussen and Andersen, p. 13):

$$S = \frac{4\pi^2 m_o}{T^2} - S_o,$$

where T = time of vibration for system with fiber, m_o = mass, and S_o = stiffness of the free system (without fiber). m_o and S_o are obtained from the following relationships:

$$m_o = m_1 \cdot \frac{T_o^2}{T_1^2 - T_o^2},$$

TABLE IX. The Dynamic Stiffness of Viscose Fibers as a Function of the Load

1		2		3		4		5	
Load mA*	Stiffness $S \times 10^{-4}$ (dynes/cm.)	Load mA*	Stiffness $S \times 10^{-4}$ (dynes/cm.)	Load mA*	Stiffness $S \times 10^{-4}$ (dynes/cm.)	Load mA*	Stiffness $S \times 10^{-4}$ (dynes/cm.)	Load mA*	Stiffness $S \times 10^{-4}$ (dynes/cm.)
5.0	53.5	5.0	34.3	5.0	45.0	5.0	41.1	5.0	45.5
10.1	82.9	10.0	78.5	10.0	78.4	10.0	80.2	10.0	74.3
15.0	96.6	15.1	96.8	15.0	94.7	14.7	98.0	15.2	94.0
20.0	102.0	20.0	105.8	20.5	104.3	20.2	110.6	20.2	101.1
25.1	107.3	25.1	108.7			25.5	115.2	25.4	104.3
20.0	102.4	20.0	107.1			20.2	112.2	20.2	101.7
15.1	100.7	15.1	102.0			15.2	107.3	15.2	95.7
10.1	90.6	10.1	92.5			10.0	92.9	10.0	85.0
5.0	59.9	5.0	83.9			5.0	58.6	5.0	59.3
5.0	53.5	5.0	61.7	5.0	48.4	5.0	54.9	5.0	56.7
10.0	87.6	10.1	89.2	10.0	79.3	10.0	89.3	10.0	82.7
15.0	97.9	15.0	101.3	15.1	99.8	15.2	108.2	15.2	96.5
20.0	107.6	20.0	108.0	20.0	102.2	20.2	110.9	20.2	101.1
25.0	108.0	25.1	109.0	25.1	106.4	25.1	121.0	25.5	103.7
l = 1.072 cm. m_o = 6.87 g. S_o = 8.72×10^4 dynes/cm.		l = 1.121 cm. m_o = 6.91 g. S_o = 8.73×10^4 dynes/cm.		l = 1.138 cm. m_o = 6.83 g. S_o = 8.57×10^4 dynes/cm.		l = 1.138 cm. m_o = 6.88 g. S_o = 8.80×10^4 dynes/cm.		l = 1.121 cm. m_o = 6.73 g. S_o = 8.67×10^4 dynes/cm.	

* $1mA$ = 52 dynes.

$$S_o = \frac{4\pi^2 m_1}{T_1^2 - T_o^2},$$

where T_o = time of vibration of the free system and T_1 = time of vibration of the free system loaded with the mass m_1.

The fiber, however, must have a certain degree of static stress before it can be given an impulse that will cause it to vibrate longitudinally. If this is not done the fiber will slacken during parts of the vibration cycle, and the state of the system is then undefined.

Thus, it is necessary to maintain larger stresses in the fiber for stretching measurements than for bending measurements.

In the stretching experiments the fiber was first loaded stepwise, then unloaded, and finally loaded again. After each loading and unloading the consolidated value of the stress was obtained, after which the system was made to vibrate by means of a current impulse. Since the photographic film moves with a constant known velocity, the time of vibration, T, can be calculated from the

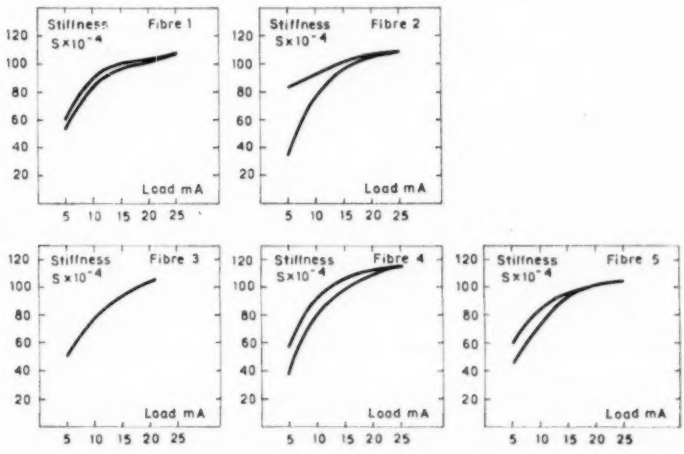

Fig. 15. *The dynamic stiffness of viscose fibers as a function of the load.*

TABLE X. YOUNG'S MODULUS BY BENDING AND BY STRETCHING ON THE SAME VISCOSE FIBERS

Fiber	$E_{bending} \times 10^{-11}$ (dynes/cm.²)	$E_{stretching} \times 10^{-11}$ (dynes/cm.²) at a load of: 0.27 g.	0.53 g.	0.80 g.	Frequency at: Bending (c.p.s.)	Stretching (c.p.s.) 0.27 g.	0.53 g.	0.80 g.
1	1.08	0.44	0.69	0.81	63	48	58	63
2	1.03	0.30	0.69	0.85	48	40	56	62
3	1.01	0.39	0.68	0.82	40	45	57	62
4	1.10	0.35	0.69	0.84	58	43	57	63
5	1.06	0.39	0.64	0.82	51	45	56	62
Mean value	1.06 ± 0.05	0.37 ± 0.06	0.68 ± 0.03	0.83 ± 0.02				

recorded vibrations. The vibration times, T_0 and T_1, for the free system without fiber, unloaded and loaded with the mass m_1, were recorded on the same film after the loading cycles were completed on the fiber. For control two different masses were used. Table IX gives the values of the dynamic stiffness for different tensile forces. The time of vibration, as determined, is the mean value of at least three impulses. The stiffness increases with increasing tensile stress in the fiber, and is generally higher in the second loading cycle (Figure 15).

The modulus of elasticity is obtained from the stiffness by means of the following equation: $E = Sl/A$, where l and A are the length and the cross section of the fiber, respectively. The values of the stiffness, S, are thus only comparable for the same fiber length and cross section.

The values of the modulus of elasticity, $E_{stretching}$, calculated from the first loading cycle are listed in Table X, together with the bending modulus, $E_{bending}$, from Table VIII.

As can be seen from Table X, the modulus of elasticity by bending is higher than that by stretching. In the bending experiments the fibers were loaded with less than 0.1 g. For reasons given above it is not possible to perform the stretching experiments with such small loads. Even for loads of 0.27 g. (5 *mA*) the stresses may have been released by the longitudinal vibrations. The comparison is therefore made with the values obtained for a tensile force of 0.53 g., which shows $E_{bending} > 1.55 \times E_{stretching}$.

It should be pointed out, however, that a comparison using the modulus by stretching for a lower value of the tensile stress will indicate an even higher ratio of the modulus by bending to that by stretching. The experiments were performed at about the same frequency.

Discussion

The higher values obtained for the bending modulus may be explained in the following ways: In the stretching experiments a mean value of the elastic properties is obtained throughout the cross section of the fiber. The bending experiments, however, give mean values, where the outer parts of the fibers play a more important role than the inner parts. According to this explanation, the outer parts of the viscose fibers investigated have a higher modulus of elasticity than the inner parts. This condition is rather usual for materials other than textile fibers (*e.g.*, the experiments with the steel filaments in Part II).

A bent fiber, however, is subjected to both tensile and compressive forces. The modulus of elasticity may have different values on the compression and elongation sides of the stress-strain diagram. As the stresses are small, this explanation seems less probable.

Meredith [13] stated that the modulus by bending usually is higher than by stretching. Khayatt and Chamberlain [10], however, obtained lower values of the modulus by bending than by stretching on wool and hair using the method mentioned in the Introduction.

The distribution of the inherent fiber properties throughout the cross section may vary widely along the fiber, causing a variation in the relationship between the modulus of elasticity in bending and in tension. This may especially be the case with natural fibers. However, the values of the bending modulus of the viscose fibers used for this investigation show a very low dispersion. It is thus reasonable to assume that the distribution of the elastic properties throughout the cross section is rather constant along the fiber for these fibers.

For these reasons it seems that the first explanation is the most probable.

Appendix 1

Equation (14), $\Delta\nu = \frac{r}{2\pi m}$, can be derived as follows:

From Courant ([5], p. 513) the following equations are obtained:

$$\phi(w) = \frac{1}{\sqrt{(k - mw^2)^2 + r^2w^2}},$$

where $\phi(w)$ is the distortion of amplitude as a function of the "exciting frequency." At resonance we have $w = w_{res}$:

$$\phi(w_{res}) = \frac{1}{r\sqrt{\frac{k}{m} - \frac{r^2}{4m^2}}}.$$

By combining these two equations:

$$\frac{\phi(w)}{\phi(w_{res})} = \frac{r\sqrt{\frac{k}{m} - \frac{r^2}{4m^2}}}{\sqrt{(k - mw^2)^2 + r^2w^2}}.$$

The band width, $\Delta\nu$, is defined as the difference between those frequencies, whose amplitudes are $1/\sqrt{2}$ times the maximum amplitude. Denoting these frequencies with w_1 and w_2, then,

$$\frac{\phi(w_{1,2})}{\phi(w_{res})} = \frac{1}{\sqrt{2}}.$$

Inserting this into the above equations gives

$$w_{1,2} = \sqrt{\frac{k}{m} - \frac{r^2}{2m^2} \pm \frac{r}{m}\sqrt{\frac{k}{m} - \frac{r^2}{4m^2}}}.$$

$(w_1 + w_2)/2$ is approximately equal to w_{res}:

$$w_{res} = \sqrt{\frac{k}{m} - \frac{r^2}{2m^2}}.$$

This assumes that w_1 and w_2 are symmetric about the resonance frequency, which is only valid at small values of r. Consequently,

$$w_{1,2} = \sqrt{w^2_{res} \pm \frac{r}{m}\sqrt{\frac{k}{m} - \frac{r^2}{4m^2}}};$$

$$w_1 - w_2 = \sqrt{w^2_{res} + \frac{r}{m}\sqrt{\frac{k}{m} - \frac{r^2}{4m^2}}} - \sqrt{w^2_{res} - \frac{r}{m}\sqrt{\frac{k}{m} - \frac{r^2}{4m^2}}}.$$

If we use the expression

$$w_{res}(w_1 - w_2) \cong \frac{(w_1 + w_2)}{2}(w_1 - w_2) = \frac{w_1^2 - w_2^2}{2},$$

we obtain

$$w_{res}(w_1 - w_2) = w_{res} \cdot 2\pi\Delta\nu \cong \frac{r}{m}\sqrt{\frac{k}{m} - \frac{r^2}{4m^2}}.$$

But

$$\sqrt{\frac{k}{m} - \frac{r^2}{4m^2}} = w_o,$$

where w_o = the natural frequency of the free system (without forced vibrations). At small values of r,

$$w_o \cong w_{res},$$

which gives

$$2\pi\Delta\nu = \frac{r}{m},$$

or

$$\Delta\nu = \frac{r}{2\pi m}.$$

Appendix 2

Table IV gives the results of an analysis of variance made on Table III.

The interaction is highly significant. The mean square values of between frequencies and between fibers are compared with the interaction, and the first of these mean square values is highly significant (at the 0.1% level) while the other is not.

Because of the significant interaction, only two sources of variance are considered—namely, between frequencies and within frequencies. The latter variance can be divided into between groups of 3 and within groups of 3 for the whole table.

An investigation shows, however, that the variance between groups of 3 is significantly greater at the frequencies 42.4 and 129.4 than at the frequency 26.8. The last group is therefore treated separately. The analysis is given in Table V.

The confidence limits of the mean values of the six fibers at each frequency have been calculated from the between groups of 3 mean squares.

The variance of the mean value $\Delta\nu = 7.44$ at the frequency 26.8 is thus $\frac{43.3}{3 \times 6} \times 10^{-2} = 0.0245$.

The confidence limits are then $\pm 2.57 \times 0.0245 = \pm 0.40$. For the other two frequencies the limits ± 0.90 are obtained.

Summary

The fundamental equations for the determination of the bending modulus using the resonance frequency method are treated in Part I. The influence of the air damping on the resonance frequency has been calculated with help of equations deduced by Stokes. The calculations have been experimentally verified for circular viscose fibers of different diameters by the measurement of band widths. The influence of the air damping decreases with increasing fiber diameter and increasing resonance frequency. For viscose fibers this influence is less than 1% at a fiber diameter $\geq 23\mu$ and a resonance frequency ≥ 100 c.p.s.

In Part II a description of the apparatus and experimental procedure is given. Different ways of clamping and exciting the fiber are discussed. Young's moduli determined by bending and by stretching have been determined for steel filaments. The bending moduli for nylon fibers, human hair, and coarse wool fibers are given.

A comparison between Young's modulus determined by bending and by stretching has been made on the same viscose rayon fibers. Dynamic methods have been used for both bending and stretching. The experiments are described in Part III. The value of the modulus by bending is at least 1.5 times higher than the modulus by stretching. The reason for this is discussed.

Acknowledgment

The authors wish to thank Mr. B. Stjernberg and Mr. B. Jiewertz for their advice regarding the design and calibration of the apparatus. They are indebted to Prof. R. W. Asmussen and Dr. F. Andersen for putting at their disposal apparatus for the measurement of the dynamic stretching properties of single fibers. They also wish to express deep gratitude to the head of the Institute, Prof. Nils Gralén, for his never-failing interest in this investigation and for many helpful suggestions.

Literature Cited

1. Asmussen, R. W., and Andersen, F., *Trans. Danish Acad. Tech. Sci.* No. 5 (1947); Andersen, F., *Trans. Danish Acad. Tech. Sci.* No. 3 (1950).
2. Ballou, J. W., and Silverman, S., TEXTILE RESEARCH **14**, 282 (1944); *J. Acoust. Soc. Am.* **16**, 113 (1944).
3. Carlene, P. W., *J. Textile Inst.* **38**, T38 (1947).
4. Carlene, P. W., *J. Textile Inst.* **41**, T159 (1950).
5. Courant, R., "Differential and Integral Calculus," London and Glasgow, Blackie & Sons Ltd., 1934, p. 512.
6. Davies, O. L., "Statistical Methods in Research and Production," London, Oliver and Boyd, 1947.
7. Hermanne, L., TEXTILE RESEARCH JOURNAL **19**, 61 (1949).
8. Hermans, P. H., "Physics and Chemistry of Cellulose Fibers," New York, Elsevier Publishing Co., 1949; Hermans, P. H., and de Leeuw, A. J., *Kolloid-Z.* **81**, 300 (1937).
9. Ising, G., "Undersökning rörande elektrometrar," Lund, Sweden, Glecrupska Universitets bokhandeln, 1919, Part II, pp. 281–3.
10. Khayatt, R. M., and Chamberlain, N. H., *J. Textile Inst.* **39**, T185 (1948).
11. Lochner, J. P. A., *J. Textile Inst.* **40**, T220 (1949).
12. Lord Rayleigh, *Phil. Mag.* **21**, 697 (1911); Faxén, O. H., Nionde Skandinaviska Matematikerkongressen, "Hydrodynamiska moståndsformler," Helsinki, Finland, Mercators trycheri, 1938, p. 165.
13. Meredith, R., *J. Textile Inst.* **37**, P475 (1946).
14. Meyer, K. H., and Lothmar, W., *Helv. Chim. Acta* **19**, 68 (1936).
15. Müller, F. H., *Kolloid-Z.* **113**, 53 (1949).
16. Nolle, A. W., *J. Applied Phys.* **19**, 753 (1948); *J. Polymer Sci.* **5**, 1 (1950).
17. Oberbeck, A., *Crelles J.* **81**, 62 (1876).
18. Sen, K. R., *J. Textile Inst.* **39**, T339 (1948).
19. Stokes, G. G., "Mathematical and Physical Papers," Cambridge, University Press, 1901.
20. Timoshenko, S., "Vibration Problems in Engineering," New York, D. Van Nostrand Co., 1928.

(Manuscript received December 4, 1952.)

Relationship Between Various Surface Properties of Wool Fibers

Part II: Frictional Properties*

Joel Lindberg†

Institute for Applied Textile Research, Gothenburg, Sweden

Abstract

Wool fibers were treated with alcoholic potash for different periods of time. The anti-scale and with-scale coefficients of friction were measured by means of a modified fiber twist friction meter. The with-scale friction increases with time of treatment, and this is explained in terms of a chemical modification of the epicuticle. There is a close relationship between friction and breaking strength of top and between friction and felting rate.

Introduction

It has been shown that wool fibers and other animal fibers have the lowest friction of all types of fibers [7, 14, 25], and Lindberg and Gralén have suggested that this low value might be associated with the chemical inertness of the epicuticle [16]. If wool fibers are treated with various agents for making them nonfelting, it is found that in general the with-scale coefficient of friction increases with the severeness of the treatment [15]. Mercer and Freney [20] remarked that the decreased felting power of alcoholic potash-treated wool might be explained by assuming an increase in surface friction. This was later confirmed by Mercer [18, 19] and Lindberg and Gralén [15, 17]. Their results show that both the with-scale and the anti-scale coefficients of friction increase upon treatment, and a constant difference between the two coefficients is maintained. Since the difference depends upon the average scale resistance [14] and this is unaffected by the treatment, the explanation of the increase of friction must be found in a surface modification. In order to obtain further confirmation of these experiments and to correlate frictional properties with other physicochemical properties, frictional measurements were carried out on samples pretreated according to Part I.

* Part I appeared in the February, 1953, issue of Textile Research Journal. Parts I–IV constitute a thesis for the degree of Doctor of Technology, Chalmers University of Technology.

† Director of Research.

Apparatus

Various methods for measuring friction between single fibers have been developed and described [9, 11, 21]. The fiber twist method developed by Lindberg and Gralén [14] has proved very satisfactory for wool fibers.

Two fibers are twisted around each other a certain number of turns (Figure 1). While the fibers are kept under tension, one of them is pulled through the twist, which is then distorted according to Figure 2. The force necessary to cause slippage is equal to the frictional force. Assuming Amontons'

Fig. 1. *Fiber arrangement in the twist friction meter.*

Fig. 2. *Distorted fiber twist.*

first law, $F = \mu W$, to be valid, where F is the frictional force, W is the normal load between the fibers, and μ is the coefficient of friction, the following equation can be derived

$$\mu = \frac{l \cdot \ln \frac{P_2}{P_1}}{4\pi^2 n^2 r}, \tag{1}$$

where P_2 and P_1 are the loads applied to the ends of one fiber, n is the number of turns, r is the fiber radius, and l is the length of the twist [14].

It has been shown, however, that Amontons' first law is not valid for fiber friction [22], and therefore the relation between the frictional force and the load has been derived in a different way. The frictional force, F, might be given as

$$F = P_2 - P_1. \tag{2}$$

The normal load between the fibers over a length dz is dW. The radius of curvature at some point of the twist is R_z, the arc φ and the axial load P_z:

$$R_z \cdot d\varphi_z = dz \tag{3}$$

$$dW = P_z \cdot d\varphi_z \tag{4}$$

$$dW = \frac{P_z}{R_z} \cdot dz. \tag{5}$$

P_z and R_z are both functions of z, which is the axial coordinate of the twist. It is now assumed that the ratio P_z/R_z is approximately constant along the twist (Figure 2)—that is,

$$\frac{dW}{dz} = \text{constant}.$$

The value of P_z/R_z may be obtained from the conditions at the mid-point of the twist, $z = l/2$. At this point, $P_{l/2} = (P_1 + P_2)/2$ and $R_{l/2} = l^2/(4\pi^2 n^2 r^2)$, for a helix with radius r, length $z = l$, and number of turns n. Integrating gives

$$W = \frac{2(P_1 + P_2)n^2\pi^2 r}{l}, \tag{6}$$

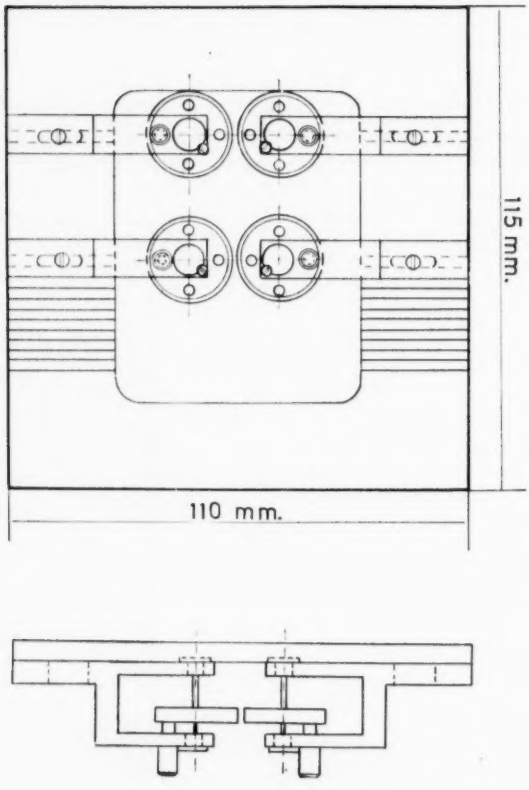

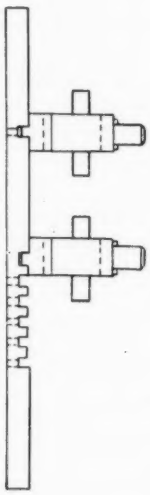

FIG. 3. *Modified twist friction meter.*

and

$$\frac{F}{W} = \frac{(P_2 - P_1) \cdot l}{2(P_2 + P_1) \cdot \pi^2 n^2 r} = \mu. \tag{7}$$

If equations (1) and (7) are compared, it is seen that

$$\frac{\mu_{(1)}}{\mu_{(7)}} = \frac{\ln (P_2/P_1)}{2(P_2 - P_1)/(P_2 + P_1)}. \tag{8}$$

If $\ln(P_2/P_1)$ is developed in series,

$$\ln \frac{P_2}{P_1} = 2 \left[\frac{P_2 - P_1}{P_2 + P_1} + \frac{1}{3} \left(\frac{P_2 - P_1}{P_2 + P_1} \right)^3 + \ldots \right] \tag{9}$$

Hence, the two equations, which are derived from different assumptions, give approximately the same value of μ.

In general, there is a difference between static and kinetic friction. If F_k, the kinetic frictional force, and F_s, the static frictional force, are known, the relative difference between F_s and F_k can be expressed by K, where

$$K = \frac{F_s - F_k}{F_k}. \tag{10}$$

The fiber twist friction meter described earlier was modified and improved [14]. The new model was equipped with four wheels mounted in sapphire bearings on a frame, as shown in Figure 3. The wheels can be arrested by small pins put into any of the four drilled holes in each wheel.

The frame is placed on the cross-head of the Instron Tensile Tester. The fibers are mounted in the apparatus by gluing the fiber ends to the wheels, as shown in Figure 4, by means of a small amount of wax (50% beeswax and 50% colophonium). The fibers are loaded by means of weights, as shown in Figure 4. One of the upper wheels is connected to the load cell in the Instron by way of a spiral spring.

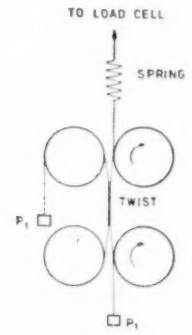

FIG. 4. *Schematic drawing of the friction meter.*

One fiber runs from the upper left wheel to the lower left wheel. The lower left wheel is arrested if the upper right wheel is attached to the load cell, and *vice versa*. The distance between the wheels can be altered both in horizontal and vertical direction to make the twist angle less than 5°.

After the fibers are mounted and three of the wheels are released, the whole frame is moved downwards at a constant speed. The load, P, on the fiber end attached to the load cell then gradually increases. The load on the other end, P_1, remains constant at the value given by the weight. If the fibers are elongated, they are wound on the wheels, and the geometrical dimensions of the fiber arrangement are maintained. Finally, $P - P_1$ attains the value of the frictional force, $F_s = P_2 - P_1$, and the fiber slips through the twist. According to Gralén and Olofsson [9] it will continue to slip until the load is $P_3 = P_2 - 2(F_s - F_k)$. Solving for F_k and replacing F_s by $P_2 - P_1$ gives

$$F_k = \frac{P_3 + P_2}{2} - P_1. \tag{11}$$

The stick-slip curve is drawn by the recorder of the Instron, and a typical example of such a curve is given in Figure 5.

Theory of Friction

Amontons' first law states that the frictional force is proportional to the load. For materials like metals and minerals this law is found to be valid. For fibrous material, however, several authors have found considerable deviations from this law [22].

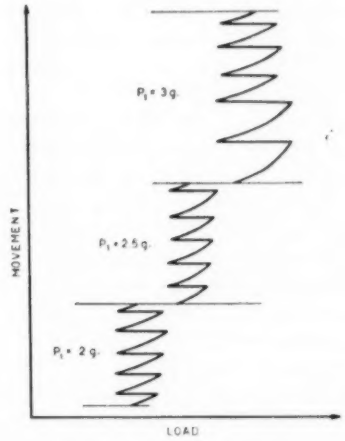

FIG. 5. *Stick-slip curve.*

Gralén and Olofsson [9], for example, give the relation between frictional force and normal load as

$$F = \mu_o W + kA, \qquad (12)$$

where F is the frictional force, W is the load, μ_o and k are constants, and A is a factor related to the area of contact. This empirical relation was also found to give a satisfactory description of the results obtained with the fiber twist method if l, the length of the twist, is substituted for A in the above equation [14].

Following the theory of Bowden and his collaborators [4] that the frictional force is proportional to the true area of contact between two bodies, Gralén *et al.* [10] derived a theoretical relationship between frictional force and normal load for the case of two parallel cylinders. Using Hertz's well-known formula for elastic deformation of two cylinders and introducing a limiting value for the maximum pressure, p_m, that the material can withstand without plastic deformation, they have, by using certain assumptions, derived the following equation:

$$F = \varphi_o(s, p_m) \cdot W + \varphi_1(s, p_m, E) \cdot rl, \qquad (13)$$

where E is the modulus of elasticity. The constant s is defined by the equation $F = sA$, where A is the true area of contact. The functions $\varphi_o(s, p_m)$ and $\varphi_1(s, p_m, E)$ have constant values for each particular type of fiber. Thus, equation (13) can be reduced to

$$F = aW + brl, \qquad (14)$$

where a and b are constants. This formula has proved to give a good description of data obtained from measurements by the fiber twist method on synthetic fibers like Terylene and nylon.

Experimental

The anti-scale and the with-scale coefficients of friction for different pairs of fibers were measured in air at 65% R.H. and in a buffer solution at pH 6 (1 part $\frac{1}{15}M$ Na_2HPO_4 + 9 parts $\frac{1}{15}M$ KH_2PO_4). One fiber was mounted with the root end up, and the other with the root end down. By switching over the weights and the spring attachment, the anti-scale and the with-scale friction could be measured at the same part of the fibers without removing them. After the measurements in air, the whole frame was immersed in the buffer solution, and after 5 min. the friction in water was determined. The weights were also immersed in water, and a correction was made for the buoyancy. The number of turns in the twist was 3.5. Five

TABLE I. ADJUSTED VALUES OF μ^* AND K FOR DIFFERENT FIBER PAIRS

Treatment	Air-dry				Buffer solution pH 6			
Untreated	μ_{2k}	μ_{1k}	K_2	K_1	μ_{2k}	μ_{1k}	K_2	K_1
	.202	.112	.13	—	.300	.133	—	—
	.187	.118	.09	—	.305	.127	—	—
	.198	.106	.11	—	.320	.132	—	—
	.194	.111	.12	—	.362	.161	—	—
	.195	.100	.08	—	.327	.126	—	—
	.270	.116	.03	—	.304	.119	—	—
	.226	.115	.06	—	.330	.116	—	—
	.213	.115	.08	—	.390	.142	—	—
					.348	.150	—	—
					.361	.145	—	—
Ether-extracted	.147	.091	.12	—	.283	.115	—	—
	.180	.107	.11	—	.333	.154	—	—
	.198	.158	.07	—	.338	.199	—	—
	.152	.086	.07	—	.345	.151	—	—
	.168	.081	.08	—	.325	.136	—	—
	.154	.091	.08	—	.305	.153	—	—
	.204	.126	.06	—	.337	.159	—	—
	.116	.088	.06	—	.327	.141	—	—
	.138	.102	.09	—	.296	.130	—	—
					.402	.212	—	—
Ether- and alcohol-extracted	.152	.111	.03	—	.296	.147	—	—
	.231	.106	.05	—	.429	.178	—	—
	.185	.085	.07	—	.334	.138	—	—
	.170	.106	.04	—	.329	.123	—	—
	.199	.147	.04	—	.348	.147	.02	—
	.190	.153	.02	—	.390	.181	.01	—
	.175	.175	.08	—	.364	.142	—	—
	.220	.147	.01	—	.357	.175	—	—
	.169	.135	.02	—	.381	.150	—	—
					.368	.134	—	—
Alcoholic potash (15 sec.)	.229	.225	.16	.24	.514	.302	.29	.48
	.176	.173	.14	—	.426	.189	.04	—
	.308	.291	.14	—	.422	.246	.08	.19
	.287	.264	.17	.11	.473	.208	.15	.16
	.181	.180	.03	—	.423	.152	.04	—
	.157	.133	.03	—	.361	.152	—	—
	.214	.227	.13	—	.419	.176	.09	.09
	.146	.175	.05	—	.394	.158	.18	.08
	.253	.188	.11	—	.470	.186	.12	.05
	.233	.143	.05	—	.426	.153	—	—
Alcoholic potash (4 min.)	.238	.161	.24	.15	.451	.228	.32	.40
	.298	.199	.17	.13	.532	.264	.26	.30
	.327	.197	.27	.14	.564	.218	.20	.25
	.313	.192	.26	.20	.534	.226	.25	.26
	.266	.226	.20	.10	.506	.269	.25	.29
	.332	.252	.21	.09	.483	.249	.27	.39
	.304	.207	.23	.14	.542	.248	.23	.32
	.249	.240	.09	.04	.533	.259	.23	.34
	.274	.170	.18	.02	.466	.241	.26	.39
					.525	.236	.24	.30
Alcoholic potash (15 min.)	.282	.210	.20	.26	.533	.295	.24	.36
	.261	.203	.24	.11	.550	.364	.31	.46
	.349	.256	.16	.17	.527	.308	.25	.30
	.261	.203	.25	.23	.526	.343	.25	.35
	.260	.200	.28	.25	.528	.303	.32	.39
	.330	.216	.27	.34	.566	.317	.23	.30
	.316	.210	.31	.33	.538	.297	.26	.32
	.243	.156	.22	.06	.515	.280	.26	.27
	.282	.186	.25	.27	.548	.299	.26	.34
	.269	.220	.22	.21	.541	.286	.29	.36

TABLE II. MEAN VALUES OF μ^* AND K FOR VARIOUS TREATMENTS

Treatment	μ_{2k}	s^2	μ_{1k}	s^2	$\mu_{2k}-\mu_{1k}$	s^2	K_2	K_1
Air-dry								
Untreated	.211	.000726	.112	.000036	.099	.000639	.088	—
Ether-extracted	.162	.000813	.103	.000607	.059	.000408	.082	—
Ether- and alcohol-extracted	.188	.000644	.129	.000837	.058	.001402	.040	—
Alcoholic potash (15 sec.)	.218	.002943	.200	.002596	.023	.001259	.101	.035
Alcoholic potash (4 min.)	.289	.001141	.205	.000914	.084	.001488	.206	.112
Alcoholic potash (15 min.)	.285	.001211	.206	.000642	.079	.000522	.240	.223
Buffer solutions pH 6								
Untreated	.335	.000889	.135	.000203	.200	.000527	—	—
Ether-extracted	.329	.001061	.155	.000889	.174	.000329	—	—
Ether- and alcohol-extracted	.360	.001341	.152	.000395	.208	.000845	.003	—
Alcoholic potash (15 sec.)	.433	.001861	.192	.002383	.241	.001165	.099	.105
Alcoholic potash (4 min.)	.514	.001310	.244	.000291	.270	.001644	.251	.324
Alcoholic potash (15 min.)	.537	.000217	.309	.000677	.228	.000645	.267	.345

* μ_{1k} = with-scale kinetic coefficient of friction; μ_{2k} = anti-scale kinetic coefficient of friction.

different values of P_1 were used on each fiber in order to determine the influence of normal load on friction—namely, 0.5, 1.0, 1.5, 2.0, and 2.5 g. The spring had a spring constant of 20 g./cm., and the downward rate of the frame was 0.2 cm./min.

A number of fibers were drawn at random from each of the pretreated samples. These fibers were first loaded with 5 g. in order to eliminate weak fibers and thus prevent breakages during the measurements. Unfortunately, this procedure introduces a bias in the sampling, but this could not be avoided with the present experimental conditions.

The diameter of each fiber was measured in air by using the vibrascope method [8]. The diameter in the buffer solution was corrected for the transversal swelling. Fibers with equal diameters were paired together and mounted in the apparatus.

From the stick-slip curves the median of nine values for F_s and the median of nine values for F_k were taken. When there were no stick-slips on the curve, the median of nine equidistant points was taken. For each fiber pair five mean values of F_s and five of F_k were obtained corresponding to the different weights. It was found that the data obtained from these measurements could be described well by equation (14), and therefore all calculations are based on that equation.

The frictional properties may be characterized by the coefficient of friction, $\mu = F/W$. From equation (14), however, it is seen that the coefficient of friction is a function of W, r, and l, and therefore different samples of fibers can be compared only if the values of the coefficient are adjusted to common values of these parameters. Equation (14) can be written

$$\mu = a + bM, \tag{15}$$

where $\mu = F/W$, and $M = rl/W$.

If there are k fiber pairs in the sample, and $\bar{\mu}_i$ and $\bar{M}_i$ are the ith values of μ and M, the value of M to which μ is adjusted might preferably be

$$\frac{\sum_{i}^{k} \bar{M}_i}{k} = \bar{M}$$

$$\bar{\mu}_{i(\text{adj})} = \bar{\mu}_i - b(\bar{M}_i - \bar{M}). \tag{16}$$

$\bar{\mu}_i$ and $\bar{M}_i$ are means of measurements at different weights, P_1, on the same fiber pair.

The value of b for each fiber pair can be determined only if a range of values of M for each fiber pair is measured. This range is obtained by changing the weight P_1. The value of r is, of course, a constant for each fiber pair. The value of $\bar{M}$ for all measurements was found to be close to 0.50, and hence all values of $\bar{\mu}$ were adjusted to this value of $\bar{M}$. The value of b for each fiber pair was determined by the method of least squares. Hence, the adjusted value of $\bar{\mu}$ is based on five measurements on each fiber pair. These values are given in Table I, together with the values of K, the relative difference between static and kinetic friction. Each value of K is the mean of five measurements on each fiber pair. The table is based on about 10,000 values of F_k and F_s. Where there are no figures for K in the table, $K < 0.01$.

In Table II the sample means of the values in Table I are given together with values of s^2, the mean square for the within-sample variation.

The value of the anti-scale frictional force can be regarded as composed of the value of the with-scale

frictional force plus a term for the effect of the scales [14]. Therefore, if we want to interpret the friction in terms of surface properties, the with-scale friction should be studied. The difference between anti-scale and with-scale friction, on the other hand, is an estimate of the mechanical resistance of the scales, and can be taken as an indication of scale modification [15]. Judging from the values of μ_{1k}, both dry and wet, it is evident that the extractions had little influence on the frictional properties. The values of μ_{1k} for the untreated sample in the buffer solution is, however, significantly lower than μ_{1k} for the ether-extracted and ether- and alcohol-extracted samples.

The friction both in the dry and the wet state increases with alcoholic potash treatments. The values of μ_{1k} are plotted against the time of treatment in alcoholic potash in Figure 6. The value of the ether- and alcohol-extracted sample is taken as the zero value. It is obvious from the curve that there is an almost instantaneous reaction between the surface layer and the alcoholic potash.

From the values of s^2 in Table II it is seen that the variation between fibers for the 15-sec. sample is significantly greater than for the other treatments. This means that the treatment is not uniform, and that the frictional values for the fibers which have received a milder treatment therefore tend to lower the mean value.

The values discussed so far are kinetic values. If it is assumed that the normal load is the same for both F_k and F_s, the static values, μ_s, can be calculated from μ_k and K. The results are given in Figure 7.

If the values for $\mu_{2k} - \mu_{1k}$ given in Table II are studied, it is seen that there is a tendency for this value to increase with the alcoholic potash treatment, at least in the wet state. It is difficult to give an explanation for this increase, and further experiments must be made to verify this behavior. The absence of a decrease, however, further confirms the conclusion drawn in Part I—that these treatments are confined to a thin surface layer.

If a wool sample is progressively treated with alcoholic potash, the handle becomes more and more scroopy [21]. It has been suggested that the scroopy handle of silk and some types of rayon and synthetic fibers is due to a difference between static and kinetic friction [23]. From values of K_1 in Table II it is seen that there is a similar relation between this difference and the handle of wool. The harshness can, of course, also be attributed to the high values of the with-scale friction, which already has been pointed out by Mercer and Makinson [21].

The variation in friction between different fibers is rather great, which means that a large number of fibers must be measured in order to get an accurate estimate of the sample mean. Therefore, a method for estimating fiber friction which would give the mean of several fibers directly should be of value.

If the only relevant property changed by a treatment is friction (friction is here taken as the friction of the fiber surface and does not include any effect of the scale edges) and if the same type of material is used for the various treatments, some mechanical properties of a fiber mass might be taken as an estimate of the frictional properties. The material

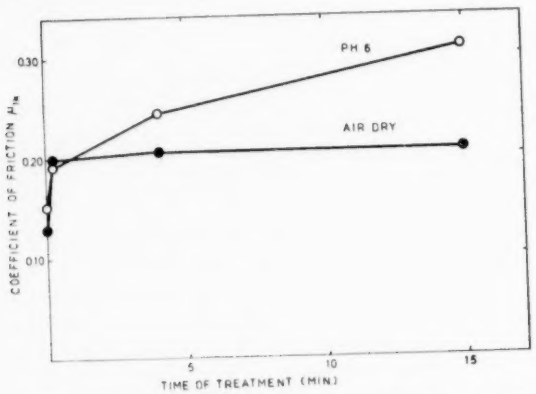

FIG. 6. *Kinetic coefficient of friction of fibers treated for different periods of time with alcoholic potash.*

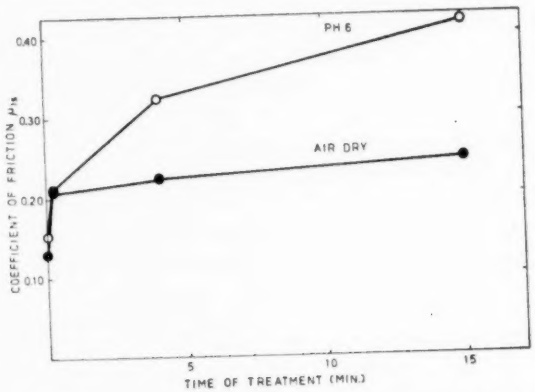

FIG. 7. *Static coefficient of friction of fibers treated for different periods of time with alcoholic potash.*

TABLE III. BREAKING STRENGTH (KG.) OF TOP

Sample No.	Untreated	Alcoholic potash 15 sec.	4 min.	15 min.
1	2.39	3.44	6.63	3.09
2	2.23	3.67	3.90	4.15
3	2.44	4.40	6.30	5.14
4	2.60	6.23	4.89	6.00
5	2.50	3.22	4.02	5.44
6	2.31	5.44	3.54	5.82
7	2.61	3.70	4.16	4.70
8	3.03	3.69	3.40	4.92
9	2.96	3.89	7.21	4.07
10	3.54	3.88	6.31	4.64
Mean value	2.66	4.16	5.04	4.80

used here was top. The breaking strength of the top is a mechanical property related to friction. Friction also determines the mobility of fibers during felting, all other properties being constant, and therefore the felting of top can be used to estimate how frictional properties are influenced by various treatments.

Breaking Strength of Top

By means of the Instron Tensile Tester it is possible to determine a load-elongation curve for top and other untwisted fiber strands. In Figure 8 a typical load-elongation curve for top is shown. The sample length is greater than the maximum fiber length. The maximum force is the breaking strength of the top. At this point the fibers start to slip apart, and therefore the maximum force is a measure of the frictional force keeping the strand together. If all properties of the fibers except surface properties are kept constant, the frictional force might be used as an estimate of the coefficient of friction.

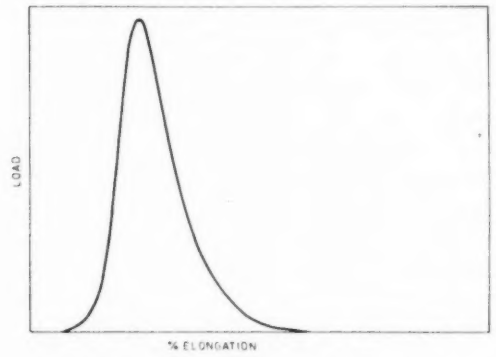

FIG. 8. *Load-elongation curve for top.*

Ten 20-cm. pieces of the top from each of the following pretreated lots were taken: untreated; alcoholic potash, 15 sec., 4 min., and 15 min. The breaking strength of each piece was measured in the Instron at 65% R.H. The gage length was 15 cm. and the rate of elongation 10 cm./min. The pieces were weighed afterwards, and the breaking strength corrected for difference in weight per unit length. The results are given in Table III. The standard error of the difference between any two treatment means is 0.89. If the means of the breaking strength are plotted against $\left(\frac{\mu_{1s} + \mu_{2s}}{2}\right)_{air}$, calculated from Table II, a good linear relationship between these two variables is obtained (Figure 9). These experiments thus confirm the reliability of the direct frictional measurements.

Felting of Top

The difference between anti-scale and with-scale friction is now widely considered to be the primary cause of felting of wool fibers. There are also a number of secondary factors—*e.g.*, mechanical properties—which might influence the rate and degree of felting [1, 3, 28]. In the present experiments these secondary factors were assumed to be unchanged by the different pretreatments of the samples (see Part I), and thus frictional properties alone are considered here in relation to felting. The direct frictional measurements showed a small increase in the difference $\mu_2 - \mu_1$ upon treatment with alcoholic potash. This increase, however, is difficult to explain and might be due to biased sampling.

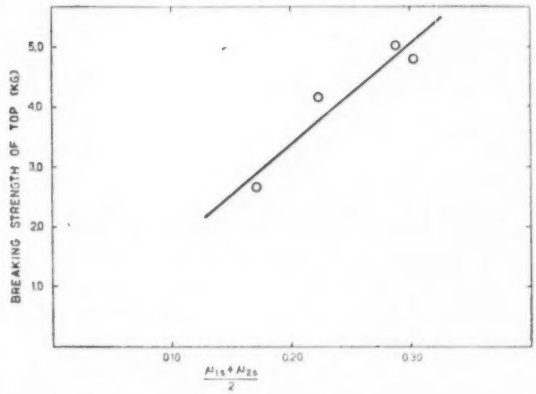

FIG. 9. *Relationship between breaking strength of top and* $(\mu_{1s} + \mu_{2s})/2$.

If numerical values of all relevant fiber properties were known, it might be possible to calculate the redistribution of fibers, which takes part on felting, by means of statistical mechanics. No serious attempt to do so has been made so far, but many authors have tried to find an empirical relationship between friction and felting [13, 18, 27]. None of these empirical relationships, however, were found to correlate with felting data, probably because they all contain the difference $\mu_2 - \mu_1$, which is subject to great experimental error. The problem was therefore attacked in another way. The difference $\mu_2 - \mu_1$, which is the operating characteristic of felting, was assumed to be constant for all samples. The energy, Q, required to move the fibers certain distances relative to each other during the redistribution is a function of the average coefficient of friction, $(\mu_{2k} + \mu_{1k})/2$:

$$Q = \lambda \bar{W} \cdot \frac{\mu_{2k} + \mu_{1k}}{2}, \tag{17}$$

where λ is the total distance all fibers have moved, and $\bar{W}$ is the average load on each fiber (it should be remembered that for long fibers different parts might move rather independent of each other). Thus,

$$\frac{d\lambda}{dQ} = \frac{1}{\bar{W}} \cdot \frac{1}{\frac{1}{2}(\mu_{2k} + \mu_{1k})}. \tag{18}$$

If felting is expressed by means of volume change of the material, the following equation for the felting rate might be suggested:

$$\frac{dV}{dt} = -CV, \tag{19}$$

where V is the volume, t is the time, and C is a rate constant. Creely and Le Compte [6] found, for instance, by measuring the felting of yarn that the rate of felting could be expressed by

$$\frac{dL}{dt} = -CL,$$

where L is the length of the yarn.

If the energy transferred to the material is a linear function of time, dQ could be substituted by dt. If it is further assumed that dV is proportional to $d\lambda$ and $1/\bar{W}$ is proportional to V, the following relation is obtained:

$$C = \frac{2c_1}{\mu_{2k} + \mu_{1k}} \tag{20}$$

where c_1 is another constant.

Experimental

Since the experimental material was in the form of top, it was convenient to use a method for top felting. Such a method has been developed by Bogaty *et al.* [2]. The samples are sewn in bags of cheesecloth and secured to the bag by two rows of stitches 25 cm. apart. The samples are soaked in the liquid to be used for felting. After squeezing by hand, the sample length is measured. The sample is suspended vertically and loaded at the bottom with 300 g., and the length is measured by means of a ruler. An appropriate number of samples were put into a tumble jar having a volume of 5 l. The jar made 50 revolutions per minute. The tumble jar contained 1 l. of a buffer solution. The tumble jar was equipped with a counter, and after tumbling for a number of revolutions the samples were removed and squeezed, and their lengths were measured. The samples were then put back into the jar, and the tumbling was continued. The felting was made at room temperature. The top shrinkage is $T = 100\,(L_o - L_n)/L_o$, where L_o is the initial and L_n the length at n revolutions.

With this experimental arrangement, one might suspect that there are differences between different runs due to different positions of the samples in the jar. It was therefore desirable to include one sample from each treatment in each run. The number of pretreatments to be investigated were six, but 6 samples were regarded as too heavy a load on the tumble jar, and therefore two experiments were made. The untreated sample and the samples treated with alcoholic potash were included in the first experiment. Four runs were made, and all four pretreatments were represented in each run. The felting liquid was the same as the buffer solution used for the frictional measurements. The samples were measured after 200, 400, 600, 800, 1,000, 1,200, and 1,400 revolutions. All samples were then run until there was no further decrease in length, which took about 30,000 revolutions. The values of the top shrinkage are given in Table IV.

It is obvious from the table that there are large differences in felting rates between the different treatments. To find out if the anticipated difference between different runs was significant and to isolate the experimental error, an analysis of variance of the data from Table IV was made (Table V). The values at 30,000 revolutions were ex-

TABLE IV. Values of Top Shrinkage

Treatment	Run	Number of revolutions: 200	400	600	800	1,000	1,200	1,400	30,000
Untreated	a	8.0	18.5	29.0	34.3	37.5	40.2	43.2	55.5
	b	11.3	24.3	31.3	38.8	41.5	45.9	47.9	60.8
	c	7.5	19.7	28.0	33.8	37.4	43.0	46.5	61.0
	d	9.4	19.1	26.1	34.3	37.5	40.6	41.8	57.7
Mean values		9.1	20.4	28.6	35.3	38.5	42.4	44.9	58.8
Alcoholic potash (15 sec.)	a	10.8	13.2	21.0	26.0	33.1	35.3	37.7	63.0
	b	6.1	12.9	18.7	25.3	27.5	32.0	36.5	58.0
	c	7.0	14.4	18.8	23.8	28.5	32.4	38.2	59.7
	d	5.1	12.0	16.7	23.7	27.7	33.5	37.8	56.0
Mean values		7.3	13.1	18.8	24.7	29.2	33.3	37.6	59.2
Alcoholic potash (4 min.)	a	7.9	12.5	17.5	21.3	26.0	28.0	31.5	58.7
	b	6.0	13.0	19.8	24.8	29.0	34.3	38.2	57.2
	c	4.8	10.2	16.8	22.0	24.7	30.6	33.7	60.0
	d	4.7	10.9	14.8	21.4	25.2	30.0	33.5	56.0
Mean values		5.9	11.7	17.2	22.4	26.2	30.7	34.2	58.0
Alcoholic potash (15 min.)	a	4.0	9.9	15.0	19.5	24.7	26.6	29.3	57.8
	b	3.5	8.6	15.2	20.0	23.0	27.0	31.2	53.0
	c	3.2	7.5	11.8	15.8	20.0	22.5	26.8	56.1
	d	3.9	8.1	12.4	17.3	20.0	23.5	27.0	51.1
Mean values		3.7	8.5	13.6	18.2	21.9	24.9	28.6	54.5

cluded from this analysis. The experimental design is of the split-plot design type [5]. The error made in subsequent measurements on the same top sample is likely to be smaller than the top sampling error. The presence of these two types of error is characteristic for the split-plot design. Since only one treatment can be made on each sample, the top sampling error (error I) must be used to estimate differences between treatments. Differences between number of revolutions and the interactions are compared against the within-top-sample error (error II).

TABLE V. Analysis of Variance of Data from Table IV

Source of variation	Degrees of freedom	Sum of squares	Mean square†
Total	111	14671.90	
Between treatments	3	3012.52	1004.17***
Between runs	3	124.28	41.43
Error I	9	114.64	12.74
Between number of revolutions (n)	6	11051.77	1841.96***
Interaction: $n \times$ treatments	18	269.52	14.97***
Error II	72	99.16	1.38

† In this and subsequent tables the asterisks *, **, and *** are used to indicate statistical significance at the 95%, 99%, and 99.9% levels, respectively.

Error II is much less than error I, which means that the method of measuring the top length is satisfactory. Differences between runs are not significant to $P = 0.95$, but the precaution taken to eliminate these differences has nevertheless reduced the error mean square. By carrying the analysis further and calculating the mean square for the treatment effects for each value of n, it is found that the greatest differences between the treatments occur around $n = 1{,}000$. Hence, in further experiments the top shrinkages are determined only at $n = 1{,}000$.

The coefficient of variation corresponding to error I and based on the grand mean for $n = 1{,}000$ is found to be 4.7%. This value is considerably less then the value of 14% reported by Bogaty *et al.* [2], and shows that the method can be used to detect small differences in felting properties of wool fibers. A separate analysis shows that there are no significant differences between the equilibrium values at $n = 30{,}000$.

If L, the length of the top sample, is substituted for V in equation (19), the following equation

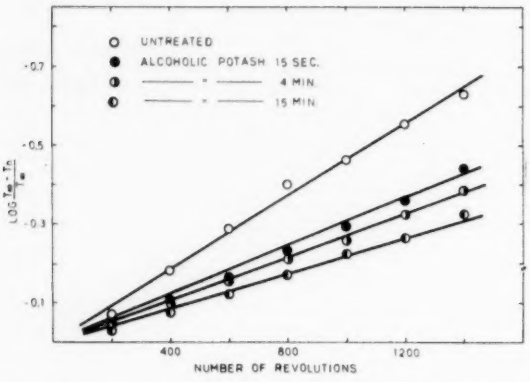

FIG. 10. *The logarithm of top shrinkage plotted against number of revolutions.*

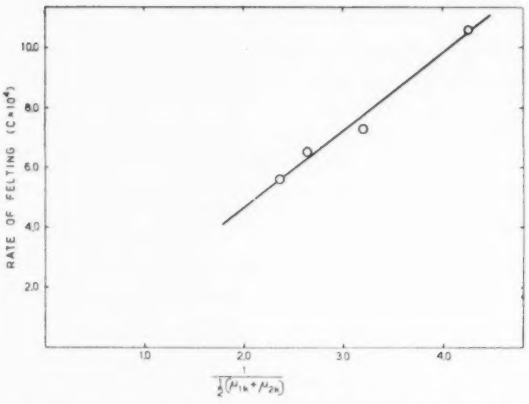

FIG. 11. *Relationship between felting rate,* C, *and* $1/\frac{1}{2}(\mu_{2k} + \mu_{1k})$.

might be used to describe the top felting:

$$\frac{dL_n}{dn} = -C(L_n - L_x), \tag{21}$$

where L_n is the length of the top at n revolutions, L_x is the length of the top at equilibrium, and C is the rate constant. Integrating and introducing the boundary condition $L_n = L_o$ for $n = 0$:

$$\log \frac{L_n - L_x}{L_o - L_x} = -0.4343 \cdot Cn, \tag{22}$$

or

$$\log \frac{T_x - T_n}{T_x} = -0.4343 \cdot Cn.$$

If $\log \dfrac{T_x - T_n}{T_x}$ for the treatment means in Table IV are plotted against n (Figure 10), practically straight lines are obtained, except for the untreated sample, which shows a slight curvature. The values of C are calculated by the method of least squares and are given in Table VI.

The validity of equation (20) is tested by plotting C against $1/\frac{1}{2}(\mu_{2k} + \mu_{1k})$. From Figure 11 it is seen that a good linear relationship is obtained.

If equation (20) is valid, it is obvious that the felting rate is a more accurate estimate of the with-scale friction than direct frictional measurements. This statement is, of course, subject to the limitations mentioned above. The work necessary to obtain the same standard error is greater with the frictional measurements than with the felting measurements.

TABLE VI. VALUES OF C

Treatments	$C \times 10^4$
Untreated	10.6
Alcoholic potash (15 sec.)	7.3
Alcoholic potash (4 min.)	6.5
Alcoholic potash (15 min.)	5.6

Peryman and Speakman [24] have found that extraction with ether and alcohol greatly reduces the felting of fabrics. They attribute the greater shrinkage of the unextracted samples to a lubrication effect, the lubricating agents being soap and fatty matter, which are always present on normally scoured samples. Especially in acid solutions the soap is hydrolyzed and felting is promoted by the presence of fatty acid.

Hitherto it has been difficult to confirm these findings by direct frictional measurements, probably because of the large variation between different fibers. The results in Table II, however, indicate that there is a difference between untreated and ether- and alcohol-extracted samples. If, now, the felting is a good measure of the friction, it should be possible to estimate the difference in friction between the untreated and the extracted samples simply by measuring the felting rate of these samples. If the true fiber friction is sought, it is also important to know how contaminating substances like fatty matter influence the friction, so that precaution can be taken to remove these.

Unextracted and extracted samples were run in the tumbling jar in buffer solutions at three different pH values. The experimental conditions were the same as before, except that the samples were removed from the jar and measured only after $n = 1{,}000$. Three samples were used in each run, one from each of the untreated, ether-extracted, and

TABLE VII. Values of Top Shrinkage

Treatments	pH 2.0	pH 6.0	pH 10.0
Untreated	42.8	46.2	45.6
	43.0	47.0	43.8
	43.5	45.2	45.7
Mean values	43.1	46.1	45.0
Ether-extracted	33.6	40.4	40.1
	35.0	39.4	39.5
	36.2	37.9	39.2
Mean values	34.9	39.2	39.6
Ether- and alcohol-extracted	35.6	35.2	36.6
	34.8	33.0	32.3
	34.8	32.3	35.6
Mean values	35.1	33.5	34.8

ether- and alcohol-extracted lots. Three runs for each buffer solution were made, which makes a total of nine runs. The results are given in Table VII.

The statistical analysis of these data is shown in Table VIII. It is important to note that differences between buffer solutions should be compared with differences between runs because of the split-top design.

From Table VII it is seen that the untreated top felted more than the ether-extracted and the ether- and alcohol-extracted top in the pH 2 buffer solutions, whereas there was no difference between the latter two samples. In the pH 6 and 10 buffer solutions the ether-extracted sample was intermediate between the other two. Run differences are here significant to the 0.95 limit. These results confirm the findings of Peryman and Speakman, although the differences between untreated and alcohol-extracted samples are not so great with the top as with the fabrics used by them. The results also confirm that the differences found by direct frictional measurements are real.

TABLE VIII. Analysis of Variance of Data from Table VII

Source of variation	Degrees of freedom	Sum of squares	Mean square
Total	26	578.61	
Between buffer solutions	2	24.72	12.36
Between runs	6	16.07	2.68*
Between treatments	2	493.49	246.75***
Interaction: buffer solutions × treatment	4	34.12	8.53***
Error	12	10.21	.851

Discussion

All measurements of friction, both direct and indirect, have shown that there is an almost instantaneous increase in friction when the fibers are subjected to treatments with alcoholic potash. The chemical reaction between the surface layer and the alkali responsible for this increase is very rapid during the first few seconds, but slows down considerably with time. It is impossible to tell from the data if it is a homogeneous surface reaction with a definite reaction constant or if the reaction progressively penetrates deeper into the surface layer. After longer times of treatment, it is obvious that the reaction must go deeper into the cuticle and might even eliminate the difference $\mu_2 - \mu_1$ by degrading the scale substance.

It has been shown by Shooter and Thomas [26] that there is a close connection between chemical constitution and surface friction. Weakly polar structures like polytetrafluorethylene and polyethylene have lower friction than polar substances like styrene and methylmethacrylate. When the low friction of the wool fibers is increased, this might be due to a structural change of the epicuticle—for instance, by transforming it from a weakly polar to a polar structure by use of alkali. A discussion of what kind of reaction this might involve is futile because we still lack knowledge of the chemical composition of the epicuticle. It is obvious from electron microscopical investigation that the main structure of the epicuticle is more or less unaffected by these treatments [12], and therefore the change of friction can hardly be due to the exposure of a new chemically different layer of the fiber. A change in chemical structure of the surface may thus affect the value of s in equation (13). But this equation also contains the modulus of elasticity, E, and the yield limit, p_m. If these quantities are changed as a result of a chemical reaction proceeding to a sufficient depth beneath the surface, the value of the friction might also change. The change in surface friction, therefore, can theoretically be brought about in two different ways. It is difficult to tell from the data which of these are responsible for the change in friction, but, because of the very rapid increase after short times of treatment, it is most likely that the main factor is a chemical change of the surface. After longer reaction times the other factor also might become operative.

Acknowledgment

My thanks are due to Professor N. Gralén for his unfailing interest and helpful advice, to Mrs. E. Bernehed, who skillfully carried out the experimental work, and to the board of the Institute for permission to publish this paper. The International Wool Secretariat, London, sponsored part of this work.

I also wish to acknowledge the work of Erling Sörvik, which stimulated me to modify the fiber twist meter.

Literature Cited

1. Barr, T., and Speakman, J. B., *J. Soc. Dyers Colourists* **60**, 335 (1944).
2. Bogaty, H., Frishman, D., Sookne, A. M., and Harris, M., TEXTILE RESEARCH JOURNAL **20**, 270 (1950).
3. Bogaty, H., Sookne, A. M., and Harris, M., TEXTILE RESEARCH JOURNAL **21**, 822 (1951).
4. Bowden, F. P., and Tabor, D., "The Friction and Lubrication of Solids," Oxford, Oxford University Press, 1950.
5. Cochran, W. G., and Cox, G. M., "Experimental Designs," New York, John Wiley & Sons, Inc., 1950.
6. Creely, J. W., and Le Compte, G. C., *Am. Dyestuff Reptr.* **30**, 247 (1941).
7. Frishman, D., Smith, A. L., and Harris, M., TEXTILE RESEARCH JOURNAL **18**, 475 (1948).
8. Gonsalves, V. E., TEXTILE RESEARCH JOURNAL **17**, 369 (1947).
9. Gralén, N., and Olofsson, B., TEXTILE RESEARCH JOURNAL **17**, 488 (1947); *Proc. Swedish Inst. Text. Research* No. 3 (1947).
10. Gralén, N., Olofsson, B., and Lindberg, J., TEXTILE RESEARCH JOURNAL (in press).
11. Howell, H. G., *J. Textile Inst.* **42**, T52 (1951).
12. Lagermalm, G., and Philip, B., TEXTILE RESEARCH JOURNAL **20**, 668 (1950).
13. Lindberg, J., TEXTILE RESEARCH JOURNAL **18**, 470 (1948); *Proc. Swedish Inst. Text. Research* No. 8 (1948).
14. Lindberg, J., and Gralén, N., TEXTILE RESEARCH JOURNAL **18**, 287 (1948); *Proc. Swedish Inst. Text. Research* No. 6 (1948).
15. Lindberg, J., and Gralén, N., TEXTILE RESEARCH JOURNAL **19**, 183 (1949); *Proc. Swedish Inst. Text. Research* No. 10 (1949).
16. Lindberg, J., and Gralén, N., *J. Textile Inst.* **41**, T331 (1950).
17. Lindberg, J., and Gralén, N., *Nature* **162**, 112 (1948).
18. Mercer, E. H., *J. Council Sci. Ind. Research* **18**, 188 (1945).
19. Mercer, E. H., *Nature* **155**, 573 (1945).
20. Mercer, E. H., and Freney, M. R., Council Sci. Ind. Research, Pamphlet No. 94, Part II (1940).
21. Mercer, E. H., and Makinson, K. R., *J. Textile Inst.* **38**, T227 (1947).
22. Olofsson, B., TEXTILE RESEARCH JOURNAL **20**, 476 (1950).
23. Olofsson, B., and Gralén, N., TEXTILE RESEARCH JOURNAL **20**, 467 (1950).
24. Peryman, R. V., and Speakman, J. B., *J. Textile Inst.* **41**, T241 (1950).
25. Postle, L. J., and Ingham, J., *J. Textile Inst.* **43**, T77 (1952).
26. Shooter, K. V., and Thomas, P. H., *Research* **2**, 533 (1949).
27. Speakman, J. B., and Stott, E., *J. Textile Inst.* **22**, T339 (1931).
28. Speakman, J. B., Stott, E., and Chang, H., *J. Textile Inst.* **24**, T273 (1933).

(Manuscript received January 19, 1953.

SUMMER LABORATORY COURSES

Polytechnic Institute of Brooklyn

The tenth in the annual series of courses for advanced instruction in modern laboratory techniques will be held this summer at the Graduate School of Physics and the Institute of Polymer Research of the Polytechnic Institute of Brooklyn.

Professional representatives—industrial and institutional—are invited to enroll in one or more of the courses. Attendance at each course is limited in order to insure intensive individual attention and contact between instructors and participants.

For information write to Professor I. Fankuchen, Polytechnic Institute of Brooklyn, 85 Livingston Street, Brooklyn 1, New York.

Program of the 1953 series is given below.

June 1–June 12—"Industrial Applications of X-Ray Diffraction," Professor I. Fankuchen, in charge

July 27–July 31—"Weight and Shape of Macromolecules in Solution, Including Polyelectrolytes," Professor H. F. Mark, in charge

August 3–August 7—"Progress in Polymerization and Copolymerization Techniques," Professor C. G. Overberger, in charge

Mechanical Properties of Cotton Fibers

Part I: Relaxation in Air and Water*

J. A. Lasater, E. L. Nimer, and H. Eyring†

University of Utah, Salt Lake City, Utah

THIS is the first in a series of reports on the investigation of the effect of present commercial handling on the properties of cotton fibers. The cotton used in this work was from the following stock: Upland Cotton Strain No. 234 (grown, Las Cruces, N. M., 1949; grade, Strict Middling or Good Middling). The samples were from a set of eleven that were obtained when a bale of this cotton was processed by current manufacturing methods. The first sample was the field or seed-containing sample, and the other samples were drawn after each stage in the processing, including even simple operations such as washing. The final sample was the finished thread. The samples weighed from 5 to 10 lbs. each. This complete set of samples was supplied through the courtesy of Dr. Carlyle Harmon of Chicopee Mills, Chicopee Falls, Mass.

The results of the relaxation studies in air and water on the sample containing seed and on that which was gin-processed are reported in this paper. The results of other types of investigations will be reported later. These samples will be designated in the following discussions as the "seed" and the "gin" cotton. Also, the terms "cotton fiber" and "cotton hair" will refer to the lint fiber. The work of Fröde Andersen [2] is interesting in that he reports results similar to some of those presented here.

Experimental

The tests were conducted on individual cotton fibers. The fibers obtained from the seed cotton were carefully cut from the seed with a sharp razor blade in such a manner as to subject the fiber to the minimum possible strain. The gin cotton was used as received. Throughout the investigations, an attempt was made to use random sections of the cotton samples at each of the experimental conditions. A small portion of the bulk sample was chosen at random, and some of the fibers were mounted and tested. The excess fibers were discarded following the preparation of the set. During the testing, there was duplication of the experimental conditions with the exception that the fibers employed were from different sets of fibers. It is believed that the method employed in selecting the fibers was such as to give representative values for the entire sample.

The individual cotton hairs were mounted with a small glass hook on one end and a copper wire hook on the other. The fiber was wrapped around the hooks several times and bonded to the hooks with an acryloid resin (Rohm & Haas, A-10). This method of mounting had the advantage that the section of the fiber tested was from the central portion. This resin "sets" without the application of heat. The bonding agent was given at least 24 hrs. to set before further treatment was undertaken.

The mounted, air-dry fibers were stored in a special rack so that no strain acted on the fiber. The fibers tested in the water-saturated state were conditioned in distilled water, under no strain, for a period of 48 hrs. or more. The initial length of the fibers, hook to hook, was generally about 2 cm., with some fibers as short as 1 cm. and some as long as 3 cm.

The apparatus used in these experiments was a modified form of the Sookne-Rutherford [7] autographic balance. This instrument is an automatic balance that records continuously the instantaneous force on the fiber. The data from this balance were reproducible to ± 10 mg.

For the force-relaxation studies, the fiber was mounted on the adjusted balance and the fiber was elongated at a rigidly controlled constant rate of 0.0712 cm./min. until the force supported was from 1 to 3 g. The elongation was then stopped and held at a constant value, and the fiber was allowed to relax. The instrument automatically recorded the decay of the force—the so-called "autograph." The time of relaxation was generally 1 hr., although in some cases it was considerably longer. In one set of tests, the fiber was re-elongated after it had been allowed to relax for approximately 1 hr. In

* This work was supported in part by the Office of Naval Research.

† Dean of the Graduate School, University of Utah.

all instances where the fiber was re-elongated, it was subjected to a force greater than that initially used.

In all experiments, the temperature of the medium surrounding the fiber was controlled to ±0.1°C by circulating water from a thermostatted bath through the outer jacket of the test chamber.

Results

It was found that the relaxation curve for cotton fiber could be reasonably approximated by the following empirical equation:

$$F = C_1 e^{-r_f t} + C_2 e^{-r_s t}. \quad (1)$$

The experimental and the calculated curves are compared in Figure 1. They are shown to be in good agreement over the entire range. The major divergence occurs during the first minute of relaxation. In one set of measurements, the relaxation was carried out for over 400 min. without any apparent change in the shape of the relaxation curve. The relaxation constants were highly reproducible and were independent of the initial force acting on the fiber in the range from 1 to 3 g., but were markedly influenced by temperature.

A summary of the relaxation constants for seed cotton is given in Tables I and II. A similar set of data was obtained from the relaxation studies using the gin cotton. These data are given in Tables III and IV.

The relaxation constants given in the tables at the temperatures 0°, 20°, 40°, and 60°C are the averages of from five to ten runs. In the studies with the air-dry fibers, it was not possible to make measurements at 0°C due to the condensation of water from the air. The data represent the behavior of from 90% to 95% of the fibers tested. It was observed that occasionally the relaxation curve for a single fiber was totally inconsistent with those for the usual fiber. In this analysis, the small fraction of fibers that were "inconsistent" with the majority of the data were considered as nonrepresentative of the fibers' behavior. These data were rejected on the following bases: (*1*) The force-elongation curves for the fibers that gave inconsistent data were markedly different from those for the "average" fibers. The force-elongation curves of the former were very flat; in the case of the water-saturated fibers, the force-elongation curves did not exhibit the two-slope curve (a minimum and then a maximum slope) but a single uniform slope. In later measurements it was possible to predict during the elongation the fibers that would give inconsistent relaxation data. (*2*) The relaxation constants obtained from these fibers were generally from 4 to 6 times the "normal" values. (*3*) The inconsistent data usually occurred under conditions—*i.e.*, elevated temperature—that would cause imperfections in the bonding to appear more readily. The authors are convinced that these inconsistent values represent faulty bonding and not a variation in fiber properties. While it would have

TABLE I. RELAXATION CONSTANTS FOR AIR-DRY SEED COTTON

Temperature (°C)	r_f (sec.$^{-1}$)	r_s (sec.$^{-1}$)
20	1.25×10^{-2}	2.05×10^{-5}
40	1.09×10^{-2}	2.48×10^{-5}
60	1.05×10^{-2}	4.34×10^{-5}

TABLE II. RELAXATION CONSTANTS FOR WATER-SATURATED SEED COTTON

Temperature (°C)	r_f (sec.$^{-1}$)	r_s (sec.$^{-1}$)
0	1.04×10^{-2}	0.471×10^{-5}
15	1.09×10^{-2}	1.16×10^{-5}
20	1.18×10^{-2}	1.61×10^{-5}
25	1.21×10^{-2}	2.27×10^{-5}
35	1.22×10^{-2}	2.30×10^{-5}
40	1.23×10^{-2}	2.48×10^{-5}
60	1.48×10^{-2}	4.14×10^{-5}

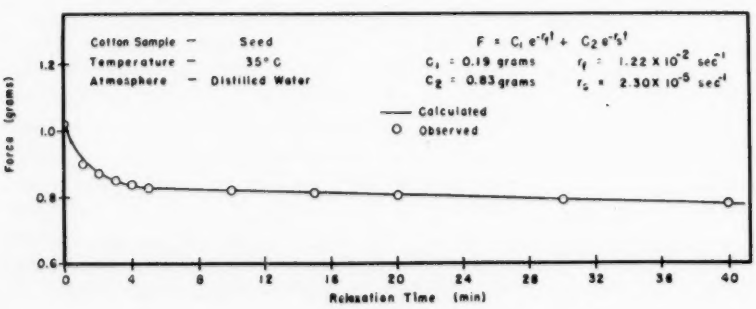

FIG. 1. *A typical force-relaxation curve of cotton fibers.*

TABLE III. Relaxation Constants for Air-Dry Gin Cotton

Temperature (°C)	r_f (sec.$^{-1}$)	r_s (sec.$^{-1}$)
20	0.896×10^{-2}	2.91×10^{-5}
40	0.998×10^{-2}	3.53×10^{-5}
60	1.08×10^{-2}	4.54×10^{-5}

TABLE IV. Relaxation Constants for Water-Saturated Gin Cotton

Temperature (°C)	r_f (sec.$^{-1}$)	r_s (sec.$^{-1}$)
0	1.24×10^{-2}	2.27×10^{-5}
20	1.15×10^{-2}	2.91×10^{-5}
40	1.11×10^{-2}	3.12×10^{-5}
60	1.07×10^{-2}	4.55×10^{-5}

been desirable to make more determinations at each of the various experimental conditions, the number of determinations was limited by the time required to collect and treat the data. It required approximately 2 man-hours to prepare the fiber, carry out the measurements, and determine the characteristics of each fiber tested.

In the experiments where the fiber was re-elongated after it had been allowed to relax for a period of approximately 1 hr., it was found that the relaxation constants were, within experimental error, the same as those obtained in the earlier relaxation studies. It was ascertained that the relaxation constants obtained from the subsequent relaxation curves were not influenced by the time of relaxation in the prior studies, provided the time interval was of sufficient length to permit the completion of the fast relaxation process. In some cases, the fiber was elongated and allowed to relax three times, with good consistency in the relaxation constants. However, consistency in the relaxation constants was not obtained if the stress was ever completely removed from the fiber. This change in the fiber properties may be due to an increased crystallization of the fiber.

The emphasis in this work was on the obtaining of a general survey of the behavior of the fibers under a wide variety of conditions, rather than restricting the investigations to a few conditions and so obtaining a statistical distribution for the relaxation constants. The authors recognize the value of a statistical treatment, but it was thought that the over-all behavior should be investigated first. Further measurements may require some revision of the relaxation constants, but such revisions will probably be of minor importance.

Theoretical Treatment of Relaxation

Although there are certain serious limitations to a simple mechanical model approach to fibers such as cotton ([1], p. 340), it has been possible to draw some conclusions as to a possible mechanism of the relaxation processes.

Considering the relaxation curves for cotton fibers and the fact that the "elasticity" is imperfect, it is possible to propose the model shown in Figure 2, which is at least qualitatively correct. The participating elements in the relaxation processes observed in this work are represented by the two Maxwell elements in parallel. The dashpot located at the top of the model is necessary to explain the region of plastic flow observed in the initial elongation of the wet fiber. This dashpot is water-sensitive, and, unless the fiber is wet, it is inactive in the elongation process. The relaxation studies carried out using the water-saturated fibers were not conducted until the fiber had been elongated to the region of "Hookean" behavior; thus, this dashpot was fully extended and did not influence the relaxation. Under these experimental conditions, the model behaved as though it had the form shown

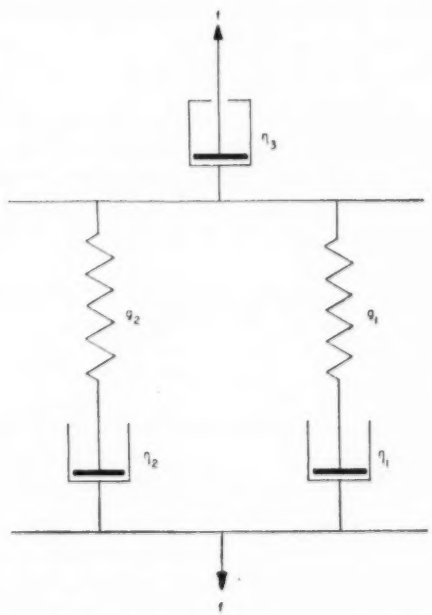

Fig. 2. *Proposed mechanical model for raw cotton fibers.*

in Figure 3A. This portion of the model can be put in a different but equivalent form ([1], p. 125), as shown in Figure 3B. In this second form, the model shows a close resemblance to the model used by Houwink [4], shown in Figure 4.

The rate of elongation of an elastic unit according to Hooke's law is

$$\frac{ds}{dt} = \frac{1}{g}\frac{df}{dt}.$$

In the case of the flow unit, the rate of elongation has been shown to be [8]:

$$\frac{ds}{dt} = \frac{\lambda}{\lambda_1} 2k' \sin h\left(\frac{f\lambda_2\lambda_3\lambda}{2\,kT}\right).$$

The total rate of elongation of the Maxwell unit is equal to the sum of these elongation rates:

$$\frac{ds_i}{dt} = \frac{\lambda}{\lambda_1} 2\,k' \sin h\left(\frac{f_i\lambda_2\lambda_3\lambda}{2\,kT}\right) + \frac{1}{g_i}\frac{df_i}{dt}. \qquad (2)$$

As a first approximation, the hyperbolic sine term can be expanded, and equation (2) is approximated by

$$\frac{ds_i}{dt} = \frac{1}{g_i}\frac{df_i}{dt} + \frac{\lambda}{\lambda_1} k' \frac{\lambda_2\lambda_3\lambda f_i}{kT}.$$

By collecting terms and using Eyring's expression for the viscosity ([3], p. 483), it is possible to obtain the usual differential equation for the Maxwell unit:

$$\frac{ds_i}{dt} = \frac{1}{g_i}\frac{df_i}{dt} + \frac{1}{\eta_i} f_i. \qquad (3)$$

For the relaxation curves obtained with the fiber held at constant elongation, the restriction is that the total elongation rate of the model must be zero, or

$$\frac{ds_i}{dt} = \frac{ds_1}{dt} = \frac{ds_2}{dt} = 0.$$

Under such conditions, the solution of the differential equation for the Maxwell element is

$$f_i = f_i{}^o\, e^{-\frac{g_i}{\eta_i} t}. \qquad (4)$$

The total force on the model is the sum of the forces on each element, or

$$f = f_1 + f_2 = f_1{}^o\, e^{-\frac{g_1}{\eta_1} t} + f_2{}^o\, e^{-\frac{g_2}{\eta_2} t}. \qquad (5)$$

The force supported by the fiber is obtained by multiplying by the appropriate cross-sectional area:

$$F = f_1{}^o A_1\, e^{-\frac{g_1}{\eta_1} t} + f_2{}^o A_2\, e^{-\frac{g_2}{\eta_2} t}. \qquad (6)$$

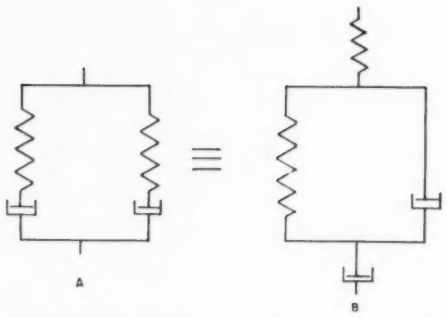

FIG. 3. *Equivalent forms of the mechanical model.*

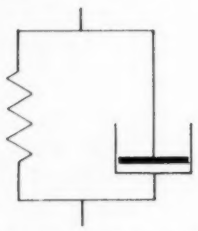

FIG. 4. *Mechanical model used by Houwink.*

It is seen that equation (6) has the same form as the empirical equation (1).

Eyring's expression for viscosity ([3], p. 483) is

$$\eta = \frac{\lambda_1\, kT}{\lambda_2\lambda_3\lambda^2 k'}.$$

The rate constant from the Theory of Absolute Reaction Rates is:

$$k' = \mathrm{H}\frac{kT}{h}\, e^{-\Delta F^{\ddagger}/RT}.$$

Using the above expressions, it is possible to express the relaxation constant in terms of fundamental values:

$$r_i = g_i/\eta_i = k'_i \frac{\lambda_2\lambda_3\lambda^2}{\lambda_1\, kT} g_i.$$

Solving for the free energy of activation, one gets

$$\Delta F_i^{\ddagger} = 2.303\, RT \log\left(\frac{r_i\lambda_i h}{\lambda_2\lambda_3\lambda^2 g_i}\right). \qquad (7)$$

In the numerical evaluation of the free energy of activation, the values of the various λ's were obtained using the model for the unit cell of cellulose developed by Meyer and Misch [6]. The relaxation probably occurs primarily in the amorphous region. The unit cell should give the minimum distances between the cellulose chains in the cotton fiber. For the purposes of these calculations, dis-

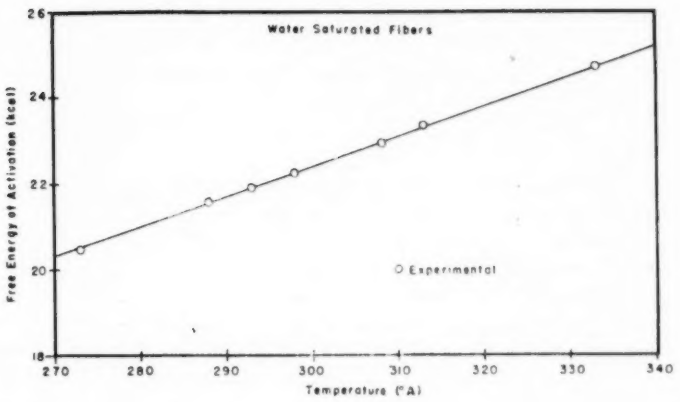

FIG. 5. *Variation in the free energy of activation with temperature for the fast relaxation process of seed cotton*

tances slightly larger than the crystal distances were chosen. The elastic constant was taken from the literature ([5], p. 996). The values used in the calculations were: $g = 5 \times 10^{11}$ dynes/cm.^{2}; $\lambda_1 = 4$ Å.; $\lambda = 5.2$ Å.* (length of anhydroglucose unit); $\lambda_2 = 3$ Å. (*a* dimension); and $\lambda_3 = 4$ Å. (*c* dimension). From thermodynamics, it is known that

$$\Delta F = \Delta H - T\Delta S.$$

The various values of the enthalpy and entropy of activation were calculated, since an excellent linear relationship was obtained between the free energy of activation and the absolute temperature. An example of these results is shown in Figure 5. The entropy and enthalpy of activation for air-dry and water-saturated seed cotton are given in Table V. Similar calculations were carried out for the gin cotton fibers. The results are given in Table VI.

In the previous development, the relaxation was treated using the classical expression for the viscosity. It would have been desirable to use the nonlinear viscosity expression of Eyring, but the mathematical complexity prevented its use at this time.

Mechanism of Relaxation

In the previous calculations, it is observed that the enthalpies of activation have small positive values, while the entropies of activation have high negative values. The maximum value observed for the enthalpy of activation is considerably less than the strength of the hydrogen bond in cellulose, 7.25 kcal. ([5], p. 1003). In a completely ordered system there may be two hydrogen bonds between adjacent hydroxyl groups.

* 5.2 Å. represents the minimum distance between equilibrium conditions along the cellulose chain.

This low heat of activation indicates that the relaxation proceeds through a rearrangement of hydrogen bonds, as proposed by Mark ([5], p. 1034). The results indicate that the slippage of the chain is somewhat more complex than the simple transport of the hydroxyl groups to new positions.

If n of the vibrational degrees of freedom each have one-Bth as many states in the activated complex as in the normal state, the rate constant for the relaxation process when written in terms of the partition functions has the form

$$k'_{\text{relax}} = \text{H} \frac{kT \left| \frac{1}{1 - e^{-\frac{k\nu}{kT}}} \right|^{n-1} \Phi_{\ddagger} e^{-E_0/kT}}{h \left| B \frac{1}{1 - e^{-\frac{k\nu}{kT}}} \right|^{n} \Phi_{\text{normal}}}.$$

The degrees of freedom which are assumed unchanged in passing to the activated complex cancel out of the rate constant. Assuming that the activation leaves the frequencies unchanged, it is seen

TABLE V. ENTHALPY AND ENTROPY OF ACTIVATION OF RELAXATION OF SEED COTTON

Fiber state	$\Delta H_f^{\ddagger}$ (kcal.)	$\Delta S_f^{\ddagger}$ (e. u.)	$\Delta H_s^{\ddagger}$ (kcal.)	$\Delta S_s^{\ddagger}$ (e. u.)
Air-dry	0.5	−84.4	4.6	−83.1
Water-saturated	0.7	−83.3	5.6	−80.0

TABLE VI. ENTHALPY AND ENTROPY OF ACTIVATION OF RELAXATION OF GIN COTTON

Fiber state	$\Delta H_f^{\ddagger}$ (kcal.)	$\Delta S_f^{\ddagger}$ (e. u.)	$\Delta H_s^{\ddagger}$ (kcal.)	$\Delta S_s^{\ddagger}$ (e. u.)
Air-dry	0.5	−81.1	2.9	−86.2
Water-saturated	0.5	−83.9	2.6	−88.7

that the entropy of activation is related to the number of elements, n, that must assume the preferred orientation before slippage of the chains can occur. This leads to the simplified expression:

$$B^{-n} = e^{\Delta S^{\ddagger}/R}.$$

The exact numerical value of B is uncertain; however, if B is taken to have an average value of 3, the average n is found to be 38. This value of $n = 38$ suggests that the relaxation results from small segmented motions of the chains rather than from the whole chain moving at one time. The relaxation must occur at least partly in the amorphous region of the fiber. Presumably, n will differ in the crystalline and the amorphous regions; thus, the n determined in these calculations is an average value for the two regions.

The air-water relaxation studies provide certain information concerning the nature of the relaxation elements. A discussion of these elements will be reserved until later since the investigations using acids are especially significant.

Summary

The relaxation at constant elongation of cotton fibers showed that the relaxation process is complex. The relaxation curve for both the air-dry and the water-saturated cotton fibers can be successfully approximated using the sum of two exponential terms. The relaxation constant for the fast relaxation process is approximately 1,000 times larger than the constant for the slow process. A mechanical model consisting of two Maxwell units in parallel has a relaxation equation, at constant elongation, of the same form as the equation for the relaxation of the cotton fibers. Using this model, it is possible to treat the relaxation constants further, and it is found that the principal portion of the free energy of activation relaxation is in the entropy term.

The theoretical treatment of the data from this work indicated that the relaxation occurs through segmented motion of the chains rather than the whole chain moving at one time.

Table of Chemical and Mathematical Symbols

A—area
C—constant that depends on the force
f—force per unit area
F—force (total)
ΔF—free energy (Gibbs) change
Φ—partition function less vibrational function
g—spring constant
ΔH—enthalpy change
h—Planck's constant
k—Boltzmann's constant
k'—reaction constant
H—transmission coefficient
λ—lateral spacing of relaxation elements
λ_1, λ_2, λ_3—dimensions of relaxation element
η—coefficient of viscosity
R—universal gas constant
r—relaxation constant
ΔS—entropy change
s—elongation
t—time
T—absolute temperature

Subscripts or Superscripts

i—general
f—fast or first process
s—second or slow process
o—initial or zero concentration
$\ddagger$—activation

Literature Cited

1. Alfrey, T., Jr., "Mechanical Behavior of High Polymers," New York, Interscience Publishers, Inc., 1948.
2. Andersen, F., *Trans. Danish Acad. Tech. Sci.*, A.T.S. No. 3 (1950).
3. Glasstone, S., Laidler, K. J., and Eyring, H., "The Theory of Rate Processes," New York, McGraw-Hill Book Co., 1941.
4. Houwink, K., "Elasticity and Plasticity and Structure of Matter," Cambridge University Press, 1937.
5. Mark, H., "Cellulose and Cellulose Derivatives" (E. Ott, editor), New York, Interscience Publishers, Inc., 1943.
6. Meyer, K. H., and Misch, L., in Meyer, K. H., "Natural and Synthetic High Polymers," New York, Interscience Publishers, Inc., 1950, 384 *et seq.*
7. Sookne, A. M., and Rutherford, H. A., *J. Research Natl. Bur. Standards* **31**, 218 (1942).
8. Tobolsky, A., and Eyring, H., *J. Chem. Phys.* **11**, 125 (1943).

(*Manuscript received July 21, 1952.*)

The X-Ray Pattern of Sericin and Silk Wax from *Bombyx mori**

E. H. Mercer† and F. H. Meyer

Textile Research Institute, Princeton, New Jersey

Abstract

Several x-ray reflections occurring in raw silk and in some preparations of sericin, and previously thought to be characteristic of sericin, are shown to arise from silk wax. The wax is associated with the sericin fraction most strongly attached to the fibroin and it is present within the silk gland prior to spinning.

SEVERAL authors [4, 5, 7, 9, 10] have described x-ray patterns believed to be characteristic of sericin, the protein constituent which gums together the fibroin filaments of cocoon silk and which constitutes about 25% of the weight of the cocoon. Certain spacings in the x-ray pattern of raw silk have also been attributed to sericin. The most extensive study was made by Simizu [9], who described three sericins (*I*, *II*, and *III*) distinguished by their ease of removal from raw silk. Since analytical studies [2, 6, 8] show that "sericins" of differing amino acid composition can be extracted, there is little doubt that sericin is not a single protein. Simizu believed that he had shown that sericin *III*, the fraction most difficut to remove from the fiber, gave a number of different spacings from those of the more easily extracted sericins, and therefore had a different structure.

The work described here shows that all sericins give similar x-ray patterns and that the special spacings believed to characterize sericin *III*, and which also are prominent in the pattern given by raw silk, arise from the silk wax, a constituent forming a small fraction (0.5%–1%) of the weight of the cocoon.

Experimental

Preparations

All materials used in this study were obtained from silkworms (*Bombyx mori*) raised in this laboratory.

Sericin

The sericin was extracted from raw silk by aqueous solutions using well-known methods [8, 9]. Other preparations were obtained from the silk glands of mature silkworms in which both sericin and fibroin are found in solution in forms clearly separated from each other. The sericin closely adheres to the inner surface of the skin of the gland and the fibroin forms a core entirely surrounded by sericin [11]. The same relative position of the two proteins is maintained during the passage of the silk stream to the spinnerets and is that found in the extruded thread. This separation made it possible to prepare specimens of the two proteins direct from the gland.

Sericin specimens were made from freshly excised glands by three methods: (*a*) by extracting the glands for 24 hrs. with 1% sodium bicarbonate solution, which dissolves the fibroin core and leaves a hollow tube of sericin; (*b*) by hardening the glands in 25% ethanol in water for 4 hrs., which coagulates both proteins, and the sericin peels off without difficulty; (*c*) by soaking the glands in 1% acetic acid for 1 hr., which also coagulates both proteins. By stretching the gland the fibroin is converted into a strong thread, while the sericin breaks into irregular patches on the surface of the thread and thus separates from the fibroin. Partial orientation of sericin specimens was obtained by stretching and pressing. Fats and waxes were removed when desired by washing in warm ethanol followed by prolonged extraction in boiling toluene.

* This research was sponsored in part by the Office of Naval Research, Navy Department, Contract No. Nonr-09001.

† Staff member, Commonwealth Scientific and Industrial Research Organization, Melbourne, Australia; at present, Visiting Fellow, Textile Research Institute.

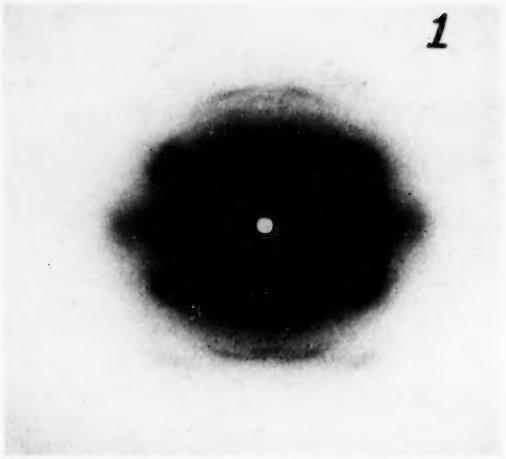

Raw cocoon silk. Note the sharp rings (touched up for emphasis) due to wax impurity.

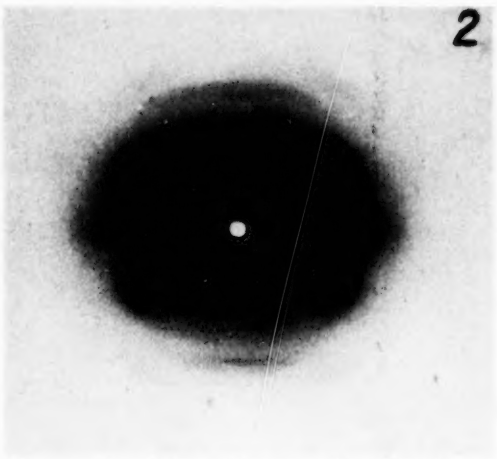

Degummed and dewaxed cocoon silk. Rings due to wax are absent.

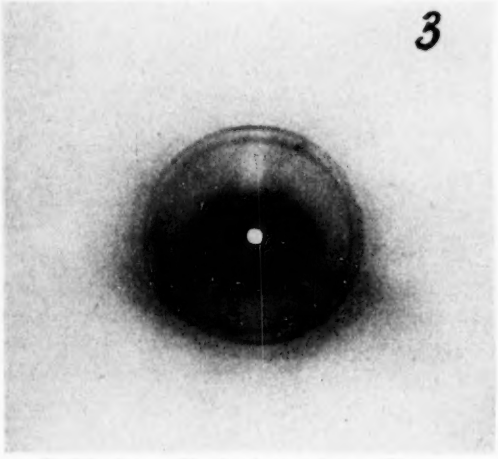

Sericin from silk gland containing silk wax.

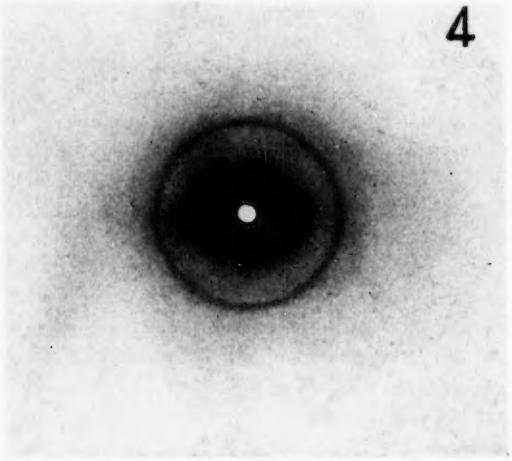

Dewaxed sericin from silk gland.

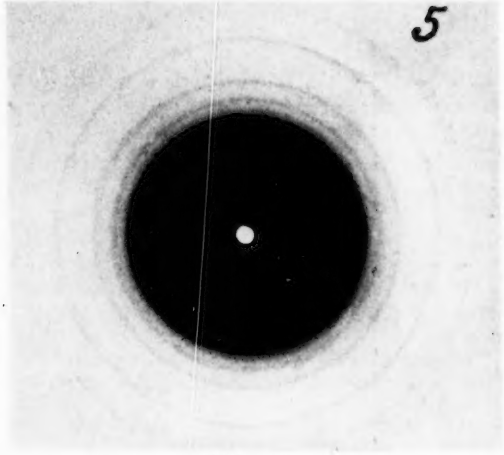

Silk wax.

FIG. 1. *X-ray photographs of silk and silk derivatives. Specimen-to-film distance in each case is 4.0 cm. Copper* K_α *radiation.*

TABLE I

(1) Non-fibroin diffractions of raw cocoon silk		(2) Sericin *I* and *II*			(3) Sericin *III*			(4) Gland sericin		(5) Dewaxed sericin		(6) Silk wax	
d Å.	Int.*	Index	d Å.	Int.*	Index	d Å.	Int.*	d Å.	Int.*	d Å.	Int.*	d Å.	Int.*
		A_1	7.7_2	S	A_1	7.1_2	S	7.7	MS	7.6	S		
		A_2	4.6_5	VS	A_2	4.6_9	MS	4.6	VS	4.6	S		
4.5_9	S	α†	4.6_6	VS	(1)	4.6_9	VS	4.6	S	4.6	S	4.5_5	MS
		A_3	2.9_7	S	A_3	3.0_5	VS						
4.1_2	VS				(2)	4.1_2	VS	4.1	VS			4.1_0	VS
3.7_8	W	I	3.7_4	S	(3)	3.7_6	MS	3.7	MS	3.7	W	3.7_0	S
		$II_{3,1}$	3.3_6	MS				3.4	W	3.4	VW	3.2_5	W
												2.9_6	W
		II_2	2.7_9	W				2.8	W				
												2.4_8	MS
		III_1	2.2_3	W	(4)	2.2_2	W	2.2	W			2.2_0	W
		III_2	2.0_6	W	(5)	2.0_5	W	2.1	W			2.0_8	VW

* VS = very strong; S = strong; MS = moderately strong. d = interplanar spacing.

† α = meridional diffraction (Simizu's notation). It does not fit into the first layer line of the sericin pattern. If it is a sericin diffraction, its presence on the meridian together with a strong diffraction on the equator at 4.6 Å. signify a double orientation of the crystallites in stretched sericin [9].

Fats and Waxes

Freshly spun cocoons were extracted with boiling benzene; the extract was filtered and allowed to evaporate. The residue from white cocoons was yellow in color, that from the yellow variety was brown. Ten grams of raw silk yielded 0.5 g. of wax, as already noted by Bergmann [1].

X-Ray Diffraction

Patterns were recorded on flat films using K_α (filtered) radiation from a Philips copper anode tube. The film-to-specimen distance was 4 cm.

Results

The principal spacings found in raw silk, degummed silk, various sericin preparations, and silk wax are recorded in Table I. The results for silk and sericin are in good agreement with values obtained by earlier workers. Typical x-ray patterns of raw silk, degummed silk, sericin from the gland (*cf.*, Simizu's sericin *III*), dewaxed sericin, and silk wax are reproduced in Figure 1.

Discussion

A comparison of the x-ray photographs in Figure 1 or of the calculated spacings in Table I shows that the strong reflection at 4.1 Å. found in patterns of raw silk (column 1) and some sericins arises from silk wax (column 6). When thoroughly dewaxed, cocoon silk and gland sericin (column 5) do not yield this reflection. The special unit cell proposed by Simizu for sericin *III* on the basis of this reflection is not necessary as there is no x-ray evidence to suggest that sericin *III* differs in structure from sericins *I* and *II*.

It is of interest to note that in the cocoon silk the wax is mainly associated with the most tenaciously held fraction of the sericin—*i.e.*, that most closely adhering to the fibroin core. The observations on the gland show that this wax is secreted in the gland along with the sericin and is not added to the silk at the time of spinning.

Recently Kratky, Schauenstein, and Sekora [3] have reported that certain reflections found in fibroin arise from a wax impurity. Their findings agree with those described here except that in the present material the wax seems to be mostly associated with the sericin and little trace can be found in fibroin when the sericin has been thoroughly removed.

Acknowledgment

The authors would like to thank Miss Dorothy O'Reilly for her aid in printing the x-ray patterns of Figure 1.

Literature Cited

1. Bergmann, W., Textile Research Journal **9**, 175 (1939); **8**, 195 (1938).
2. Bryant, F., Textile Research Journal **22**, 523 (1952).

3. Kratky, O., Schauenstein, E., and Sekora, A., *Nature* **170**, 796 (1952).
4. Matsunaga, Y., *J. Soc. Chem. Ind., Japan* **39**, B465 (1936).
5. McNicholas, H. J., TEXTILE RESEARCH JOURNAL **11**, 39 (1940).
6. Rutherford, H. A., and Harris, M., TEXTILE RESEARCH JOURNAL **10**, 221 (1940).
7. Sakurada, I., and Matusita, Y., *J. Soc. Chem. Ind., Japan* **40**, 58B (1937).
8. Shaw, J. T. B., and Smith, S. G., *Nature* **168**, 745 (1951).
9. Simizu, M., *Bull. Imp. Sericult. Expt. Sta., Japan* **10**, 441 (1941).
10. Trogus, C., and Hess, K., *Biochem. Z.* **260**, 376 (1933).
11. Yamanouchi, M., *J. Coll. Agr., Hokkaido Imp. Univ.* **X**, Part 4 (1921).

(*Manuscript received January 2, 1953.*)

The Identification of Synthetic Fibers by Their Refractive Indices and Birefringence

A. N. J. Heyn*

School of Textiles, Clemson Agricultural College, Clemson, South Carolina

Abstract

A simple method is described for the differentiation of synthetic fibers by their refractive indices and birefringence, using the technique of central illumination.

IN a previous communication [2] the results were reported of a comparative study of the refractive index and birefringence of synthetic fibers with special reference to their identification. The present paper is a continuation of this study and applies the data in a simple method of differentiation and identification of these fibers.

It is possible, of course, to identify the fibers by determining exactly their refractive index and birefringence with the methods used in the former article and by comparing the values obtained with the data reported there. The accurate determination of the two indices of refraction by the Becke-line method, however, not only requires the use of a complete set of accurately calibrated immersion liquids, but in certain cases also involves a great deal of eyestrain and concentration. The determination of birefringence from the polarization colors, furthermore, is not very accurate for noncylindrical fibers, and requires special care and precaution in cases where the birefringence is either very low or very high (see [4] for the case of Dacron).

For the purpose of differentiation, quicker methods can be worked out which do not involve accurate determination of the indices. The present study describes such a method. The most important requirements for such a simple routine method are: ease of operation; use of only a limited number of easily available immersion liquids; and exclusion of the use of complicated polarizing accessories or a special microscope.

Of the various possibilities tried, the method described here met all of the requirements and proved very useful. It is not claimed that the method suggested is the only answer; many other methods can be worked out along the same lines.

Principles Applied for a Simple Method of Identification

Use of the Central Illumination Method

Apart from the observation of the Becke line, two other immersion methods are known for the determination of refractive index—namely, the method of central illumination and the method of oblique il-

* Professor of Natural and Synthetic Fibers.

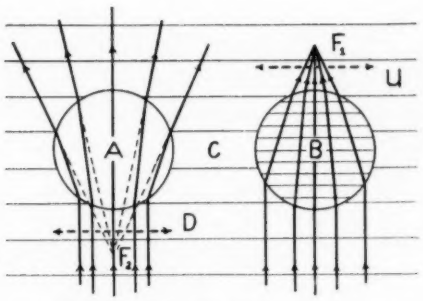

Fig. 1. *Diagram showing the refraction of light by a fiber of lower* (A) *and higher* (B) *refractive index than that of the medium* (C). *In the first case a bright line is observed in focusing down* (*plane* D), *and in the second case in focusing up* (*plane* U).

lumination. The latter method does not offer a great simplification over the Becke method, since Saylor [5] pointed out that it must be carried out with special precautions in order to give reliable results. The method of central illumination, however, proved to be extremely easy and suitable for the investigation of fibers in cases where high accuracy is not required.

The principle of this method is that any solid of roughly lenticular or circular cross section embedded in an immersion medium acts as a biconvex lens. If the fiber is immersed in a medium of lower index, it will act like a convex lens, so that a light concentration is formed at some distance above the fiber (see Figure 1). If the microscope is focused on the fiber, this light concentration will not be observed, but if the microscope is raised and focused above the fiber, the light concentration is observed as a bright band in the center of the cylindrical fiber. If the refractive index of the medium is higher than that of the fiber, the light concentration will be observed when the microscope is lowered and focused below the fiber (when the microscope is focused above the fiber, a dispersed brightness is observed outside the fiber edge). Similar light concentrations are observed when the fiber is not exactly cylindrical, but in that case the bright band may be found somewhere else than in the center or sometimes more than one bright band may be observed (*e.g.*, in fibers with dog-bone-shaped cross section, where two bands generally appear). The phenomenon of central illumination is distinct from the phenomenon of the Becke line in that the former is mainly the result of the refraction of light by the fiber and the latter the result of the reflection of light at the interface of fiber and liquid. In practice, the fiber shows a composite effect in which both central illumination and the Becke effect play a part in such a way that they reinforce each other. In changing the focus, the Becke line may be seen to move towards the inside of the fiber and to fuse together with the central light band.

Use of Intermediate Immersion Liquids for Fibers of High Birefringence

If the method of central illumination is used with a fiber of high birefringence immersed in a liquid of a refractive index intermediate between the two indices of the fiber, the following interesting phenomena will be observed (see Figure 2): if the fiber is observed with polarized light vibrating parallel to the fiber axis, the central bright light band will appear when the microscope is focused up; if the fiber is observed with light vibrating perpendicular to the fiber axis, the bright band will appear when the microscope is focused down.* When these phenomena are observed, it may be concluded that the index of the liquid used lies between the indices of the fiber. A single Polaroid polarizing disc inserted in the eyepiece or somewhere under the stage is sufficient to produce the polarized light; it is not even necessary to know its vibration axis, and no complicated polarizing devices or special microscope are necessary.

In this way the birefringence and refractive indices of a fiber can be used in a simple way for its identification, as is shown in more detail below.

The Absence of Birefringence in Certain Fibers

Some synthetic fibers, like glass fiber and Vinyon HH, have been found to have no birefringence at all. These fibers can be identified easily. When rotating the fiber in the dark field between crossed polarized discs, no polarization colors will be observed.

Use of a Few Selected Liquids

Of the commercially available liquids, those are selected which have refractive indices intermediate between the two indices of the fibers in question. For a fiber of high birefringence, many liquids of various refractive indices will meet this requirement, and a large difference will exist between the intermediate index of the liquid and each of the refractive

* Presuming that the fiber has positive birefringence; in the case of negative birefringence, the reverse would be true.

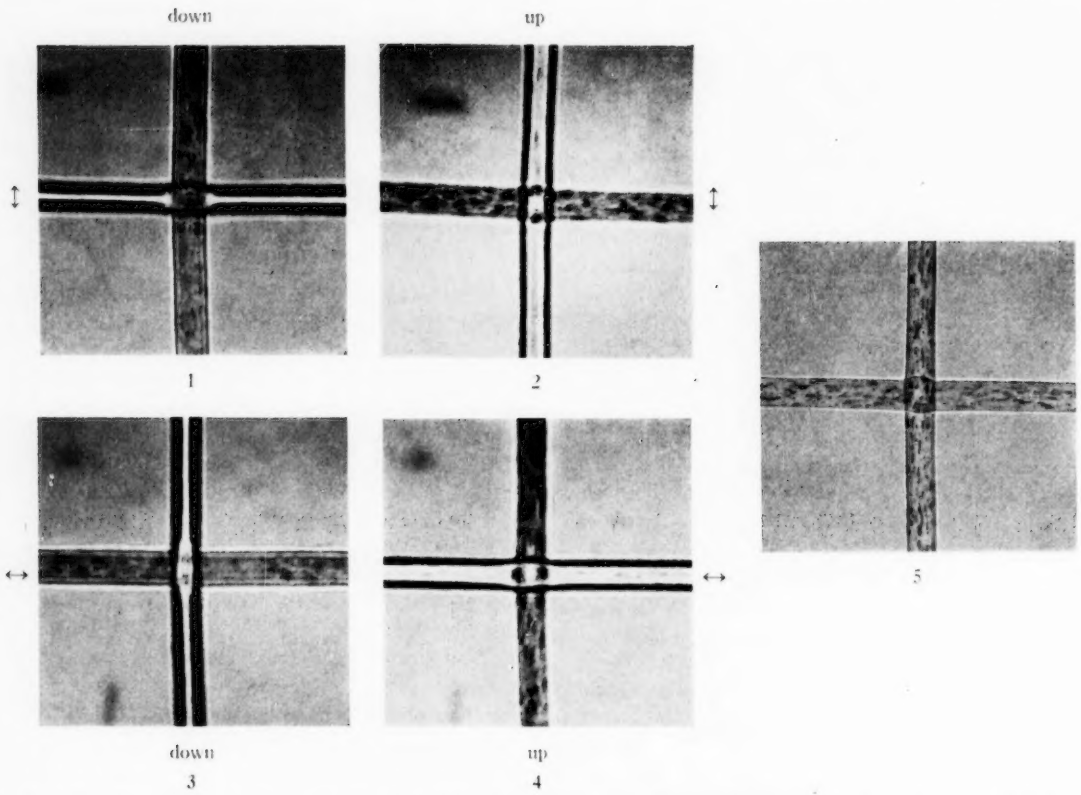

FIG. 2. *Photomicrographs (magnification, 200 ×) of two crossed Dacron fibers immersed in α-bromonaphthalene (n = 1.657). Plane of light vibration is along vertical line in 1 and 3 (refractive index of vertical fiber 1.700 and of horizontal fiber 1.532), and along horizontal line in 2 and 4 (refractive index of vertical fiber 1.532 and of horizontal fiber 1.700). The microscope was focused down in 1 and 3 and up in 2 and 4, and was in correct focus in 5. A stronger lens action is observed when focusing down in 1 and 3 because the difference between the refractive indices of the medium and the fiber (1.657 and 1.532) in these cases is larger than when focusing up in 2 and 4, where the difference is smaller (1.657 and 1.700). The same phenomena are observed with nylon mounted in methyl salicylate.*

indices of the fiber. Under these conditions the phenomena of central illumination will always occur.

For a fiber of low birefringence, the index of the liquid will be very near to that of the fiber, and the difference in indices will be too small to result in a clear appearance of the central illumination bands. In this case the fiber will be almost invisible in all positions under the polarizing disc, and this will usually allow identification. The observation of the Becke line may be used in addition.

The liquids selected after some experimentation were *alpha*-bromonaphthalene ($n = 1.657$), methyl salicylate ($n = 1.537$), and monochlorobenzol ($n = 1.522$). Of course, other similar liquids may be used in the same way.

Description of Special Procedure for Identification

The fiber is mounted in the test liquid and illuminated by a symmetrical cone of light focused for the best results approximately in the plane of the fiber. It is necessary that the angular aperture of the light cone be less than the aperture of the objective.

The behavior of various synthetic fibers in the three liquids listed above is summarized in Table I. The first column in this table gives the various fibers in the order of their refractive indices (given in the second column), and the other columns described the behavior of the fiber in each of the three immersion liquids.

Bromonaphthalene has a refractive index inter-

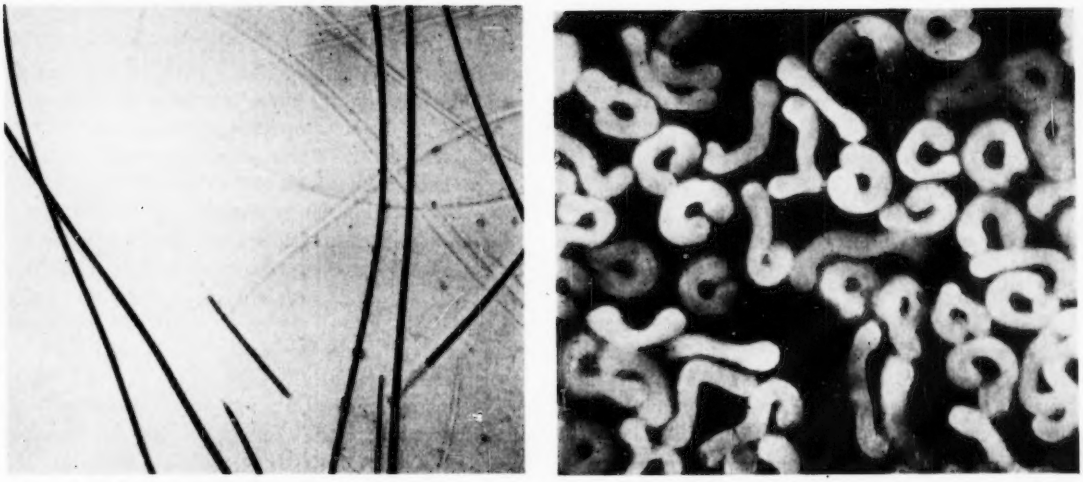

Fig. 3. Left—*Dynel mounted in methyl salicylate; the fibers are almost invisible except for lines of entrapped air (magnification, 100 ×).* Right—*Cross sections of fibers from which the presence of entrapped air can be understood (magnification, 500 ×).*

TABLE I. Differentiation of Synthetic Fibers by Their Refractive Indices, Following the Method of Central Illumination‡

Fiber	Refractive index n_γ*	Refractive index n_α†	Immersed in α-bromonaphthalene (n = 1.657)	Immersed in methyl salicylate (n = 1.537)	Immersed in monochlorobenzol (n = 1.522)
Orlon	1500–1510	1500–1510	Down	Down	Down (clear fibrillation)
X-51	1.520	1.516	Down	Down	Almost equal (Becke line indicates lower n; little structure)
Acrilan (Vinyon HH)	1.524	1.520	Down	Down	Equal (intense pitting)
	1.526	1.526	Down	Down	Almost equal (no pitting)
Dynel (Vicara-Alginate)	1.536	1.531	Down	Equal	Up
Nylon		1.519	Down	Intermediate Down	Up
	1.582		Down	Up	Up
Dacron		1.532	Intermediate Down	Up	Up
	1.700		Up	Up	Up

* The vibration direction of light is parallel to the fiber axis except for X-51 and Acrilan, where the direction is perpendicular to the fiber axis.

† The vibration direction of light is perpendicular to the fiber axis except for X-51 and Acrilan, where the direction is parallel to the fiber axis.

‡ Up: bright band observed when the microscope is focused up; refractive index of fiber is higher than that of the medium. Down: bright band is observed when the microscope is focused down; refractive index of fiber is lower than that of the medium. Equal: no bright band observed on either focus; refractive index of fiber is close to that of the medium. Intermediate: bright band is observed when the microscope is focused up when the light is vibrating in the one direction of the fiber, and when the microscope is focused down when the light is vibrating in the other direction of the fiber; refractive index in one direction of the fiber is higher and in the other direction is lower than that of the medium.

mediate between those of Dacron,* and therefore the phenomena of central illumination are exhibited by the fiber in this medium (see Figure 2).

The same holds true for nylon when immersed in methyl salicylate. Dynel, Vicara, and alginate fibers have low birefiringence and become practically invisible in this liquid. The presence of air trapped in the surface folds of Dynel results in typical dark streaks over long areas in parts of the fiber (see Figure 3); no central illumination band is observed on defocusing.

In monochlorobenzol Acrilan becomes almost invisible except for the external and internal pitting which is overemphasized as a result of the high transparancy of the fiber. No central illumination is observed on defocusing. X-51 is not fully invisible in monochlorobenzol, and a faint outline (but very little further structure) may be observed in either position under the polarizer. (Becke lines corresponding to a slightly lower refractive index may be observed.) Orlon immersed in monochlorobenzol shows clear central illumination on focusing down, which distinguishes this fiber from the foregoing ones; clear fibrillation is observed. The refractive indices of the various types of this fiber—no. 81, no. 41, and staple—were found to vary between 1.502 and 1.510.

Glass fiber and Vinyon HH are differentiated from the above fibers by the absence of birefringence, as discussed previously.

The following identification key is based on the above procedure:

1(a)	Fiber does not show any polarization color under crossed polarizers.	Vinyon HH or glass fiber
(b)	Fiber shows stronger or weaker polarization colors under crossed polarizers.	*2*
2(a)	Refractive index of *alpha*-bromonaphthalene is intermediate between the indices of the fiber, as shown by bright band observed on focusing up with one setting and on focusing down with the other setting of the polarizer disc.	Dacron
(b)	Refractive index of *alpha*-bromonaphthalene is higher than the indices of the fiber, as indicated by bright band only on focusing down.	*3*
3(a)	Refractive index of methyl salicylate is intermediate between the indices of the fiber, as shown by bright band observed on focusing up with one setting and on focusing down with the other setting of the polarizer disc.	Nylon
(b)	Refractive index of methyl salicylate is equal to that of the fiber, as shown by very faint visibility.	Dynel (Vicara, alginate)
(c)	Refractive index of methyl salicylate is higher than that of the fiber, as indicated by bright band on focusing down.	*4*
4(a)	Refractive index of monochlorobenzene is equal to that of the fiber, as shown by the faint outline and the absence of bright band on either focus; strong pitting is observed throughout the fiber.	Acrilan
(b)	Refractive index of monochlorobenzene is slightly lower than that of the fiber, as indicated by the absence of bright band on either focus and the presence of Becke lines corresponding to a lower refractive index; very little structure.	X-51
(c)	Refractive index of monochlorobenzene is considerably higher than that of the fiber, as indicated by one or two bright bands on focusing down; clear fibrillation is observed in this liquid.	Orlon

Comparison of the Method of Refractive Indices with Other Identification Methods

It is hoped that the principle indicated here and the method suggested may be helpful in the identification of synthetic fibers.

The few methods suggested previously combine tests of density, morphological characteristics, and solubility [1], or use a combination of morphological characteristics, color tests (identification stains), and solubility tests [6], and are therefore rather compli-

* The refractive index, n_γ, of Dacron was found to be 1.700 with three commercial samples investigated with the Becke-line method. This finding complements the determination of n_α in the author's previous paper [3] and is in agreement with the observations by Quynn and Steele [4].

cated. The use of the refractive index and birefringence as described here is both easy and effective for the main differentiation of these fibers, especially when the outstanding morphological characteristics mentioned are also taken into account. A special advantage of the method is that it can also be applied in most cases with dyed fibers (color tests, for example, require that the fiber be stripped). Circumstances should decide which method is to be used, and one method may complement the other. For further discussion and comparison of methods refer to [3].

Acknowledgment

Appreciation is expressed to Assistant Professor J. S. Graham of the School of Textiles, Clemson Agricultural College, for drawing Figure 1.

Literature Cited

1. Fisher, D. C., and Roberts, E. D., Analysis of Staple Fiber Mixtures, Textile Research Journal **22**, 509 (1952).
2. Heyn, A. N. J., Observations of the Birefringence and Refractive Index of Synthetic Fibers with Special Reference to Their Identification, Textile Research Journal **22**, 513 (1952).
3. Heyn, A. N. J., "Fiber Microscopy," New York, Interscience Publishers, Inc. (in press).
4. Quynn, R. G., and Steele, R., Letter to the Editor, Textile Research Journal **23**, 258 (1953) (this issue).
5. Saylor, C. P., Accuracy of Microscopical Methods for Determining Refractive Index by Immersion, *J. Research Natl. Bur. Standards* **15**, 277 (1936).
6. Wilson, W. R. (American Viscose Corp.), "A Systematic Scheme of Fiber Analysis by Solvent Action," paper given at a meeting of the Am. Assoc. Textile Technologists, Oct. 1, 1951.

(Manuscript received January 26, 1953.)

Magnetic Anisotropy of Cellulosic Materials*

L. Loeb and L. A. Welo†

Southern Regional Research Laboratory,‡ New Orleans, Louisiana

Abstract

The results of a survey of the magnetic anisotropy of a group of cellulosic materials measured according to the Krishnan "oscillation" method are presented. The technique is described for the application of this method to the measurement of the anisotropy of fibrous materials.

Experimentally it was found necessary to subject the samples to brief pretreatment with cold, dilute acid in order to obtain concordant results for a given material. Data are given to show the effect on the observed anisotropy of variations in this pretreatment.

The results of magnetic anisotropy measurements are discussed as to their possible usefulness in characterizing molecular orientation. It is shown that for materials of a given crystalline modification (cellulose *I* or *II*) the observed anisotropy is primarily a function of molecular orientation, but that the anisotropy varies with orientation in a different manner for the two crystalline modifications. The influence of variations in the amount of crystalline material on the observed anisotropy is also briefly discussed.

WHILE magnetic anisotropy has thus far received little attention in fiber research, other anisotropic properties have been known for many years and have been studied in detail. The direction-dependence of the refractive index was probably the first of the anisotropic properties observed in fibers, and was cited by early workers as proof of the presence of crystalline elements within the fiber. It is now known that the double refraction arises from the inherent optical anisotropy of the chainlike macromolecules and from the preferred axial orientation of the molecular chains which constitute the fiber. Preston and Bhat [11] discussed the evaluation of molecular orientation from swelling anisotropy and double refraction data, and

* Report of a study made under the Research and Marketing Act of 1946. Presented at the Southwide Chemical Conference, American Chemical Society, held at Auburn, Ala., Oct. 23–25, 1952.

† Present address: 924 Fillmore Ave., New Orleans, La.

‡ One of the laboratories of the Bureau of Agricultural and Industrial Chemistry, Agricultural Research Administration, U. S. Department of Agriculture.

concluded that these two anisotropies depend upon the orientation of the fiber as a whole, including both the crystalline and amorphous regions. Hermans [3] has also shown that, at least for highly oriented fibers, the orientation parameter for the whole fiber as determined by double refraction measurements agrees well with the orientation parameter for the crystallites as determined by x-ray diffraction.

For materials which can be obtained as single crystals, Krishnan [5, 6] has shown that a knowledge of the principal magnetic susceptibilities measured on the crystal can in some cases give a great deal of information concerning the relative orientation of the molecules in the unit cell. Although Selwood [14] suggested the utility of such magnetic studies in determining molecular orientation in fibrous high polymers, the literature reveals few such studies.

Cotton-Feytis [1, 2] demonstrated the generality of magnetic anisotropy by the examination of several types of natural cellulosic and proteinaceous fibers and of stretched crude rubber. All of the fibers studied showed varying degrees of anisotropy, the magnitude of which roughly paralleled the degree of orientation as measured by x-ray diffraction.

Nilakantan [9] made a detailed magnetic study of wood cellulose derived from teakwood. He examined the samples after various treatments leading to the isolation of high-purity *alpha*-cellulose, and found the specific anisotropy to be proportional to the cellulose content of the specimen. The raw wood after extraction with alcohol-benzene and boiling water exhibited a specific anisotropy of 39×10^{-10} in c.g.s. electromagnetic units; the high-purity *alpha*-cellulose obtained after complete chlorination gave a value of 92×10^{-10}. His results further showed that the more negative diamagnetic susceptibility lay along the fiber axis, and that in the cellulose macromolecule the axis of greater diamagnetic susceptibility was along the direction of the main-valence chains.

Selwood, Parodi, and Pace [15] have shown magnetic anisotropy to be an extremely sensitive criterion for evaluating changes in molecular orientation in fibrous materials. In their work on the polymer polyethylene terephthalate they measured the magnetic anisotropy on a series of filaments which had been subjected to varying degrees of stretch during preparation. They found that the anisotropy increased linearly as a function of stretch up to a draw ratio of about 3.8:1. Beyond this point the anisotropy began to increase very rapidly with increasing draw ratio. They interpreted the break in the curve as indicating the inception of crystallization due to stretching the substantially amorphous polymer.

In view of the work on other polymers, it appears that magnetic anisotropy should be useful in characterizing molecular orientation in cellulose. In the present study, magnetic anisotropy measurements have been made on a series of cellulosic materials, including both native and regenerated fibers, as well as on some materials which had been modified in this laboratory by chemical treatment. The possible usefulness of such magnetic measurements in characterizing molecular orientation in cellulosic fibers is discussed, and an attempt is made to compare the results with those obtained with some of the better-known methods for evaluating orientation.

The results presented here should be considered only as a preliminary survey of the magnetic anisotropy of certain cellulosic materials, and the correlation presented should be taken as tentative but indicative of the possible direction for further work.

Method of Measurement

In his work on the magnetic anisotropy of crystals, Krishnan devised two experimental methods for measuring directly the difference between any pair of principal magnetic susceptibilities. The anisotropy values reported here have all been made by using Krishnan's "oscillation" method [5], with some modification required in order to apply the method to fibrous materials. Although the method gives no information concerning the absolute values of the magnetic susceptibility, it does measure with high accuracy the difference between principal susceptibilities. When a sample of anisotropic matter is suspended in a uniform magnetic field, a couple is set up due to the anisotropy, which tends to set the axis of greater susceptibility in the plane of oscillation parallel to the field direction. Throughout this paper, the term "greater," when applied to susceptibility, refers to its alegbraic value. In the case of a diamagnetic substance, such as cellulose, all principal susceptibilities are negative; the axis of less negative susceptibility will therefore align itself with the field direction. When the torsion of the suspension filament is known, the couple due to the anisotropy can be evaluated from the period of oscillation of the sample in the magnetic field.

The difference in susceptibility for the two axes in the plane of oscillation is related to the observed pe-

riod of oscillation and the constants of the system according to the following equation:

$$\chi_1 - \chi_2 = \frac{T_a^2 - T_i^2}{T_i^2} \cdot \frac{C}{H^2} \cdot \frac{1}{m},$$

where χ_1 and χ_2 are the maximum and minimum values of the specific susceptibility of the sample in the plane of oscillation; T_i is the period of oscillation in magnetic field and T_a is the period with the influence of the field removed; C is the torsion constant of the suspension filament in dyne-centimeters per radian; H is the field strength of the magnetic field in oersteds; and m is the mass of the sample in grams.

It is generally accepted that fibers may be considered as uniaxial, symmetrical bodies with random orientation about the fiber axis [4]. Thus, the anisotropy of a fiber is completely specified by determining $\chi_{\parallel} - \chi_{\perp}$, where $\chi_{\parallel}$ is the susceptibility parallel to the fiber axis and $\chi_{\perp}$ is the mean of the two principal susceptibilties in the plane perpendicular to the fiber axis. In order to bring these two axes of principal susceptibility onto the plane of oscillation, the sample bundles were suspended with the fiber axis horizontal. The oscillation took place about a transverse axis through the center of the bundle, and the anisotropy ($\chi_{\parallel} - \chi_{\perp}$) was determined by a single measurement.

Apparatus

The magnetic field employed was furnished by a large permanent magnet which was fitted with pole pieces designed to give a uniform field in an air gap 1.0 in. in length and 2.0 in. in diameter. The field strength was determined in the usual manner with a small test coil and ballistic galvanometer; the field strength was found to be 8360 ± 20 oersteds. The uniformity of the field was mapped by noting the period of oscillation of a small, well-formed crystal of potassium nitrate at various points in the field within the region normally occupied by the sample bundles. The maximum deviation in field strength relative to the average strength at the center was found to be less than 0.5%.

This magnet was mounted on a brass turntable which allowed the magnet to be rotated about a vertical axis. The turntable was set upon a chain-driven rolling carriage which served to move the magnet over a horizontal distance of 16 in. With the magnet removed the full 16 in., the field strength of the sample was effectively zero.

Fine gold filaments (.0008–.001 in. nominal diameter) were employed as suspension fibers. The torsion constant of each filament used was determined by measuring the period of oscillation of a nonmagnetic mass of known inertia. For the several suspensions employed during this work, the torsion constant, C, varied within the range .008 to .030 dyne-centimeters per radian.

A short straight length of number 30 copper wire was soldered to the lower end of the suspension filament. The bottom end of this copper wire was bent up to form a small flat hook on which the sample bundles were hung.

The upper end of the suspension filament was soldered to a ¼-in. brass rod; this rod was in turn affixed to the center of rotation of a torsion head. The whole of the suspension system was protected from disturbing air drafts by a glass tube. The lower end of the glass tube was silvered on the inner surface and grounded in order to eliminate interferences due to electrostatic attraction between the sample bundle and the tube. The sample bundles were illuminated

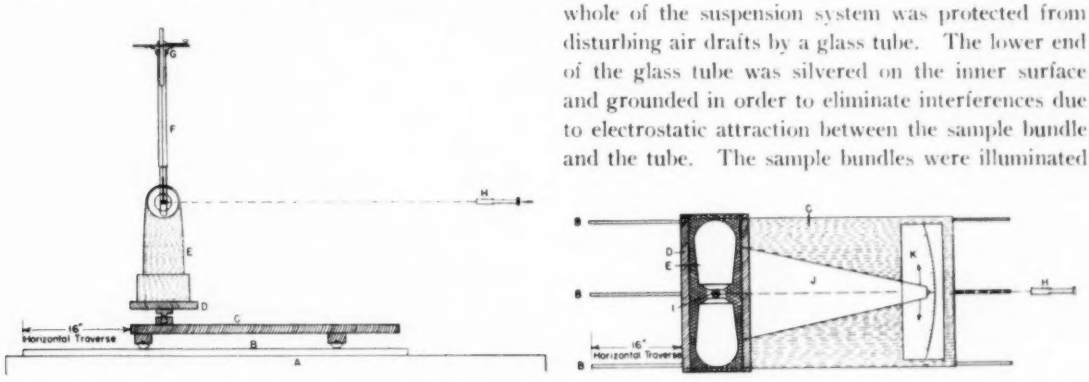

Fig. 1. *Schematic drawings of magnetic anisotropy apparatus.* Left—*Elevation view.* Right—*Plan view.* A, *table top;* B, *tracks;* C, *rolling carriage;* D, *turntable;* E, *magnet;* F, *suspension fiber;* G, *torsion head;* H, *telescope;* I, *sample bundle;* J, *angular indicator;* K, *angular scale.*

by a beam of light focused on the bundle, and the oscillations were observed with a small telescope approximately 1 meter from the sample. The telescope was so adjusted that its line of signs was horizontal and perpendicular to the field direction when the magnet was in its normal position. A small fiducial mark was burned on the center of one end of the sample bundle, and the oscillation period was determined by measuring the time required for this mark to pass the telescope cross hairs a given number of times.

Schematic drawings of the apparatus, shown in elevation and plan views, are given in Figure 1.

Preparation of Sample Bundles

Most of the materials studied were in the form of loose-twisted singles yarns. Small skeins of these yarns were wound on a grooved brass jig, care being taken to keep the yarns accurately parallel during the winding of the skeins. Depending upon the material, sufficient yarns were placed on the jig to give compact bundles approximately $\frac{3}{8}$ in. in diameter. The skeins were extracted with hot ethyl alcohol to remove any waxes or finishing oils. They were then compacted by drawing through a $\frac{3}{8}$-in. hole in a Bakelite form. While drawing through the form, a single turn of yarn was tied about the skein at $\frac{3}{4}$-in. intervals along the length of the skein. After tying, the skein was cut into sample bundles with an electrically heated platinum wire. The bundles thus formed were approximately $\frac{3}{8}$ in. in diameter and $\frac{1}{2}$ in. in length, with a tie at each end, and weighed 0.5 g. or less.

In some of the first measurements attempted, much difficulty was experienced in that the orientation assumed by the bundles in the magnetic field was not reproducible but varied from bundle to bundle. This erratic behavior was attributed to the presence of ferromagnetic impurities either in the sample yarns initially or introduced during the manipulation incident to preparing the bundles. A brief treatment with cold, dilute hydrochloric acid was found to alleviate this erratic action. The usual procedure was to take two skeins of each material studied. One skein was washed with normal hydrochloric acid for 30 min. at 0°C while still in skein form and again for 30 min. on the bundles after tying and cutting (referred to as the 30/30 treatment in Table I). The second skein was cut into bundles and a single 30-min. acid treatment was applied to the bundles after tying and cutting. Several variations of the acid pretreatment and the results achieved are given below. After each treatment the acid was removed by thorough washing with numerous portions of cold water; then with one portion of cold normal ammonium hydroxide; and again washed thoroughly with water. The samples were air-dried in vacuum at room temperature and then were allowed to equilibrate with the humidity of the laboratory atmosphere for at least a day before measuring.

Procedure

The measurements were made as follows: After the sample bundle was mounted on the suspension, with the long axis horizontal, the torsion head was rotated angularly so as to make the bundle axis coincident with the line of sight of the telescope. The sample was then allowed to execute torsional oscillations, these oscillations being initiated by a momentary manual displacement of the torsion head. After the quantity T_o was determined, the magnetic field was then brought up around the sample. The angular position was again adjusted so as to make the bundle axis coincide with the cross hairs of the telescope. For this adjustment the torsion head was not changed, but the magnet was rotated slightly on its vertical axis in order to achieve the required adjustment in the angular position of the bundle. This procedure insured that the suspension filament was under zero torsion when the sample was in its rest position in the magnetic field. This last condition—that the oscillation take place about a position of zero torsion—is one of the prerequisites of the method. The bundle was then allowed to execute torsional oscillations about this position of minimum torsion and the quantity T_i was determined. The samples were then transferred from the suspension to previously weighed containers, and the oven-dry weight was determined. All anisotropies were calculated on the basis of the oven-dry weight.

Crystallite Orientation Measurements

X-ray orientation measurements were performed on fiber bundles of the same materials for which magnetic measurements had been made. The angle between maximum and half-maximum intensity on the (002) diffraction arc was taken as an arbitrary measure of crystallite orientation. The intensity distribution along the (002) diffraction arc was obtained from azimuthal tracings prepared with a Geiger

TABLE I. Results of Magnetic Anisotropy Measurements for Various Cellulosic Materials

Item No.	Material and description	Magnetic anisotropy $-(\chi_n - \chi_\perp)$ 30/30* (e.m.u. × 10^{19})	30* (e.m.u. × 10^{19})	.5* (e.m.u. × 10^{19})	Angular width of 002 arc at half-maximum intensity (degrees)
1	Ramie yarn, 20/2 metric	105.4 ± 1.0	103.8 ± 1.6		9.0
2	Ramie yarn, 20/3 metric	92.1 ± 0.9	92.5 ± 0.9		9.5
3	Fortisan yarn, 1100/1440, 2.5Z			83.7 ± 0.7	7.6
4	Rayon yarn, Fiber G, 240/120	87.1 ± 0.9	83.4 ± 0.6	83.0 ± 0.5	9.2
5	Cotton yarn, kier-boiled, 20/1	66.0 ± 0.5	65.3 ± 0.8	65.5 ± 0.4	27.1
6	Cotton yarn, Wilds 1943, 17.5/1	60.4 ± 0.5	62.8 ± 1.3		27.7
7	Cotton yarn, 13.75/2	55.9 ± 0.9	56.6 ± 0.7		30.6
8	Rayon yarn, Cordura, 1100/480	56.2 ± 1.4	55.4 ± 1.2		14.4
9	Rayon yarn, textile, 150/60	50.2 ± 1.2	48.9 ± 1.0		16.3
10†	Cotton yarn, ethylamine-treated	46.8 ± 1.3	42.5 ± 1.2	44.1 ± 0.8	28.0
11†	Cotton yarn, ethylamine-treated and water-boiled 2 hrs.	49.5 ± 0.9	47.8 ± 0.7	53.1 ± 0.6	29.8
12†	Cotton yarn, mercerized constant length	64.7 ± 0.5	65.5 ± 1.4		24.0
13†	Cotton yarn, mercerized no tension	34.1 ± 0.6	31.5 ± 0.8		27.3

* Indicates minutes of acid treatment with *N* HCl at 0°C (30/30 refers to dual treatment discussed in text).
† Items 10–13 were derived from the kier-boiled singles yarn (item 5).

counter x-ray spectrometer and a special rotating specimen mount developed in this Laboratory [12]. With this rotating specimen mount, the intensity distribution along the diffraction arc is received by the counter which had been set previously at the proper radial angle. As the sample rotates, the intensity of radiation as received by the counter is automatically traced on a strip-recorder.

Results

The magnetic anisotropy results for the various materials studied are summarized in Table I. The results are entered under the column headings that indicate the time of acid treatment applied to the sample bundles prior to measurement. Each anisotropy value is the mean of at least four, and usually six or more, determinations on separate bundles. The standard error of each set is entered together with the mean value. The results of the crystallite orientation measurements are given in the last column of the table.

A brief study was made to determine the effect of various pretreatments on the measured anisotropy. The kier-boiled cotton yarn (item 5, Table I) was selected as the control, and was subjected to the pretreatment listed in Table II. It seems apparent from these data that some pretreatment is necessary prior to measurement. Although a simple wash with distilled water at room temperature is partially effective, a further increase in anisotropy is observed following a brief acid wash at 0°C. It also seems apparent that the acid wash is most effective when applied to the bundles after tying and cutting rather than to the sample in skein form. From the data for the rayon yarn, Fiber G, it is again evident that a brief acid wash of 5 min. suffices to render the resultant anisotropies consistent with the results for samples which had received the longer treatments.

As previously discussed, untreated bundles for some materials assumed erratic orientations in the

TABLE II. Effect of Pretreatment on Observed Anisotropy

Duration of treatment: 1.0*N* HCl at 0°C, Applied to skeins (min.)	1.0*N* HCl at 0°C, Applied to bundles (min.)	Water at 25°C, Applied to bundles (min.)	Anisotropy on oven-dry basis $-(\chi_n - \chi_\perp)$ (e.m.u. × 10^{19})
Cotton yarn			
0	0	0	44.3
0	0	60	55.0
30	0	0	56.3
30	0	60	61.6
0	5	0	65.5
0	30	0	65.3
30	30	0	66.0
Rayon yarn			
0	5	0	83.1
0	10	0	82.2
0	15	0	83.8
0	30	0	83.4
30	30	0	87.0

magnetic field. After the briefest acid treatment, all of the materials studied invariably assumed an orientation with the long axis perpendicular to the field direction. From theory it is known that the axis of greater susceptibility in the plane of oscillation will set itself parallel with the field. In cellulose the axis perpendicular to the fiber axis has therefore the greater algebraic susceptibility and is less diamagnetic; and the fiber axis is the greater diamagnetic axis. It follows that in the cellulose macromolecule the axis of greater diamagnetic susceptibility lies along the length of the main valence chains. This is in conformity with the results of Nilakantan [9] on cellulose from teakwood and with the general rule of Lonsdale [7], which states that for organic molecules containing few or no multiple bonds the maximum diamagnetic susceptibility and maximum refractivity correspond to the greatest dimension of the molecule.

Discussion

It is known that long-chain diamagnetic molecules are, in general, anisotropic [7]; and that when such anisotropic molecules are arranged in a regular manner, as in a crystal, the resultant anisotropy of the gross structure is primarily dependent upon the relative orientation of the molecules in the unit cell. Thus, it is the arrangement of the cellulose chains, with their lengths more or less parallel to the fiber axis, which gives rise to the observed anisotropy, and the magnitude of this anistropy should in turn give a measure of the degree of molecular orientation.

Hermans [3] has shown that cystallite orientation as determined by x-ray diffraction and that as determined for the whole fiber from double refraction measurements agree well, at least for highly oriented fibers. Since according to theory magnetic and optical anistropy studies can be expected to give analogous results [5], it seemed reasonable that the magnetic data would also correlate well with x-ray data. The relation between the half-maximum angles, the present measure of crystallite orientation, and the magnetic anisotropy of the various materials is shown in Figure 2; each point is identified in accordance with the item numbers from Table I.

It can be seen that the data would be meaningless if it were necessary to use a single relation for all of the points. However, if the materials are divided with respect to crystalline modification (cellulose *I* or cellulose *II*), then the data fall along two distinct lines.

In order to discuss these data further, certain pertinent results of Hermans' study of optical anisotropy will be noted here. He concluded that the following factors influence the optical anistropy of a fiber at ideal or complete longitudinal orientation: (*1*) the modification of the crystalline part; and (*2*) the percentage of crystalline material in the fiber. Thus, the molecular orientation of fibers of different crystalline modification cannot be compared in terms of the observed double refraction since they do not approach the same limiting value of optical anisotropy at ideal orientation. Experimentally he observed for native ramie a refractive index difference of 0.071. However, quite different results were obtained for a highly oriented mercerized ramie (cellulose *II*). For the mercerized ramie the specific optical anistropy was only 0.057. Hermans emphasized the fact that the orientation of this stretched mercerized ramie was as good as or better than that of the original native sample, and yet the observed optical anisotropy was only 78% of the first value. The results of Hermans have been cited because by analogy they seem to give a plausible explanation for the orientation *vs.* magnetic anisotropy relations shown in Figure 2. It seems evident from the data in Figure 2 that the crystalline modification has greatly influenced the observed magnetic anisotropy, and that the anisotropy varies with orientation in a different manner for the two modifications. It is of interest to compare the magnetic anisotropy of two materials of different modification at equal orientation. The ramie yarn (item 1) and the rayon yarn, Fiber G (item 4), both exhibit high and nearly equal

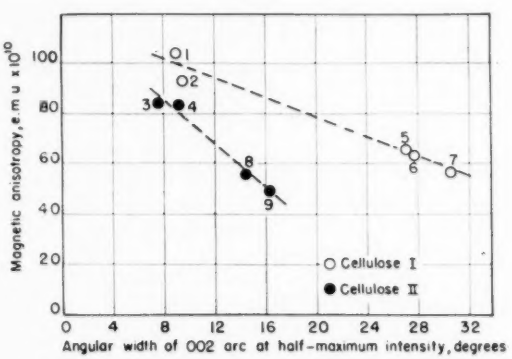

FIG. 2. *Variation of magnetic anistropy with crystallite orientation.*

crystallite orientation, and yet the ratio of the anisotropy for these two materials is 0.80, a value approximately equal to the ratio given by Hermans for native and mercerized ramie.

It is more difficult to decide from the present limited data whether the observed anisotropy is influenced by the percentage of crystalline material. The ethylamine-treated samples are of particular interest in this connection. Treatment of cotton with anhydrous ethylamine followed by chloroform extraction of the amine has been shown to reduce the percentage of crystalline material [13]. Subsequent water-boiling of the amine-treated cotton causes a partial restoration of crystallinity. The percentages of crystalline material, as estimated by the acid-hydrolysis residue technique [8, 10], for the control, the amine-treated, and the amine-treated water-boiled cottons were 91%, 33%, and 55%, respectively. It has further been shown that the "decrystallized cotton" still possesses the native modification. Since the half-maximum angles given in Table I were not appreciably different for these three materials (Table I, items 5, 10, and 11), the comparatively large differences in the anisotropy for these samples must be due solely to differences in the percentage of crystalline material. It seems, therefore, that the same factors which influence the optical anisotropy of a fibrous material also operate when magnetic anisotropy is considered as a criterion of molecular orientation.

The extreme difference in the observed anisotropy for the cotton yarn mercerized at constant length and with no tension again presents a case which is not explainable on the basis of variations in crystallite orientation alone.

Certain points are mentioned below which should be considered in any further magnetic study of cellulosic fibers. In order to effect a more rigorous correlation with other methods of molecular orientation, it would be necessary to measure the anisotropy of fibers rather than bundles of yarns. While the use of bundles of parallel fibers is a little more tedious experimentally, the bundles can be made quite small if the torsion constant of the suspending filament is reduced accordingly. The disorienting effect of twist in the yarns undoubtedly influences both the absolute and relative values reported here. Furthermore, the magnetic anisotropy should be compared with those criteria which reflect the orientation of the fiber as a whole—*i.e.*, optical or swelling anisotropy rather than crystallite orientation, which does not take into account the amorphous cellulose.

Reliable limiting values at ideal longitudinal orientation must be obtained for the two crystalline modifications in order to use magnetic anisotropy as a measure of orientation. Less well oriented actual fibers could then be compared to these two limiting values. However, further study of the effect of differences in crystallinity between the ideal and actual fiber would still be required in order to give the method any general usefulness.

Literature Cited

1. Cotton-Feytis, E., *Compt. rend.* **214**, 485, 996 (1942); **215**, 299 (1942).
2. Cotton-Feytis, E., *Rev. gen. caoutchouc* **21**, 26 (1944).
3. Hermans, P. H., "Contributions to the Physics of Cellulose Fibers," New York, Elsevier, 1946, chaps. V–VI.
4. Hermans, P. H., "Physics and Chemistry of Cellulose Fibers," New York, Elsevier, 1949, chap. IV.
5. Krishnan, K. S., Guha, B. C., and Banerjee, S., *Phil. Trans. Roy. Soc., London* **A231**, 235 (1933).
6. Krishnan, K. S., and Banerjee, S., *Phil. Trans. Roy. Soc., London* **A234**, 265 (1935).
7. Lonsdale, K., *Proc. Roy. Soc., London* **171**, 541 (1939).
8. Nelson, M. L., and Conrad, C. M., Textile Research Journal **18**, 149 (1948).
9. Nilakantan, P., *Proc. Indian Acad. Sci.* **7A**, 38 (1938).
10. Philipp, H. J., Nelson, M. L., and Ziifle, H. M., Textile Research Journal **17**, 585 (1947).
11. Preston, J. M., and Bhat, R. V., *J. Textile Inst.* **39**, T211 (1948).
12. Segal, L., Creely, J. J., and Conrad, C. M., *Rev. Sci. Instruments* **21**, 431 (1950).
13. Segal, L., Nelson, M. L., and Conrad, C. M., *J. Phys. & Colloid Chem.* **55**, 325 (1951).
14. Selwood, P. W., *J. Research Natl. Bur. Standards* **41**, 151 (1948).
15. Selwood, P. W., Parodi, J. A., and Pace, A., *J. Am. Chem. Soc.* **72**, 1269 (1950).

(*Manuscript received November 17, 1952.*)

Letters to the Editor

Short communications in the form of Letters to the Editor are intended to provide prompt publication of significant new research results and to permit an exchange of views on papers previously published in the JOURNAL. These communications are not submitted to formal review as are research papers, and the editors do not assume any share of the author's responsibility for the information given or the opinions expressed. When work previously published in the JOURNAL is the subject of critical comment, the authors of the original paper are given an opportunity to submit a reply, which will be published concurrently when possible.

The Birefringence of Dacron Polyester Fiber

TEXTILE RESEARCH INSTITUTE
Princeton, New Jersey
December 15, 1952

To the Editor
TEXTILE RESEARCH JOURNAL

Dear Sir:

The recent paper of Heyn [1], concerned with refractive index and birefringence measurements of synthetic fibers, prompts us to point out a possible error in his determination of the birefringence of Dacron polyester fiber, and to indicate a different method of birefringence measurement which makes the possibility of such an error less likely.

Heyn reports a value of 0.015 for the birefringence of Dacron, corresponding to a retardation of 140 mμ per 10μ thickness of fiber. No information about the extent of stretching is given, but presumably it is sufficient to result in the characteristic x-ray pattern of Dacron [2], which begins to appear at about 250% stretch. We have measured the birefringence of Dacron as a function of stretching, with the following results:

Stretch (%)	Birefringence
0	0.001
102	0.042
199	0.110
299	0.140
402	0.167
499	0.181

Thus, Dacron stretched only 100% appears to have a birefringence nearly three times the value reported by Heyn. Measurements by the immersion liquid technique confirm the very high birefringence of Dacron recorded above. We found that the refractive index perpendicular to the fiber axis is approximately that given by Heyn, but that the index parallel to the axis, which he was unable to measure, is quite high and depends strongly on the degree of stretching.

The methods of measuring birefringence described by Heyn become difficult to apply in the case of fibers with a very large retardation, because of the uncertainty of the order of interference. Determination of the birefringence of such fibers by visual examination of the polarization colors becomes impossible, since at the higher orders the colors become less distinctive and very closely spaced; even the use of retardation plates or the quartz wedge is hampered at the interference orders which may be encountered with Dacron—eighth or ninth.

The method used in this laboratory (suggested to us by Dr. E. H. Mercer) is to cut a flat wedge at the end of the fiber and to observe the black interference bands exhibited by the wedge between crossed nicols in monochromatic light. The number of such bands gives directly the order of interference plus one. The remaining steps involve the principle of the Sénarmont compensator [3]. In order to permit a greater range of rotation, the upper prism of the polarizing microscope is replaced by a small piece of Polaroid fitted into the eyepiece, which is equipped with a pointer and circular scale. A $\frac{1}{4}$-wave plate, with its slow direction parallel to the polarizer vibration direction, is used above the specimen, and illumination is provided by a sodium vapor lamp. Against the dark background of the crossed polarizer and analyzer, the fiber (immersed in mineral oil) is adjusted in the 45° position, where its center appears brightest. The angle θ ($< \pi$ radians) through which the eyepiece analyzer must be turned in order to pro-

duce extinction down the center of the fiber is measured. The birefringence is then given by

$$n_\gamma - n_\alpha = \frac{(\theta + n\pi)\lambda}{\pi d},$$

where n ($= 0, 1, 2, \ldots$) is the number of interference bands seen on the fiber wedge in monochromatic light. λ is the wave length of the illuminating light, and d is the thickness of the fiber.

These measurements were made as part of a program supported by the Office of Naval Research under Contract No. Nonr-09000. The samples of Dacron polyester fiber were obtained through the kindness of E. I. du Pont de Nemours and Company.

Literature Cited

1. Heyn, A. N. J., Textile Research Journal **22**, 513 (1952).
2. Heyn, A. N. J., *Rayon Textile Monthly* **31**, No. 10, 42 (1950).
3. Hartshorne, N. H., and Stuart, A., "Crystals and the Polarising Microscope," London, Edward Arnold & Co., 1950, pp. 452, 455–7.

Richard G. Quynn
Richard Steele

Author's Comments

The data obtained by the above writers with Dacron polyester fiber of different stretch on the one hand confirm our findings on the great influence of "drawing" on the birefringence of synthetic fibers, but on the other hand suggest that the birefringence of *commercial* Dacron is much higher than found with our original material (which was an older experimental product of the Fiber V type). Determinations with the latest commercial Dacron fiber confirm this suggestion; the *commercial* fiber has the highest birefringence of all synthetic fibers so far (in the order of the highest values given above).

The elegant "wedge" method described above offers a means for easy differentiation of this fiber under the polarizing microscope and furnishes a valuable addition to our comparative study and identification procedure of synthetic fibers with the polarized light method.

A. N. J. Heyn
School of Textiles
Clemson Agricultural College
Clemson, S. C.

(*January 5, 1953.*)

The Rapid Identification of Fibers by the Christiansen Effect

Beaunit Mills, Inc.
New York, N. Y.
December 30, 1952

To the Editor
Textile Research Journal

Dear Sir:

Two recent discussions of fiber refractive indices in Textile Research Journal by H. de Vries [4] and A. N. J. Heyn [10] indicated that a method used in our laboratory may be of interest as an aid in the qualitative analysis of fibers. There is nothing new in the method, it having been shown many years ago by Christiansen that if a material is placed in a liquid having a similar refractive index but a higher dispersion, under certain conditions varying chromatic effects are visible to the naked eye [3]. Since Christiansen's time, his technique has been improved [15], rediscovered [11], and variously explained [2, 9, 16], and developments of his experiment have been applied to fibers by various workers who added special instruments. Preston and Freeman observed the colors without special equipment, but their goal was the determination of precise refractive indices, and they added a spectroscope [13, 14]. More recently, Douglass and Crossman used the Christiansen effect observed with a special dark-field microscope for the qualitative analysis of a few fibers with a few liquids [5], but the fibers listed are more easily and surely differentiated with less equipment, and their excellent approach does not seem to have had practical employment.

The Becke line method for refractive index is also based on the microscope and is often difficult [6, 7, 8, 10]. In addition, the literature contains different values, which sometimes are given as if commercial fibers had refractive indices as absolute as those of nonfibrous crystalline materials [1, 12]. Actually, as

Preston, Heyn, Matthews, and others have pointed out, the refractive indices of different samples of the same commercial fibers can and do vary considerably, so that painstaking Becke line determinations to 0.002 or better are not normally required for qualitative analysis and can be misleading.

In our method we have gone back to the original Christiansen principle, with merely the addition of a small oblong of Polaroid. Tufts of white or only lightly dyed fiber mounted in matching refractive index liquids of high dispersion seem to be brilliantly colored when inspected at the edge of an approximately parallel beam of light or at the edge of illumination from an overhead daylight fluorescent tube or a frosted incandescent globe. One can determine n_α and n_γ adequately for the purposes of qualitative analysis using a set of liquids differing by 0.005 in n_d^{20} by viewing the fibers illuminated through a small oblong of Polaroid. The Polaroid may be placed in front of or behind the sample. Fibers with n_d^{20} almost equal to that of the liquid are seen as red-blue. If the liquid index is too high, cold colors—blues which vary from indigo to paler shades—are visible. If the liquid n_d^{20} is slightly too low, warm colors—brick red, amber, and yellow—are produced. The following table shows the complementary nature of the colors:

Visible color	Color of corresponding wave lengths
Sky blue	Red
Violet-blue	Orange
Purple	Yellow-green
Magenta	Green
Orange	Blue
Yellow	Blue-violet

Not all fibers produce colors of high intensity; Celcos, cotton, Dacron, and X-51 may give dim shades. Twist, overlapping, crimp, and delustrants

Refractive index	No polaroid	Perpendicular	Parallel
1.475	Acetate rayon	Acetate rayon	Acetate rayon
1.480	Acetate rayon	Acetate rayon	Acetate rayon
1.485	Celcos*	Celcos*	Celcos*
1.500	German polyacrilonitrile staple	German polyacrilonitrile staple	German polyacrilonitrile staple
1.510	Bemberg staple	Bemberg staple, Fortisan	
1.515	Orlon staple, X-51 staple, Bemberg staple, SpunLo viscose	Viscose, Orlon staple, X-51 staple, Bemberg staple	Orlon staple, X-51 staple
1.520	Orlon, Acrilan, acetate†	Viscose, Fiber B, linen, nylon, Acrilan, Orlon	Orlon, Acrilan
1.525	X-51,* viscose, Perlon	X-51,* nylon, ramie, Cordura, Bemberg, Perlon	X-51*
1.530	Viscose, Dynel staple	Dynel staple, cotton*	Dynel staple
1.535	Vinyon N, Aralac, Bemberg, Dynel, Vicara	Vinyon N, Aralac, silk, Dynel, Vicara	Vinyon N, viscose, Aralac, Dynel, Vicara
1.540	Viscose	SpunLo viscose,† silk	Viscose
1.545	Fiberglas, Fiberfrax, Cordura, soybean (Drackett), Bemberg staple	Wool, Fiberglas, Fiberfrax, soybean (Drackett), Bemberg staple†	Fiberglas, Fiberfrax, viscose, soybean (Drackett), Bemberg staple
1.550	Wool, Soylon	Soylon, Dacron*	Wool, Soylon, Cordura, Bemberg staple
1.555			Fortisan, Bemberg
1.560	Angora	Angora	Angora
1.565			Fiber B
1.570	Vicara	Vicara	Vicara
1.580	Perlon, ramie	Dacron†	Perlon, nylon, linen
1.585			Silk
1.590			Ramie, silk
1.600	Saran staple	Saran staple	
1.605			Saran

* Dim colors.
† Spectral effect (R–Gr–B).

cut down the color. For good results, a few well-parallelized fibers should be mounted under a small cover glass. In this way, several checks can be made on a single glass slide. In addition to the Christiansen colors, fibers may produce prismatic colors, as the liquid refractive index goes well above that of the fiber refractive index by about 0.030. These prismatic colors are easily distinguished from the Christiansen colors since there is a color change in prismatic order (red, green, blue) as the angle of illumination increases.

We have made up test liquids using acetyl acetone, anisol, oil of fennel, butylcarbitol, and α-chloronaphthalene, and have blended them in order to cover the range from 1.47 to 1.615 in steps of 0.005. This approach has its disadvantages because of uneven evaporation of the constituents and corresponding changes in the refractive index. Preston has given a series of liquids of high dispersion [14], but it is, of course, not possible to find a practical group of pure liquids which closely covers the entire range. Here too, literature index values and the index values of commercial products differ. It is not necessary that the liquids have very high dispersions for the chromatic effect to be visible. Limonene, with its relatively low dispersion, will give dim Christiansen colors with acetate rayon. The list opposite indicates the fibers which have been tested in our laboratory and which will show purple using the above technique. Naturally, a correct and current table of fiber refractive indices would be a good guide. One should bear in mind that liquids change n_d with temperature, and some fibers change with moisture content. Our list is based on liquids and fibers tested at just below American standard textile conditions, 65% R.H. and 68°F (20°C). In general, if a higher n_d liquid is used, an amber color will be seen, and if a lower n_d liquid is used, the color will be blue. We have also marked the beginning of the distinct prismatic effect of some fibers.

Literature Cited

1. American Society for Testing Materials, "A.S.T.M. Standards on Textile Materials," Philadelphia, Oct. 1952, p. 536.
2. Chamot, E. M., and Mason, C. W., "Handbook of Chemical Microscopy," Vol. I, New York, John Wiley & Sons, 1938, p. 101.
3. Christiansen, C., *Wiedemann's Annalen* (Nov. 1884).
4. de Vries, H., Textile Research Journal **22**, 619 (1952).
5. Douglass, P. C., and Crossmon, G. C., Textile Research Journal **19**, 644 (1949).
6. Emmons, R. C., and Gates, R. M., *Am. Mineral.* **33**, 612 (1948).
7. Fox, K. R., Textile Research Journal **10**, 79 (1939).
8. Fox, K. R., and Finch, R. B., Textile Research Journal **11**, 62 (1940).
9. Francis, A. W., *J. Phys. Chem.* **56**, 510 (1952).
10. Heyn, A. N. J., Textile Research Journal **22**, 513 (1952).
11. Holmes, H. N., and Cameron, D. H., *J. Am. Chem. Soc.* **49**, 71 (1922).
12. Mauersberger, H. R. (editor), "Matthews' Textile Fibers," 5th ed., New York, John Wiley & Sons, 1947, p. 60.
13. Preston, J. M., and Freeman, K., *Chemistry & Industry* **13**, 338 (1935).
14. Preston, J. M., and Freeman, K., *J. Textile Inst.* **34**, T19 (1943).
15. Lord Rayleigh, *Phil. Mag.* **20**, 358 (1885).
16. Wood, R. W., "Physical Optics," 3rd ed., New York, Macmillan Company, 1934, p. 115.

Braham Norwick

INDUSTRIAL SECTION

The Measurement of Fabric Thickness

R. E. Seaman

Characterization Research Laboratory, Textile Research Division, Textile Fibers Department, E. I. du Pont de Nemours & Company, Inc., Wilmington, Delaware

Abstract

A discussion of the principles underlying the measurement of fabric thickness is presented. The instruments and procedures in current use are outlined, together with their advantages and disadvantages. A procedure based on the one adopted by the British Standards Institute for measuring fabric thickness under low pressures is outlined and recommended. The necessary equipment is discussed, together with the results obtained on over 200 fabrics.

Introduction

Research on such fabric properties as bulk, warmth, hand, and resilience indicates the importance of reliable methods for measuring thickness. Since most fabrics are compressed rather easily, the type of instrument and method of measurement used can influence the results markedly. As an example, woven conveyor belting or heavy cotton duck are both quite stiff and relatively incompressible under the pressures encountered in normal usage. Therefore, if a dead-weight gage is used to measure their thicknesses, the pressure applied to the presser foot of such an instrument is not an important factor in the test procedure. In direct contrast to this is the case of a pile liner or fur-faced fabric. In the case of such fabrics it is apparent that the value reported as fabric thickness will be dependent on the pressure exerted on the fabric during the test. This difference in behavior is shown in Figure 1. Both fabrics have been subjected to the standard A.S.T.M. pressure of 3.4 p.s.i. The extreme deformation of the double-pile liner is quite apparent.

It is evident from the foregoing that one standard method of measuring thickness which utilizes an appreciable pressure cannot give accurate results on all types of fabrics. On the other hand, it is possible that for quality control work, which is concerned primarily with reproducibility, once the specifications for measurement have been established using a particular instrument and procedure, such a method may be entirely satisfactory regardless of its relative accuracy. However, in research work it is recognized that there are some fabric constructions (pile-faced lining material or blankets, for example) which are used in situations where their usefulness depends on their ability to maintain their original form (and thickness) under relatively low pressures. Even for such relatively "hard" materials as worsted suitings, it is misleading to measure their thicknesses under 3.4 p.s.i. since the maximum pressure in service (on the seat of a man's trousers) is about 1.5 p.s.i.

Standard A.S.T.M. Test

Several different methods are available at the present time. The only official method, however, is the standard A.S.T.M. procedure D-39–49, and this is used on many types of fabrics. The current A.S.T.M. procedure is based on the use of a dead-weight gage with a presser foot (diameter 0.375 in.) attached to a micrometer dial graduated to read directly in increments of .001 in. In operation, a fabric specimen is placed horizontally, without tension, on an anvil, and the presser foot is applied normal to the fabric surface under a pressure of 3.4 lbs./sq. in. The separation of anvil and presser foot, as indicated on the dial, is reported as a measure of fabric thickness.

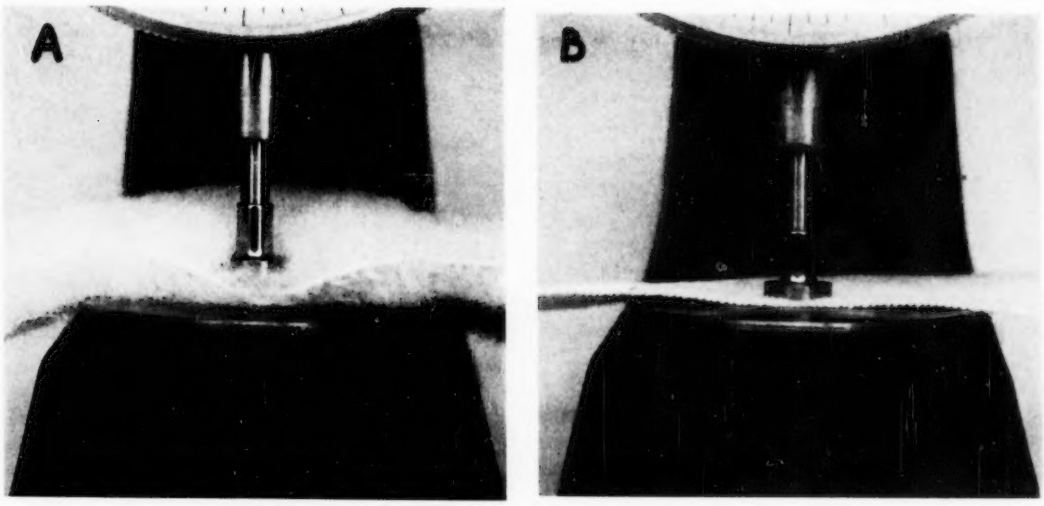

Fig. 1. *Compression of different fabric constructions under standard A.S.T.M. pressure (3.4 p.s.i.).* A—*21-oz. wool double-pile liner.* B—*12-oz. cotton duck.*

Many variables are present in such measurements. Haven [2] has stated that the following variables are present when the conventional micrometer type of equipment is used. They may be classified as: controlled variables, such as size of and weight on the presser foot, which determines the pressure applied to the fabric, shape of presser foot, and stability or rigidity of equipment; operative techniques, such as rate at which the load is applied to the specimen, and time elapsing during measurement; and specimen variations within a given sample.

It is apparent that these variables exist as listed in such thickness measurements, and also that the topic headings could apply to practically all test equipment and procedures. However, in view of this list and the discussion in the previous section, it is evident that the present A.S.T.M. test should not be used for all types and constructions of fabrics.

The A.S.T.M. test is well established in this country, and in many instances is satisfactory. It does, however, penalize soft fabrics such as the pile-liner fabric shown in Figure 1. In such a fabric the individual elements in the pile may be considered to be Euler columns which, when subjected to an axial stress in excess of the critical load, will bend laterally. Since such a condition is self-aggravating, the mass of fibers exposed to such a load will buckle and the pile will be compressed until the density of the compressed mass becomes great enough to resist further lateral deformation. Such a condition is always observed to some degree when the thicknesses of soft fabrics are measured according to the A.S.T.M. procedure. The elimination or reduction of this condition is necessary in order to determine the thickness of the fabric under loads frequently found in service.

Other Methods

An instrument called a "Compressometer," designed by H. F. Schiefer, has been used for thickness and resilience measurements in many laboratories [4]. It consists of two micrometer gages mounted with a rack and pinion which moves vertically. The two gages are connected by means of a helical spring. A threaded shaft connected to the lower gage permits attachment of any one of three different diameter presser feet.* In practice, the specimen to be tested is placed on a horizontal anvil without tension, and the rack and pinion operated to lower the presser foot on the specimen. By means of calibration curves for each size presser foot, the desired pressure may be applied, as indicated on the upper gage. The reading on the lower gage, which is reported as specimen thickness, is the distance between anvil and presser foot when the pressure has been increased to a stated amount. This equipment has merit in that it is easy

* It is understood that a fourth foot of larger diameter (8 in.) to secure still lower pressures has recently been put on the market.

to operate and the test may be carried out quickly; and pressures from .002 to 2.00 p.s.i. may be used. Among its disadvantages are: a hysteresis effect due to friction is observed, a different value of thickness being obtained for a given pressure dial reading depending on whether the desired pressure is approached from the high or low side; the equipment must be recalibrated frequently due to changes in the coefficient of friction of lubricated parts with time; at low pressures the compression of a specimen under its own weight is not taken into consideration; and when using the larger presser feet at low pressures, care must be exercised to be sure the foot remains parallel with the anvil and is not deflected by accidental tilting or is out of level due to warping of the foot itself.

It is also possible to measure fabric thicknesses on an Instron tensile tester fitted with a compression unit.* This machine operates as a constant-rate-of-deformation tester, the deformation and load being registered autographically on the chart of a modified Leeds and Northrup recorder. In practice, a fabric is placed on an anvil attached to the sensing cell, and is then compressed by a presser foot actuated by a movable cross-head. Bonded-wire strain gages incorporated in the cell translate the pressure into an electrical signal which is recorded on the recorder chart. The thickness value reported is obtained by measuring the chart travel during the time the presser foot moves from a predetermined initial position. While this method is very precise and a variety of pressures may be employed, the necessary equipment is expensive and the test is time-consuming.

Other methods have been considered, such as projecting a cross section of a fabric on a screen and measuring or photographing the enlarged image, but the preparation of cross sections is time-consuming and the technique may result in the introduction of operator errors so that it is not used extensively.

Low-Pressure Tester

Since no standard method for the measurement of thickness at low pressures exists in this country, an instrument was constructed which had been described originally by Marsh [3] and adopted as standard by the British Standards Institute [1]. This instrument utilizes low pressures of from 1 to 100 g./cm.^{2} (.015 to 1.5 p.s.i.).

* Instron Engineering Corporation, Quincy, Mass.

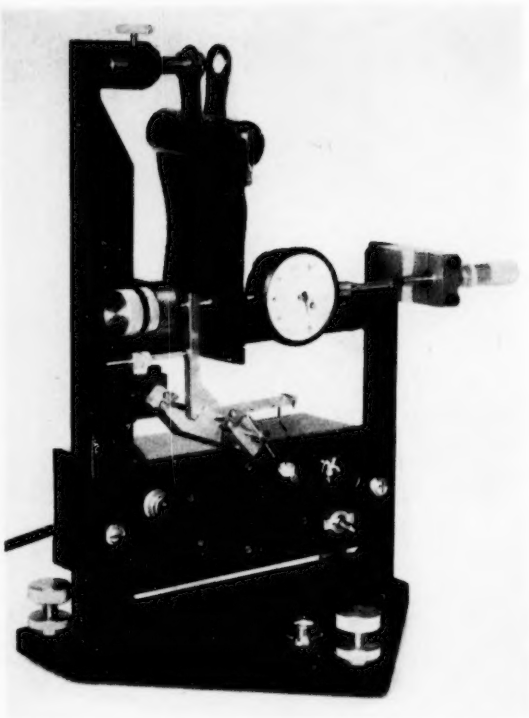

FIG. 2. *Instrument for measuring fabric thickness under low pressures.*

A modification of the equipment described by the B.S.I. was constructed in our laboratory in order to get high reproducibility. The apparatus is shown in Figure 2. The modifications consisted of the addition of a more stable mount and frame and the incorporation as an integral part of the equipment of an electrical circuit to indicate the test end-point.

A specimen is held vertically between an anvil 1 sq. cm. in area and a presser foot connected to a micrometer dial graduated in mils. The anvil is part of a lever arm arranged so that both arms are of equal length. Therefore, a weight hung in the notch of the horizontal arm gives direct pressure measurements in g./cm.^{2} A weight of 5 g. is used in this laboratory. The lever arm is suspended by a length of .002 shim stock to provide a frictionless bearing. A perspective view of this assembly is shown in Figure 3. When the presser foot is moved against the fabric by means of a vernier screw, the fabric and anvil are moved to the left until the anvil contacts an adjustable zeroing screw, the contact being indicated by completion of an electrical circuit which flashes a

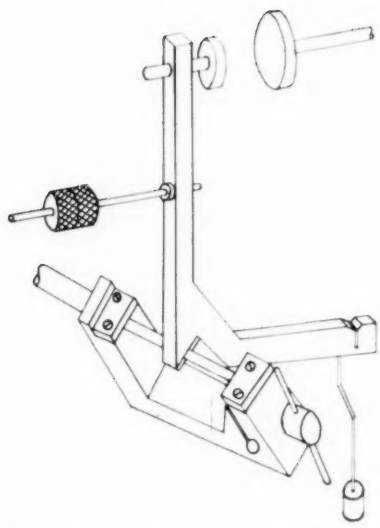

FIG. 3. *Perspective drawing of presser foot and balance arm assembly of the low-pressure thickness tester.*

red light. If the equipment has previously been adjusted to zero without a specimen, the specimen thickness will be indicated directly on the dial. Most micrometer dials are spring-loaded so that they return to zero automatically. Therefore, when used in this apparatus, either the spring action must be reversed or the numbering of the dial reversed to provide direct reading measurements.

Advantages of Low-Pressure Tester

This instrument has two advantages inherent in its construction. First, the fabric is suspended vertically. This eliminates any compression of the fabric under its own weight, which will occur if it is tested in a horizontal plane. An example may clarify this point. The double-pile liner in Figure 1 weighs approximately .07 g./cm.^{2} If its thickness is measured under a pressure of 1.0 g./cm.^{2}, the measurement may be in error by as much as 7% if tested while lying on an anvil in a horizontal plane. (It is even conceivable that an appreciably higher error may result if the material is very compliant to small compressive forces.) Since an increasing amount of interest and effort is being directed towards the measurement of thicknesses at very low pressures (< 1 g./cm.^{2}), this point should be considered in the evaluation of such results. Second, the fabric itself determines the end-point of the test since both presser foot and anvil are free to move during the duration of the test. Thus, any compression of the fabric is related only to its construction. This is in direct contrast to conventional measurements where the fabric lies on a fixed anvil and is not free to seek an equilibrium position during the test. The instrument is also free of several of the disadvantages noted for the Compressometer.

Comparison of Fabric Thicknesses as Measured by A.S.T.M. and Low-Pressure Techniques

Figure 4 shows the relationship between the thicknesses of 212 fabrics measured by both the standard A.S.T.M. and low-pressure (B.S.I.) techniques. The plotted thickness of each fabric is the average of five measurements by each procedure. Fabric weights ranged from 2.1 to 14 oz./yd.^{2} Considering the fact that these fabrics ranged from thin, hard, monofilament fabrics to thick, soft, pile liners, the spread of values is not at all excessive. The ratio

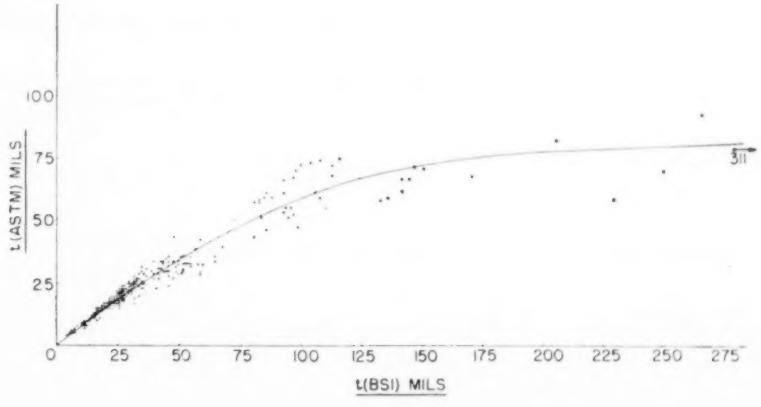

FIG. 4. *Relationship between A.S.T.M. and B.S.I. thickness for 212 fabrics.*

of the two thicknesses is about 1:1 up to approximately 10 mils. Above 10 mils, the relationship is no longer linear. It is apparent that above 40 mils (A.S.T.M. thickness) the ratio of B.S.I. to A.S.T.M. thickness increases rapidly. Since most clothing fabrics thicker than 40 mils are soft, measurement of their thicknesses by the A.S.T.M. procedure will penalize them considerably. In such cases, the use of a low-pressure technique is highly desirable.

Conclusion

The low-pressure technique has been used in this laboratory for approximately 8 months and is proving quite reliable. The thickness values obtained by this procedure have been found to contribute substantially more information to the bulk, compressibility, and insulation properties of fabrics than do results obtained using the current A.S.T.M. method.

Literature Cited

1. British Standards Institute, Methods of Tests for Textiles, in "British Standards Handbook No. 11," London, 1949, p. 119.
2. Haven, G. B., TEXTILE RESEARCH JOURNAL **3**, 229 (1933).
3. Marsh, M. C., *J. Sci. Instruments* **6**, 382 (1929).
4. Schiefer, H. F., *J. Research Natl. Bur. Standards* **10**, 705 (1933).

(*Manuscript received January 12, 1953.*)

A Theoretical Investigation of Cap and Ring Spinning Systems

J. Crank

Courtaulds Limited, Maidenhead, Berkshire, England

Abstract

This paper describes how balloon profiles and thread tensions may be calculated, given the requisite properties of the yarn and the spinning frame, by solving the equations of motion of the ballooning thread and by considering the forces acting at the cap edge or on the traveller. It is possible to include the effects of air drag and Coriolis forces by carrying out the calculations on a differential analyzer. The influence of top tension on the balloon profile is investigated in air and in vacuum, and, in particular, the characteristic licking of the cap is seen to be a consequence of air drag and low tension. It is associated with the tendency to form a double balloon at low tensions in vacuum.

Calculated profiles agree reasonably well with those observed for corresponding tensions at the top guide on a practical cap-spinning system. The balloon is shown to be determined by two parameters involving the various technical features such as yarn tension and denier and the dimensions of the spinning frame.

The forces at the cap edge and on the traveller are considered. As an example, the equation at the cap edge is combined with those of the ballooning thread to show how bobbin tension is decreased by increasing the bobbin radius and by decreasing the friction between the cap edge and the yarn. The calculations confirm that licking may arise when the bobbin is full even though it does not occur when it is empty. The bobbin tension calculated for a given bobbin radius, on the assumption of a perfectly smooth cap, agrees well with the observed tension in a practical system.

Introduction

In any cap spinning system there are three distinct problems to be considered: (*1*) the behavior of the thread in the balloon between the top guide and the cap edge; (*2*) the conditions existing at the cap edge; (*3*) the behavior of the thread between the cap edge and the bobbin. In this paper the thread between the cap edge and the bobbin is considered to be straight and its tension constant. In practice the form and tension of the ballooning thread are determined by the requirement that the forces acting on the ballooning thread and also the forces acting at the cap edge must be in equilibrium. These two sets of forces are not independent of

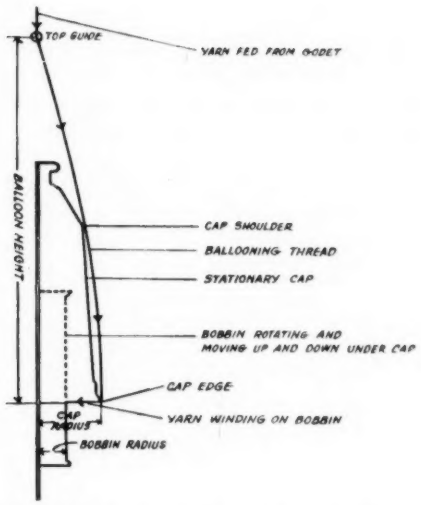

FIG. 1. *Typical arrangement for cap spinning.*

each other; the conditions at the cap edge, for example, partly control the properties of the balloon, and the forces on the ballooning thread partly determine the forces at the cap edge. Nevertheless, it is convenient in the first place to treat them as separate problems and then, by putting the two together, it is possible to predict the balloon shape and yarn tension, given the relevant properties of the yarn and the spinning frame. Similar considerations clearly apply to ring spinning, except that forces on the traveller must be considered instead of those at the cap edge.

In this paper the equations of motion of the ballooning thread are formulated first, and balloon profiles are calculated for given thread tensions at the top guide. It is then shown that the balloon and tension to be expected when a particular yarn is spinning on a given frame can be selected from the family of calculated balloons by considering the forces at the cap edge or on the traveller. In calculating balloon profiles for given tensions at the top guide, it is immaterial whether cap or ring spinning is being considered, and the same family of curves applies to both. The method of spinning comes in later in selecting the tension and balloon appropriate to a particular set of spinning conditions.

The calculated balloon profiles presented in this paper are chosen to illustrate how the ballooning thread is influenced by technical features such as yarn tension, air drag, bobbin diameter, etc., and to show that calculated balloons are in reasonable agreement with those observed under corresponding conditions. It is hoped later to publish a set of balloon profiles and thread tensions calculated systematically for a range of parameters covering practical spinning conditions.

Forces on the Ballooning Thread

A typical arrangement for cap spinning is shown diagrammatically in Figure 1 to illustrate the nomenclature and dimensions used in this paper. In setting up equations of motion for the ballooning thread, it is most convenient to take rotating axes OX, OY, and OZ, rotating about OZ with the constant angular velocity of the balloon, denoted by ω. The axis OZ is vertically downwards. In this moving frame of reference the thread curve has a constant form. We may note in passing that ω is readily calculated from spindle speed, N (r.p.s.), bobbin radius, r, and spinning speed, v, using the relation

$$\omega = 2\pi N - v/r. \qquad (1)$$

The following forces acting on an element of thread in the balloon are taken into account in this paper: (*1*) the thread tensions at the two ends of the element; (*2*) gravity in the z direction; (*3*) air resistance opposed to the direction of revolution of the thread in the balloon, assumed to be proportional to the length of the element and to act perpendicular to the radius to the element and to the axis of the balloon OZ; (*4*) the centrifugal force directed radially outwards perpendicular to the axis of the balloon; (*5*) the centrifugal force acting along the normal to the balloon curve due to the movement of the thread along its own length with speed v; and (*6*) the Coriolis force arising from the use of rotating axes.

It is not strictly accurate to assume either that the air resistance is proportional to the length of the element or that it acts only in the direction stated. The thread is somewhat inclined to the vertical, and the air-drag should more accurately be assumed to be proportional to the element of the meridian of the balloon. Also there will be some resistance tangential to the thread due to its motion along the curve. Present knowledge of the air-resistance law does not appear to justify inclusion of either of these effects, however.

In setting up equations to express the fact that an element of thread is in equilibrium under the action of the above forces, the thread is assumed to

be vertical immediately above the top guide and to have a constant velocity and tension there. The thread is assumed to be uniform and of circular cross section, perfectly flexible, and inextensible. No attempt is made to allow for possible separation of the individual filaments of the yarn as it moves through the air. Resolving forces along the three axes OX, OY, and OZ leads to the following equations of motion:

$$\frac{d}{ds}\left(T_1\frac{dx}{ds}\right) + \frac{fy}{r} + 2\,m\omega v\frac{dy}{ds} + m\omega^2 x = 0, \quad (2)$$

$$\frac{d}{ds}\left(T_1\frac{dy}{ds}\right) - \frac{fx}{r} - 2\,m\omega v\frac{dx}{ds} + m\omega^2 y = 0, \quad (3)$$

$$\frac{d}{ds}\left(T_1\frac{dz}{ds}\right) + mg = 0. \quad (4)$$

Here T_1 is a modified thread tension given by

$$T_1 = T - mv^2, \quad (5)$$

where T is true tension (g.). In most practical examples mv^2 is very small compared with T, and so T_1 can be thought of as the true tension without serious error. Distance measured along the thread curve is denoted by s, r is the radius of the balloon at the point (x, y, z), v is the spinning speed, and m is the mass of the thread per unit length (g./cm.). The air-drag acting on an element of length ds is taken to be $f(r, \omega)\,ds$, where f is a function of velocity determined by aerodynamic conditions, the diameter of the thread, and the nature of its surface. The precise form of f used is discussed in a later section.

In equation (4) the term mg can usually be neglected, in which case equation (4) is simply

$$T_1\frac{dz}{ds} = \text{constant} = T_z; \quad (6)$$

that is, the vertical component of tension is constant.

Balloon Profiles in Vacuum

The problem is a much simpler one if the effect of air-drag on the ballooning thread is neglected. This is then the problem of spinning in vacuum, which at first appears to be of little practical importance. It is worth-while considering briefly, however, because when balloon profiles in air are considered, it is instructive to compare them with corresponding balloons in vacuum. If air-drag is negligible and if the Coriolis forces are small, so that the terms $2m\omega v\,dy/ds$ and $2m\omega v\,dx/ds$ in equations (2) and (3) can also be neglected (and this is frequently the case for practical spinning speeds), then it is clear from the equations that y is everywhere negligible, and equation (2) reduces to

$$\frac{d}{ds}\left(T_z\frac{dx}{dz}\right) + m\omega^2 x = 0. \quad (7)$$

The solution of this equation in terms of elliptic integrals has been given previously by Baltz [1]. Before discussing some typical balloon profiles calculated from his solution, however, it is instructive to consider the much simpler equation obtained from equation (7) by assuming $ds = dz$—*i.e.*, by examining only long narrow balloons. Then equation (7) becomes

$$\frac{d^2x}{dz^2} + \frac{m\omega^2 x}{T_z} = 0. \quad (8)$$

This is the well-known equation for simple harmonic motion for which the solution is

$$x = A\sin(m\omega^2/T_z)^{\frac{1}{2}}\,z, \quad (9)$$

where A is a constant chosen such that $x = R$ when $z = h$ (R is the radius of cap or ring and h is the balloon height). Thus, x varies periodically with z, and the period of oscillation is $2\pi\sqrt{T_z/m\omega^2}$, which means that the distance between two successive points $x = 0$, where the balloon crosses its own axis, is $\pi\sqrt{T_z/m\omega^2}$. The point of interest is that this distance increases as T_z increases. Thus,

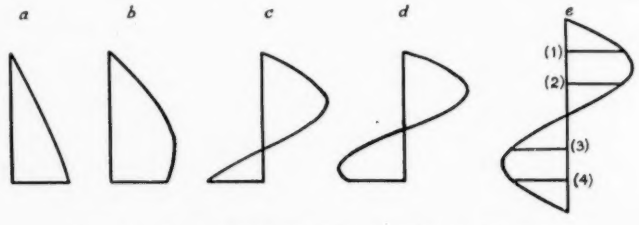

FIG. 2. *Balloon profiles approximating to sine curves.*

TABLE I

Data	System *I* (bobbin empty)	System *II* (bobbin full)
Height of balloon (h)	46.04 cm. (18.1 in.)	42.26 cm. (16.6 in.)
Radius of cap (R)	7.78 cm. (3 in.)	7.78 cm. (3 in.)
Barrel radius (r)	3.50 cm (1.37 in.)	5.67 cm. (2.23 in.)
Spindle speed (N)	133.33 r.p.s. (8,000 r.p.m.)	133.33 r.p.s. (8,000 r.p.m.)
Spinning speed (v)	833 cm./sec. (500 m./min.)	833 cm./sec. (500 m./min.)
Speed of revolution of balloon	95.44 r.p.s. (5,726 r.p.m.)	109.95 r.p.s. (6,597 r.p.m.)

consider T_z so large that the half-period $\pi\sqrt{T_z/m\omega^2}$ is greater than twice the balloon height, h. Then the balloon is qualitatively as shown in Figure 2a. If the half-period is less than $2h$ but greater than h, the profile is as shown in Figure 2b; if it is less than h, the profile is as shown in Figure 2c; and so on, the profiles showing progressively more of the complete sine curve as T_z is decreased. These forms can be regarded, of course, as derived from one long sine curve in which the base of the balloon of radius R takes the successive positions *1*, *2*, *3*, and *4* (Figure 2e). Thus, different conditions of spinning may be expected to produce one of these profiles. Returning now to the more general equation (7), Baltz used the substitutions

$$x = t(b^2 - a^2)^{\frac{1}{2}},\quad k^2 = (b^2 - a^2)/(b^2 + a^2),\quad (k')^2 = 1 - k^2, \tag{10}$$

where

$$a^2 = 2T_z/m\omega^2, \tag{11}$$

and b^2 is a constant of integration. The solution of equation (7) then takes the form

$$z = \frac{ak'}{\sqrt{2}}\int_0^t \frac{dt}{[(1 - t^2)(1 - k^2t^2)]^{\frac{1}{2}}}. \tag{12}$$

This is an elliptic integral, of which tables are available [4, 7], so that z can readily be found for given values of t, k, and k'. Here a^2 is determined from equation (11) by the spinning conditions, and b^2 is chosen so that $z = h$ when $x = R$. Furthermore, since

$$ds/dz = [1 + (dx/dz)^2]^{\frac{1}{2}}, \tag{13}$$

it follows from equation (7) after one or two steps that

$$\frac{dz}{dx} = \frac{a^2}{[(b^2 - x^2)^2 - a^4]^{\frac{1}{2}}}, \tag{14}$$

so that $T_1 = T_z\, ds/dz$, can be determined for any value of x or z.

Some balloon profiles calculated from equation (12) for several different tensions just below the top guide are shown in Figure 3. The details of the yarn and spinning conditions to which these calculations refer are those of system *I* in Table I. The significance of Table I is that the profiles of balloons in air, calculated later in the paper, are compared with balloons observed on two actual cap spinning systems. These systems are referred to as systems *I* and *II*, and details of them are given in

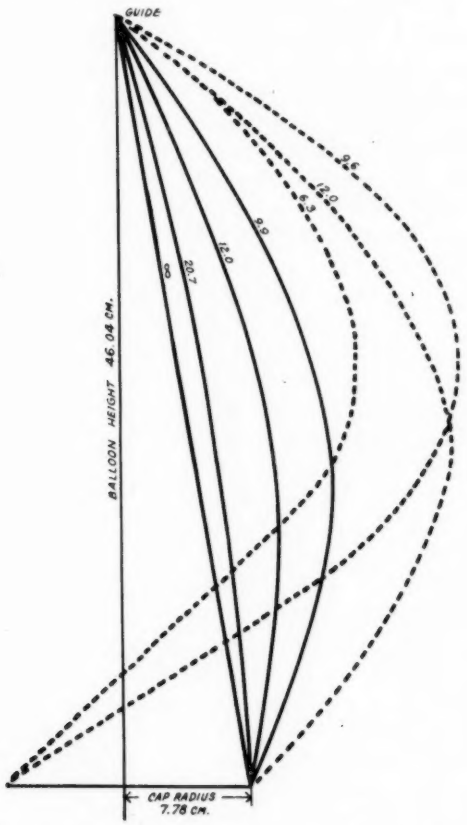

FIG. 3. *Balloon profiles in vacuum. The numbers on the curves are tensions* (g.). *The conditions are those of system I.*

Table 1. The bobbin is empty in system *I* and full in system *II*.

The main features of interest in the profiles of Figure 3 are:

1. For a very high tension the balloon is almost conical.

2. Decreasing the tension causes the balloon to move outwards, and a maximum radius greater than that of the cap eventually develops.

3. As the balloon moves outwards the initial tension reaches a minimum, after which it increases again as the balloon moves further out. Thus, in theory there are two single balloons for any given top tension greater than the minimum.

4. No *single* balloon exists for a tension below the minimum. The minimum tension depends on the yarn and the spinning conditions. For system *I* it is about 9.9 g.

5. For a tension less than the minimum a double balloon (intersecting its own axis) is formed. Examples are shown for tensions of 9.6 g. and 6.3 g.

6. For all double balloons top tension increases as the balloon radius at half-height increases. Thus, it is interesting to note that the behavior which is usually regarded as characteristic—*i.e.*, that the balloon moves outwards when the tension is decreased—is really a special case and only occurs, in vacuum, for certain single balloons.

7. There is a tension below which no double or single balloon is possible, but only treble balloons, which intersect their own axes twice.

In deriving the elliptic integral solution (12) Coriolis forces were neglected, and the thread curve so calculated lies in a plane. This is not so, even in vacuum, if Coriolis forces are appreciable. A solution was evaluated by numerical integration to include these forces for system *I*; the deviation at any point from the plane through the axis of the balloon and the point where the thread crosses the cap edge never exceeds 10% of the radius of the balloon at that point. This departure from the plane is more marked the greater the spinning speed.

Balloon Profiles in Air

The Differential Analyzer

In many practical spinning systems the air-drag on the yarn is very considerable and plays an important part in determining the balloon profile. In such cases the problem cannot be handled by formal mathematical methods. It is possible, however, to evaluate numerical solutions for specific conditions by using one of the large calculating machines available. The results presented in this paper were obtained by using the differential analyzer, which forms part of the equipment of these laboratories. This type of machine has been fully described elsewhere [2]. Its application to this problem is fairly straightforward, and solutions of the full equations (2), (3), and (6) have been obtained with the effects of air-drag and Coriolis forces included.

Air-Drag

The differential analyzer must be supplied with information about the dependence of air-drag on the velocity of the yarn—*i.e.*, on the wind speed relative to the yarn. In general, air-drag (g./cm.) of yarn may be specified by the relation

$$\text{drag/unit length of yarn} = C_D \rho u^2 D/2g, \quad (15)$$

where u is the wind speed, D the diameter of the yarn, ρ the density of the air, and C_D an empirical nondimensional parameter. Values of C_D have been obtained for a straight wire at N.P.L. [5] and also for a number of yarns at the Shirley Institute [6]. The latter results suggest that for wind speeds up to about 200 ft./sec. and the yarns in which we are interested, the N.P.L. law is a reasonably good approximation. Furthermore, in this velocity range the air-drag is found to be nearly proportional to the square of the wind speed, and so the square law is adopted in this work. The effective diameter, D, of the yarn used in systems *I* and *II* was obtained from the mean diameter of the individual filaments comprising it by assuming the cross section of the yarn to be equal to the sum of the cross sections of the 12 individual filaments.

Calculated Profiles

The following are some of the main properties of balloons in air revealed by the calculations:

1. Some calculated balloon profiles for several initial tensions are shown in Figure 4 (left) for system *I* and in Figure 4 (right) for system *II*. The profiles observed experimentally by Curtis [3] are also shown. The calculated balloons for top tensions of 15.4 g. in system *I* and 8.4 g. in system *II* agree reasonably well with the experimental ones. In particular, the characteristic "licking" is reproduced in the calculated profile for system *II* when the tension is 8.4 g.

2. These calculated tensions are to be compared with the values of 8.5 g. and 7 g., respectively, measured by Curtis. His tensions were measured above the top guide, whereas the calculated figures refer to just below the guide. Some increase in tension is to be expected as the yarn passes through the guide and so the agreement is not unsatisfactory.

3. The balloon changes with the top tension in the following way. When the top tension is high the balloon is nearly conical. As the tension is decreased the balloon moves outwards, reaching a maximum diameter when the tension is about 9 g. for system *I*. For lower tensions, the mid-point of the ballooning thread moves inwards and also the balloon develops a concavity just above the cap edge. This tendency to "lick" the cap under certain conditions is well known in practice. The behavior is similar in system *II* except that the largest balloon is obtained for a top tension of about 10 g.

4. Comparison of the profiles of Figure 4 with those of Figure 3 is instructive as regards the effect of air resistance. At high tensions the behavior is similar in vacuum and in air. The top tension for which the largest balloon occurs in air is about the same as the least tension for which a single balloon is possible in vacuum. For lower tensions the behavior is somewhat different because, whereas in vacuum a double balloon occurs, in air the profile merely develops a concavity and "licks" the cap. This suggests that the tendency to "lick" the side of the cap is caused not by air-drag, as appears to have been supposed previously, but by the low tension. Licking is, in fact, an indication that a double balloon would form were it not for the air-drag, which prevents the thread crossing the axis of the balloon by causing it to be blown round the cap. The licking is more pronounced the lower the tension. The suggestion that licking indicates a

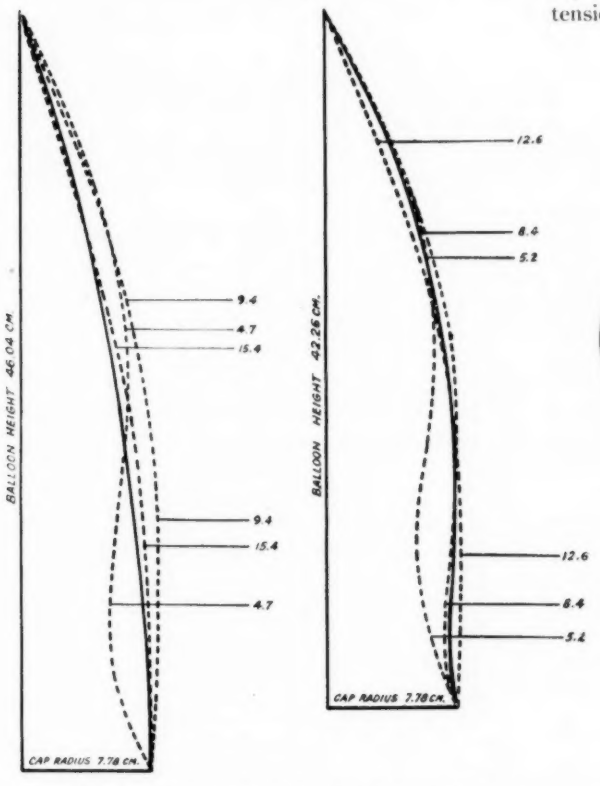

FIG. 4. *Comparison of calculated and observed balloon profiles.* Left—*System I.* Right—*System II. The numbers on the curves are tensions* (g.).

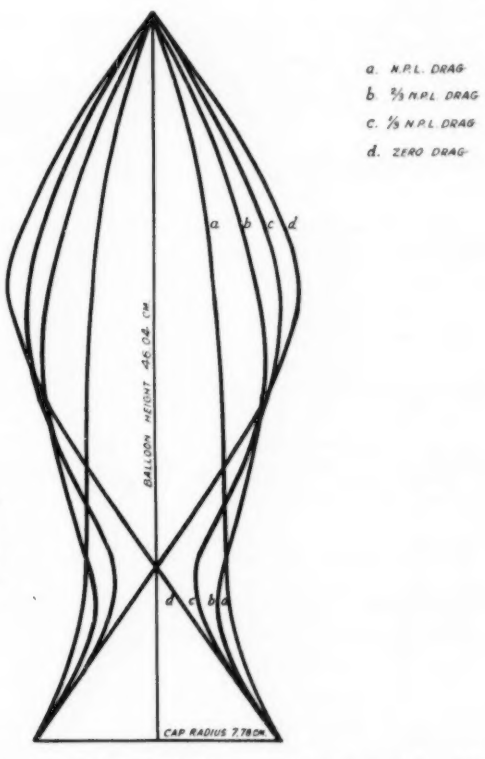

FIG. 5. *Effect of air-drag on balloon profile. The conditions are those of system I. Top tension = 3.75 g.*

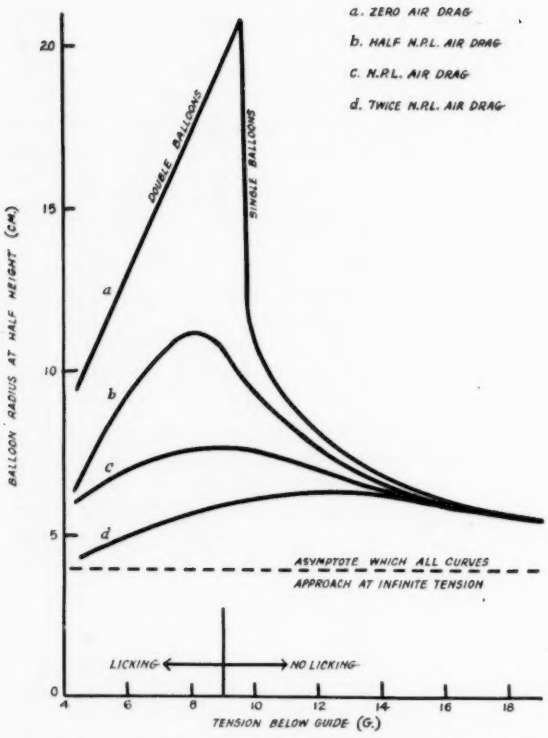

FIG. 6. *Effect of tension and air-drag on balloon size. The conditions are those of system I.*

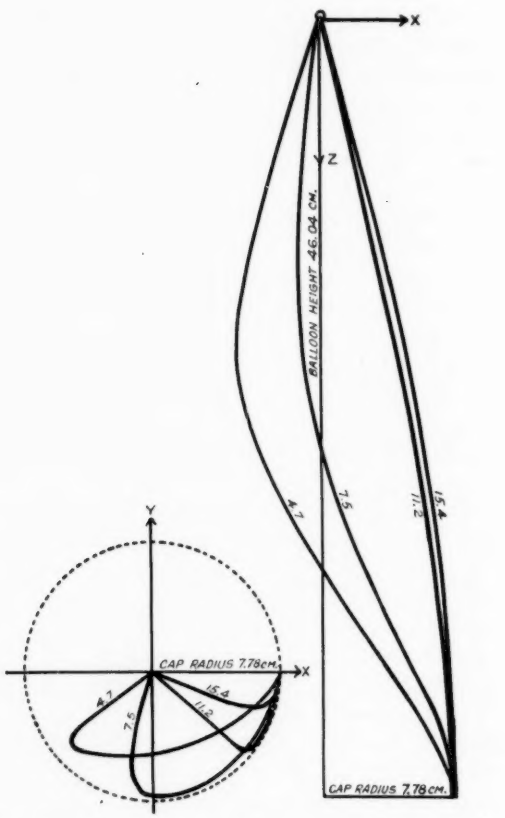

FIG. 7. *Projections of thread curve on vertical* (right) *and horizontal* (left) *planes. The numbers on the curves are tensions* (g.).

potential double balloon is strengthened by the calculated behavior of balloons for a given top tension and successively less air-drag, as shown in Figure 5. As the air is removed, the licking balloon approaches a double balloon intersecting its own axis.

5. The way in which the balloon is influenced by top tension and air-drag is summarized in Figure 6. The different air resistances could be due to different atmospheric conditions or, more likely, to different yarn diameters for the same denier (see the following section). The curves refer to system *I*.

6. So far only balloon profiles have been considered. A more complete picture of the thread curve in the balloon is provided by the projections on to the vertical XZ plane and the horizontal XY plane, as in Figure 7.

7. The variation of tension along the thread is shown in Figure 8 for the two top tensions for which the calculated balloon profiles agree best with observed profiles. In practice system *II* is usually associated with low yarn tension, as indicated by good yarn extensibility. It is possible that the calculated tensions are unduly high because of the assumptions made regarding air-drag.

Two Nondimensional Parameters

If changes in the Coriolis and gravitational forces are neglected and attention is focussed on long, narrow balloons (R^2/h^2 small), only two parameters are needed to specify a balloon calculated from equations (2), (3), and (6). Expression (15) can be written in a shorter form as

$$\text{drag/unit length of yarn} = qDu^2, \qquad (16)$$

with q a parameter depending on the yarn and on aerodynamic conditions. Then if the X and Y coordinates are expressed as fractions of the cap radius, R, and the Z coordinate is expressed as a fraction of balloon height, h, it is easily seen from

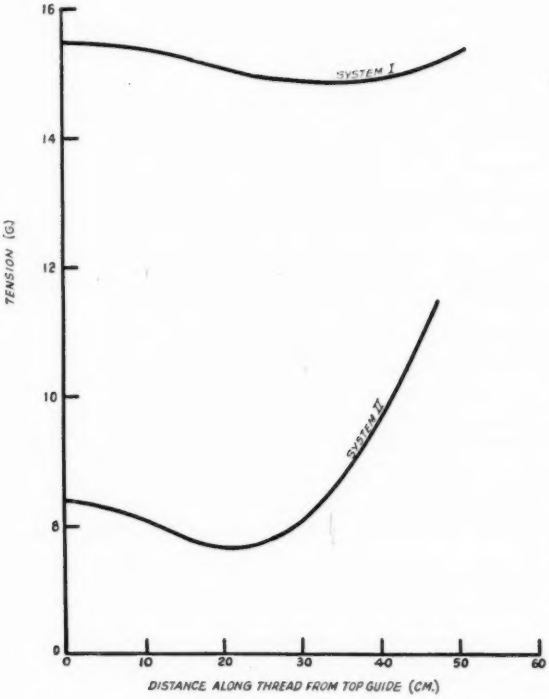

FIG 8. *Variation of tension along ballooning thread.*

the equations that the balloon depends on the two nondimensional parameters qDR/m and $T_o/mh^2\omega^2$, where T_o is the thread tension below the guide. On substituting the approximate relation

$$m = \pi D^2 d/4, \tag{17}$$

the first parameter becomes $qR/(md)^{\frac{1}{2}}$, a constant factor $2/\pi^{\frac{1}{2}}$ having been removed. This means that if any two factors are altered in such a way as to maintain both parameters fixed, the thread curve (expressed in fractional coordinates) is unchanged. Alternatively, the effect on the balloon of a change in any of the spinning conditions is determined by its effect on one or both of these parameters. For example, the speed of revolution, ω, of the balloon affects only the second parameter, $T_o/mh^2\omega^2$, and an increase in ω is clearly equivalent to a decrease in tension. Thus, if the tension is increased in the same ratio as ω^2, the balloon is unchanged.

For a balloon in a vacuum $q = 0$, and therefore only one parameter, $T_o/mh^2\omega^2$, is needed to specify such a balloon, provided the same fractional coordinates are used and attention is confined to long, narrow balloons for which Coriolis forces are negligible.

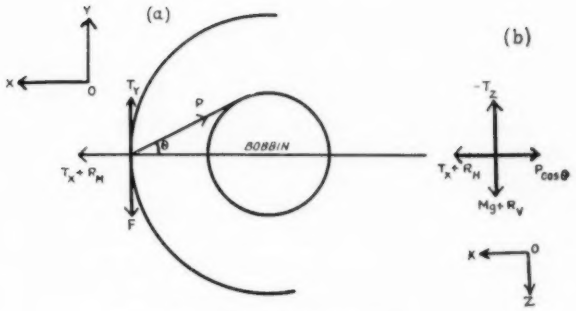

FIG. 9. *Forces on the traveller.*

Forces on the Traveller

The forces acting on the traveller are its weight, thread tensions, the reaction of the ring, and frictional forces between the traveller and the ring. These forces are shown in Figure 9 (a and b). Here T_X, T_Y, and T_Z are components of tension along the axes OX, OY, and OZ, respectively; P is the tension in the thread between the traveller and the bobbin; R_H and R_V are the horizontal and vertical components of the reaction of the ring on the traveller, and F is the frictional drag of the ring on the traveller. Resolving along the radius gives

$$P\cos\theta - T_X - R_H = MR\omega^2, \tag{18}$$

where M is the mass of the traveller, R the ring radius, and ω the angular velocity of the traveller, the same as that of the balloon. Resolving vertically,

$$Mg + R_V + T_Z = 0, \tag{19}$$

and along the tangent to the traveller motion,

$$P\sin\theta = F - T_Y. \tag{20}$$

The resultant reaction between ring and traveller is $(R_H^2 + R_V^2)^{\frac{1}{2}}$, and hence the frictional force, F, is given by

$$F = \mu_1 (R_H^2 + R_V^2)^{\frac{1}{2}}, \tag{21}$$

where μ_1 is the coefficient of friction between ring and traveller. Substituting for R_H and R_V from equations (18) and (19) and then for F in equation (20) yields

$$P\sin\theta = -T_Y + \mu_1 [(T_Z + Mg)^2 + (P\cos\theta - T_X - MR\omega^2)^2]^{\frac{1}{2}}. \tag{22}$$

Because the thread is running through the traveller,

the tension, P, exceeds T, the relation between the two being given approximately by

$$P = Te^{\mu_2\phi}, \qquad (23)$$

where ϕ is the angle through which the thread turns on passing through the traveller, and μ_2 is the coefficient of friction between the thread and the traveller. The angle ϕ is given by the usual relation for the angle between two lines whose direction cosines are given. Since in setting up equations of motion of the thread s was taken as increasing towards the traveller, the relation becomes

$$\cos\phi = dy/ds \sin\theta - dx/ds \cos\theta, \qquad (24)$$

and also in equation (22)

$$T_X = -Tdx/ds,\ T_Y = -Tdy/ds,\ T_Z = -Tdz/ds, \qquad (25)$$

where T is the tension in the thread at the traveller. On substituting for P from equation (23) and using equations (25), equation (22) becomes a relation between thread tension and direction which must be satisfied in order that the forces on the traveller will be in equilibrium. Previously in this paper values of thread tension and direction at the traveller for which the ballooning thread was in equilibrium were calculated. Balloons which are possible in practice for given spinning conditions are those for which tension and direction satisfy both traveller and balloon equations.

Forces at the Cap Edge

A rigorous treatment of the conditions at the cap edge appears to be at least as involved as that of the ballooning thread. However, the radius of the cap edge is usually about 0.01 in. compared with a cap radius of 3 to 4 in., and so it is reasonable to assume that the cap has a line edge rather than one of finite radius. Furthermore, the motion of the thread is usually much greater *along* the cap edge than across it. This means that the main component of friction is tangential to the cap edge and no appreciable change occurs in the thread tension when the thread crosses the edge. Subject to these assumptions, the problem is closely similar to that of a traveller of zero mass, and, by resolving the forces in the corresponding way, it is easily shown that the relation at the cap edge is

$$\sin\theta = dy/ds + \mu\,[1 - (dy/ds)^2 + 2\,(dx/ds)\cos\theta + \cos^2\theta]^{\frac{1}{2}}, \qquad (26)$$

which follows directly from equation (22) by putting $M = 0$ and $P = T$. In equation (26) μ is the coefficient of friction between the thread and the cap edge.

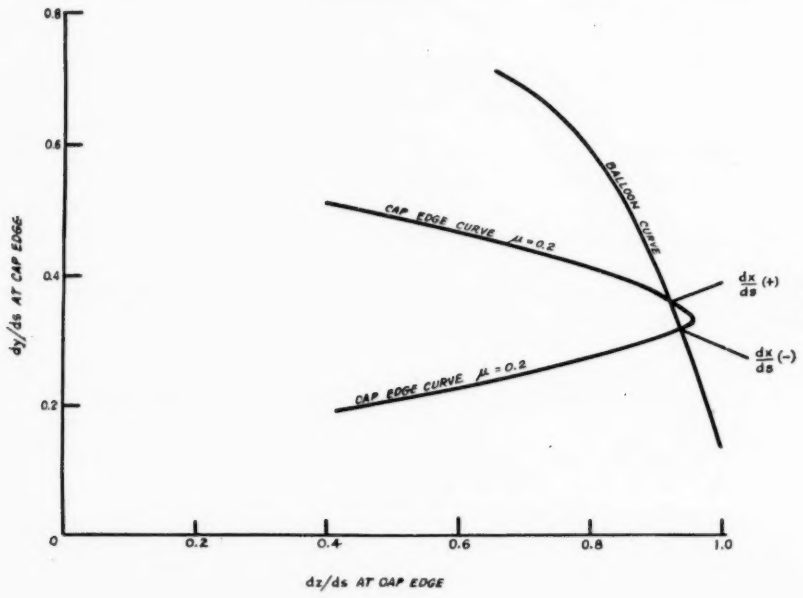

FIG. 10. *Curves showing equilibrium conditions for cap-edge and balloon forces. The conditions are those of system II.*

For given μ and θ—*i.e.*, given ratio of cap to bobbin radius—dy/ds can be plotted as a function of dx/ds (in practice dz/ds is more convenient) such that the cap edge equation (26) is satisfied. Also, on the same diagram can be plotted values of dy/ds and dz/ds calculated by the differential analyzer for ballooning threads of various top tensions. At the intersection of these two curves both the cap edge and the balloon conditions are satisfied, and the values of dy/ds and dz/ds there define the top tension and hence the balloon to be expected for given spinning conditions. An example of such a diagram is shown in Figure 10, where the conditions are those of system *II* and μ is taken to be 0.2. At one of the two intersections dx/ds calculated from equation (26) is positive, and at the other it is negative. Thus, only the one intersection, for which the sign of dx/ds agrees with the sign of the corresponding quantity on the balloon curve, is acceptable.

Treatment of equation (22) for the traveller is similar in principle though slightly more complicated in practice because there is a family of curves of dy/ds against dz/ds for different values of T. The intersection of the balloon curve with the surface defined by this family of curves in a three-dimensional diagram has to be determined to find which balloon can exist.

Effect of Bobbin Radius and Friction at the Cap Edge

Figure 11 shows how bobbin tension varies with bobbin radius and how it depends on the coefficient of friction at the cap edge. These curves are based on values calculated in the way described above for cap spinning under the conditions of system *II* apart from the different bobbin radii. The calculated bobbin tension is seen to decrease as bobbin radius increases, but increasing the coefficient of friction leads to higher bobbin tensions. These conclusions are in qualitative agreement with practical experience. Figure 11 shows that the tension increases rapidly below a certain radius, and it is clear that, for the higher coefficients of friction, spinning will be prevented by breakage of the thread unless the bobbin is almost full.

It is of interest to see how the thread tension deduced from Figure 11 agrees with that observed in practice for system *II* when the bobbin is full

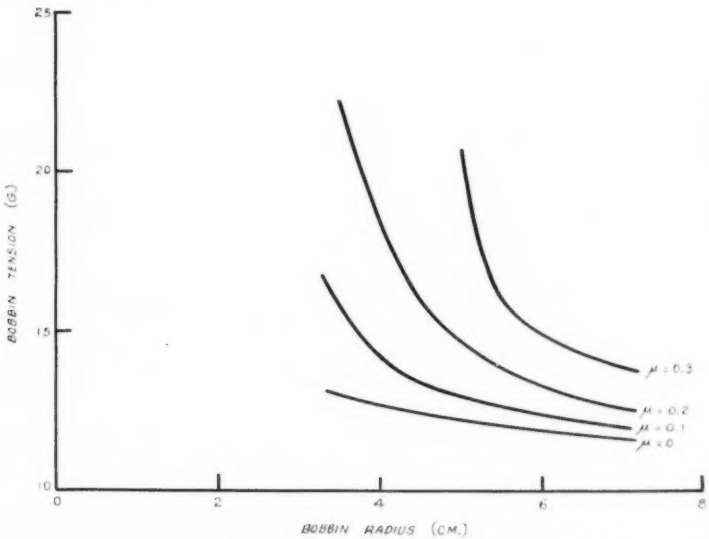

Fig. 11. *Effect of bobbin size and cap-edge friction on bobbin tension. The conditions are those of system II.*

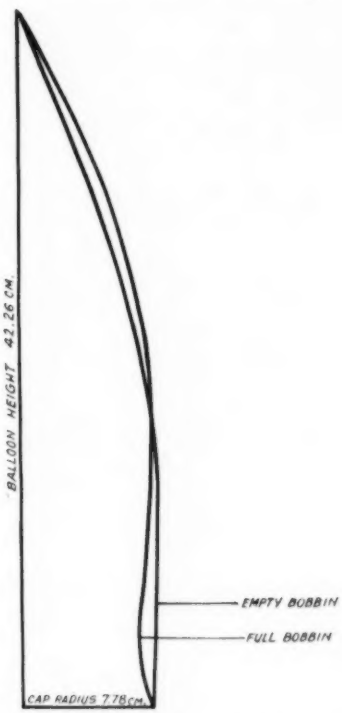

Fig. 12. *Balloons for full and empty bobbins; perfectly smooth cap ($\mu = 0$). The conditions are those of system II.*

for example (bobbin radius = 5.67 cm.). Taking a perfectly smooth cap ($\mu = 0$) the bobbin tension from Figure 11 for this radius is roughly 11.5 g., which corresponds, according to the differential analyzer solutions, to a tension below the top guide of 8.5 g. The measured tension *above* the guide for system *II* is 7 g. Clearly, the calculated tensions for rougher caps are still greater. This and other comparisons between calculated and observed tensions suggest that the coefficient of friction at the cap edge is less than 0.1. This is much smaller than would normally be expected for cellulose acetate yarn and steel. It is known, however, that the frictional properties depend greatly on local conditions. Also, as Dr. T. H. Morton has suggested in conversation, there may not be true contact between the thread and the cap edge.

The change in tension, which occurs as the bobbin fills up, produces changes in the balloon. The profiles in Figure 12 for an empty and a full bobbin show that licking can occur with a full bobbin even though it does not occur when the bobbin is empty.

Acknowledgment

The author is indebted to several colleagues, especially Dr. J. G. Oldroyd, Dr. S. Kulik, and Mr. G. Curtis, for much helpful discussion in the early stages of the work. The numerical work was carried out by Miss M. E. Henry, and the differential analyzer was operated by Mr. I. M. Groves.

Literature Cited

1. Baltz, W. E., *Kunstseide u. Zellwolle* **26**, 42 (1948).
2. Crank, J., "The Differential Analyser," London, Longmans, 1947.
3. Curtis, G., Courtaulds Ltd., Coventry, England, private communication.
4. Jahnke, E., and Emde, F., "Tables of Functions," New York, Dover Publications, 1945.
5. National Physical Laboratory, "Modern Developments in Fluid Dynamics," Vol. 2, Oxford, Clarendon Press, 1938, p. 418.
6. Shirley Institute, Manchester, England, private communication.
7. Spenceley, G. W., and Spenceley, R. M., "Smithsonian Elliptic Functions Tables," Washington, 1947.

(*Manuscript received October 27, 1952.*)

GORDON RESEARCH CONFERENCE ON TEXTILES

Colby Junior College, New London, N. H., July 13–17, 1953

Individuals interested in attending the Conference are requested to send in their applications to W. George Parks, Director, Department of Chemistry, Rhode Island State College, Kingston, Rhode Island, on or before May 1, 1953.

George S. Buck, *Chairman*

July 13—John A. Howsmon —"The Evaluation of the Submicroscopic Structure of Fibers"
Leon Segal —"Decrystallization of Cotton Cellulose"
July 14—R. J. Andres —"Pressure Dyeing of Man-Made Fibers"
Speaker and subject to be announced.
July 15—Pauline Beery Mack—"Recent Developments in the Science of Textile Maintenance"
Herman Bogaty —"Chemical, Physical and Physiological Characteristics of Blended Fabrics"
July 16—Myron J. Coplon —"Influence of Temperature on Certain Tensile Properties of Various Textile Fibers"
George Ham, Jr. —"Chemistry of Polymerization of Acrylics"
July 17—D. J. Montgomery —"Generation and Conduction of Electricity in Fibrous Materials"

. . . *what is it?*

Tomorrow's customer . . . your customer, may still remember the ironing board. But chances are, she'll have little use for one.

For women, especially, are leading busier lives today. That means less time for clothes care . . . a greater demand for fabrics that seldom need ironing.

Du Pont "modern-living" fibers make it possible for you to offer fabrics in exciting new textures and colors . . . fabrics that wash easily, dry quickly, hold their shape, stay crisp and pretty longer.

When you create fabrics, consider the Du Pont "modern-living" fibers—take advantage of Du Pont's long experience and more extensive research on fibers and fabrics—rely on Du Pont to help you produce fabrics that satisfy . . . fabrics that sell.

DU PONT

REG. U.S. PAT. OFF.

BETTER THINGS FOR BETTER LIVING . . . *THROUGH CHEMISTRY*

DU PONT'S MODERN-LIVING FIBERS

DACRON® POLYESTER FIBER

NYLON

ORLON® ACRYLIC FIBER

RAYON

ACETATE

DREW anti-static agents proved superior by every static testing method!

It's time you tried DRUSTATS & DRUSPINS—Drew Anti-Static agents. A full line of new, effective materials is now available for use with any type of fibre, yarn or fabric.

DRUSTATS & DRUSPINS have been evaluated for chemical, physical and electrostatic properties in laboratory and plant by all known procedures and have proved superior in every case.

In textile production, DRUSPIN treated fibres are manipulated without trouble. Fabrics finished with DRUSTATS are dust, lint and dirt free, they cut better, sew better and are more comfortable to wear. Used with resins they also supply increased tear resistance and quicker recoverability from crease.

Write for summary of leading Anti-Static testing devices, and the latest leaflet on using the new DRUSTATS & DRUSPINS in production for any specific fibre at any specific textile process.

TEXTILE CHEMICALS DEPARTMENT

E. F. DREW & CO., Inc.

15 EAST 26th STREET, NEW YORK 10, N. Y.

CHICAGO
PHILADELPHIA
BOSTON
GREENVILLE, S. C.